REACTIONS OF THE ALKOXIDES AND AMIDES OF MAGNESIUM, ZINC, AND ALUMINUM

A THESIS

Presented to

The Faculty of the Division of Graduate Studies

By

George Fredrick Willard, Jr.

In Partial Fulfillment

of the Requirements for the Degree

Doctor of Philosophy in the School of Chemistry

Georgia Institute of Technology

January, 1978

REACTIONS OF THE ALKOXIDES AND AMIDES OF

MAGNESIUM, ZINC, AND ALUMINUM

Approved:

E. C. Ashby, Research Advisor

H. O. House, Chairman

C. L. Liotta

E. Grovenstein

Date Approved by Chairman: 6/5/78

To

Kathy, Fredrick, and Melinda

ACKNOWLEDGEMENTS

No thesis is the product of only one person. Many individuals and organizations have made contributions to the successful completion of this thesis. I wish to acknowledge those people whom I felt made the greatest contribution.

The Georgia Institute of Technology, especially the School of Chemistry, supplied research and teaching assistantships during my research. All the faculty and staff of the School of Chemistry supported my research. I particularly would like to recognize Professor H. O. House for his aid in solving synthetic problems and Professors E. Grovenstein and C. L. Liotta for their useful kinetics discussions. Special thanks are due to John P. Oliver who "showed me the ropes" when I first started my laboratory research. Also, I wish to thank my contemporaries Steve Noding, Joe Bowers, Scott Smith and Dr. Tim Smith for their many helpful discussions.

Professor E. C. Ashby suggested the areas of study covered in this thesis and gave advice as the research progressed. He is also to be commended for taking an active interest in the welfare of his graduate students outside of the laboratory. I wish to thank him for keeping faith in me.

My mother, Geraldine R. Willard, provided moral support and financial assistance when needed.

My wife, Kathy, has made many sacrifices so that I might finish my graduate studies. She provided financial support our first few

years in Atlanta by working full time. Later, she devoted her time, energy, and patience to raising our two children. She also participated in the rough typing and editing of this thesis. Probably her greatest contribution has been her moral support when everything was going wrong.

TABLE OF CONTENTS

PART II

THERMAL DECOMPOSITION OF THE ALKOXIDES AND AMIDES OF MAGNESIUM, ZINC, AND ALUMINUM

Page

LIST OF TABLES

PART I

STEREOSELECTIVE ALKYLATIONS OF CYCLIC KETONES BY DIALKYLAMINO AND ALKOXY (METHYL) MAGNESIUM COMPOUNDS

PART II

THERMAL DECOMPOSITION OF THE ALKOXIDES AND AMIDES OF MAGNESIUM, ZINC, AND ALUMINUM

LIST OF FIGURES

PART I

STEREOSELECTIVE ALKYLATIONS OF CYCLIC KETONES BY DIALKYLAMINO AND ALKOXY (METHYL) MAGNESIUM COMPOUNDS

PART II

THERMAL DECOMPOSITION OF THE ALKOXIDES AND AMIDES OF MAGNESIUM, ZINC, AND ALUMINUM

SUMMARY

PART I. STEREOSELECTIVE ALKYLATION OF CYCLIC KETONES BY DIALKYLAMINO AND ALKOXY (METHYL) MAGNESIUM COMPOUNDS

Dialkylamino (methyl) magnesium compounds, CH_3MgNR_2 (where NR_2 = NPr^i_2, NPh_2, and 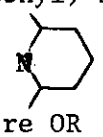), and alkoxy (methyl) magnesium compounds, CH_3MgOR (where OR = O— 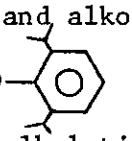 and O— 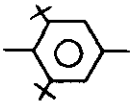), have been evaluated as stereoselective alkylating reagents. Two cyclic ketones, 4-t-butylcyclohexanone and 2,2,6,6-tetramethyl-4-t-butylcyclohexanone, were employed as model substrates. Excellent stereochemical results were obtained with diisopropylamino (methyl) magnesium and 2,6-diisopropylphenoxy (methyl) magnesium. Equatorial attack to give axial alcohol could be increased by adding triphenylphosphine to complex the reagent. Changing the solvent from diethyl ether to diphenyl ether also gave increased yields of axial alcohol. These reagents have considerable potential as stereoselective alkylating agents, especially for nonenolizable substrates.

PART II. THERMAL DECOMPOSITION OF THE ALKOXIDES AND AMIDES OF MAGNESIUM, ZINC, AND ALUMINUM

The thermal decomposition of the alkoxides and amides of magnesium, zinc, and aluminum has been studied. Kinetic and stereochemical data indicated that a cyclic, unimolecular six-center transition state was involved. The products from the alkoxides

were a hydrocarbon, an olefin, and a metal oxide, and the products from the amides were a hydrocarbon, an olefin, and a residue with empirical formula $(MgNR')_x$. The decompsoition reaction occurred in a syn stereochemical fashion and showed a large negative entropy of activation. Non-isothermal kinetic data agreed with the isothermal kinetic data to within 20%.

The product $(MgNR')_3$ represented a new class of pseudo-aromatic compounds analogous to the borazines: N-substituted magnazines. Spectroscopic and colligative property data supported this conclusion.

PART I

STEREOSELECTIVE ALKYLATION OF CYCLIC KETONES BY DIALKYLAMINO AND ALKOXY (METHYL) MAGNESIUM COMPOUNDS

CHAPTER I

INTRODUCTION

Background

A recent review[1] on the stereochemistry of organometallic compound addition to ketones points out the paucity of stereoselective alkylating reagents, especially for the case of methylation of unhindered ketones. The reaction of methyl lithium, in the presence of a lithium salt such as $LiClO_4$, with 4-tert-butylcyclohexanone to give a 94/6 ax/eq alcohol ratio is probably the best example of stereoselective methylation hitherto reported.[2]

Our success with the stereoselective reduction of cyclic and bicyclic ketones with dialkylaminomagnesium hydrides[3] prompted us to apply similar reasoning to the problem of stereoselective alkylation. Namely, if such hydrides were good stereoselective reducing agents by virtue of their bulky dialkylamino groups, then similar bulkiness in an alkylating reagent should produce the same effect.

Purpose

The purpose of the research described in Part I of this thesis is to evaluate various dialkylamino and alkoxy (methyl) magnesium compounds as potentially new stereoselective alkylating reagents. Two cyclic ketones, 4-t-butylcyclohexanone and 2,2,6,6-tetramethyl-

4-t-butylcyclohexanone, are used as models. Several experimental factors are considered including the nature of the solvent and the influence of additives such as lithium perchlorate or triphenylphosphine.

CHAPTER II

EXPERIMENTAL

Apparatus

Reactions were performed under nitrogen at the bench using Schlenk tube techniques.[4] GLPC analyses were performed on an F and M Model 720 gas chromatograph. Nmr spectra were recorded on a Jeol 100 MHz fourier transform nmr spectrometer.

Analyses

Gas analyses were carried out by hydrolyzing samples with hydrochloric acid or methanol on a standard vacuum line equipped with a Toepler pump.[4] Magnesium was determined by EDTA titration at pH 10 using Eriochrome Black T as an indicator.[5] A special apparatus was designed to facilitate gas analyses (Appendix 1).

Materials

Diisopropylamine (Aldrich), 2,6-dimethylpiperdine (Aldrich), and 2,6-diisopropylphenol (Ethyl Corp.) were dried over NaOH and fractionally distilled prior to use. Diphenylamine (Fisher), tert-amyl alcohol (Mallinckrodt), 2,6-di-tert-butyl-p-cresol (Eastman), and triphenylphosphine (Fisher) were used without further purification. 4-tert-Butylcyclohexanone (Frinton) was sublimed under vacuum prior to use.

Diethyl ether and benzene were distilled over $LiAlH_4$ and $NaAlH_4$, respectively. Diphenyl ether was fractionally distilled under vacuum. Dimethylmagnesium was prepared by the reaction of dimethylmercury with excess magnesium metal (Ventron chips) at 25°C.[6] A solution of dimethylmagnesium in diethyl ether was standardized by magnesium and methane analysis (Ratio $Mg:CH_4$ = 1.00:1.98).

Preparation of 2,2,6,6-Tetramethyl-4-tert-butylcyclohexanone

To a 1-liter three neck flask equipped with a reflux condenser and nitrogen bubbler was added 34.5 g. (1.50 moles) sodium and 178 ml (excess) tert-amyl alcohol. The mixture was stirred 24 hours under reflux until no sodium remained. Then 38.8 g. (0.252 moles) 4-tert-butylcyclohexanone in 158.4 g. (excess) methyl iodide was added dropwise and the reflux continued for one week. The reaction mixture was then quenched with water and extracted with diethyl ether. The ether extract was dried over $MgSO_4$ and reduced under vacuum to give 49.6 g. of an oil (93.7% crude yield). The material was then crystallized twice from pentane to give 8.2 g. 2,2,6,6-tetramethyl-4-tert-butylcyclohexanone (15.5% yield), mp 77.0-78.0°C. The material was sublimed at 65 to 85°C at 2 mm Hg. The yield was 7.1 g. (mp 92.0-93.0°C). The 2,2,6,6-tetramethyl-4-tert-butylcyclohexanone thus prepared was hydroscopic and was handled in a glove box. Anal. Calcd. for $C_{14}H_{26}O$: C, 79.94; H, 12.46. Found: C, 79.69; H, 12.40. Nmr in $CDCl_3$: 0.95 δ(s, 9H), 1.10 δ(s, 6H), 1.18 δ(s, 6H) and 1.62 δ(m, 5H); ir in nujol: 1715 cm^{-1} (C=O); mass spec: 210 (M^+), 153 ($M^+ - C_4H_9$).

Characterization of cis and trans (axial and equatorial) 1,2,2,6,6-Pentamethyl-4-tert-butylcyclohexan-1-ol

The methylation products from the reaction of 2,2,6,6-tetramethyl-4-tert-butylcyclohexanone and methylmagnesium bromide were collected via glpc on a 4 ft., one-half inch diameter, 5% carbowax 20M on chromosorb W column. The equatorial alcohol eluted first as will be shown later.

Trans-1,2,2,6,6-pentamethyl-4-tert-butylcyclohexan-1-ol (equatorial)

The material collected first via glpc gave the following analysis: Anal. Calcd. for $C_{15}H_{30}O$: C, 79.58; H, 13.35. Found: C, 79.39; H, 13.39. Mp = 44.0-45.0°C; nmr in $CDCl_3$: 0.85 δ(s, 9H), 0.98 δ(s, 3H), 1.05 δ(s, 6H), 1.13 δ(s, 6H), 1.26 δ(m, 4H), and 1.61 δ(m, 1H); ir as melt: 3620, 3500 cm^{-1} (OH); mass spec: 226 (M^+), 169 ($M^+ - C_4H_9$).

Cis-1,2,2,6,6-pentamethyl-4-tert-butylcyclohexan-1-ol (axial)

The material collected second via glpc gave the following analysis: Anal. Calcd. for $C_{15}H_{30}O$: C, 79.58; H, 13.35. Found: C, 79.40; H, 13.34. Mp = 35.5-36.0°C; nmr in $CDCl_3$: 0.85 δ(s, 9H), 0.95 δ(s, 3H), 1.10 δ(s, 6H), 1.15 δ(s, 6H), 1.20 δ(m, 4H) and 1.32 δ(m, 1H); ir as melt: 3620, 3500 cm^{-1} (OH); mass spec: 169 ($M^+ - C_4H_9$).

Assignment of Stereochemistry

Preliminary assignment of stereochemistry for the isomeric alcohols was based on melting point and nmr data. The axial alcohol was expected to have a lower melting point due to less hydrogen bonding because of steric hindrance to association. Also, the

α-methyl group of the axial alcohol (0.95 δ) was found at a higher field in the nmr than the corresponding signal of the α-methyl group in the equatorial alcohol (0.98 δ) since the α-methyl group is shielded more by the β-methyl groups in the axial alcohol.

In order to verify the assignment of stereochemistry, a shift reagent study was conducted. Nmr samples were prepared from standard solutions of pure axial and equatorial alcohols in $CDCl_3$. Small aliquots of a standard solution of $Eu(fod)_3$ (Bio-Rad) in $CDCl_3$ were added via microliter syringe. The nmr spectra were recorded for various shift reagent to alcohol ratios, and chemical shifts due to the tert-butyl group were followed for each alcohol. The data are plotted in Figure 1 and listed in Appendix 2. Because the tert-butyl and hydroxyl groups are cis in the axial alcohol and therefore would be expected to show the greater effect due to the addition of shift reagent, the compound responsible for the larger slope (0.854 compared to 0.283) was assigned to be the axial alcohol.[7] These data were compatible with the preliminary stereochemical assignment.

Attempts to obtain a single crystal of the axial alcohol for X-ray analysis failed to yield a suitable crystal. The p-bromobenzoyl ester derivative was prepared but was also unsuitable.

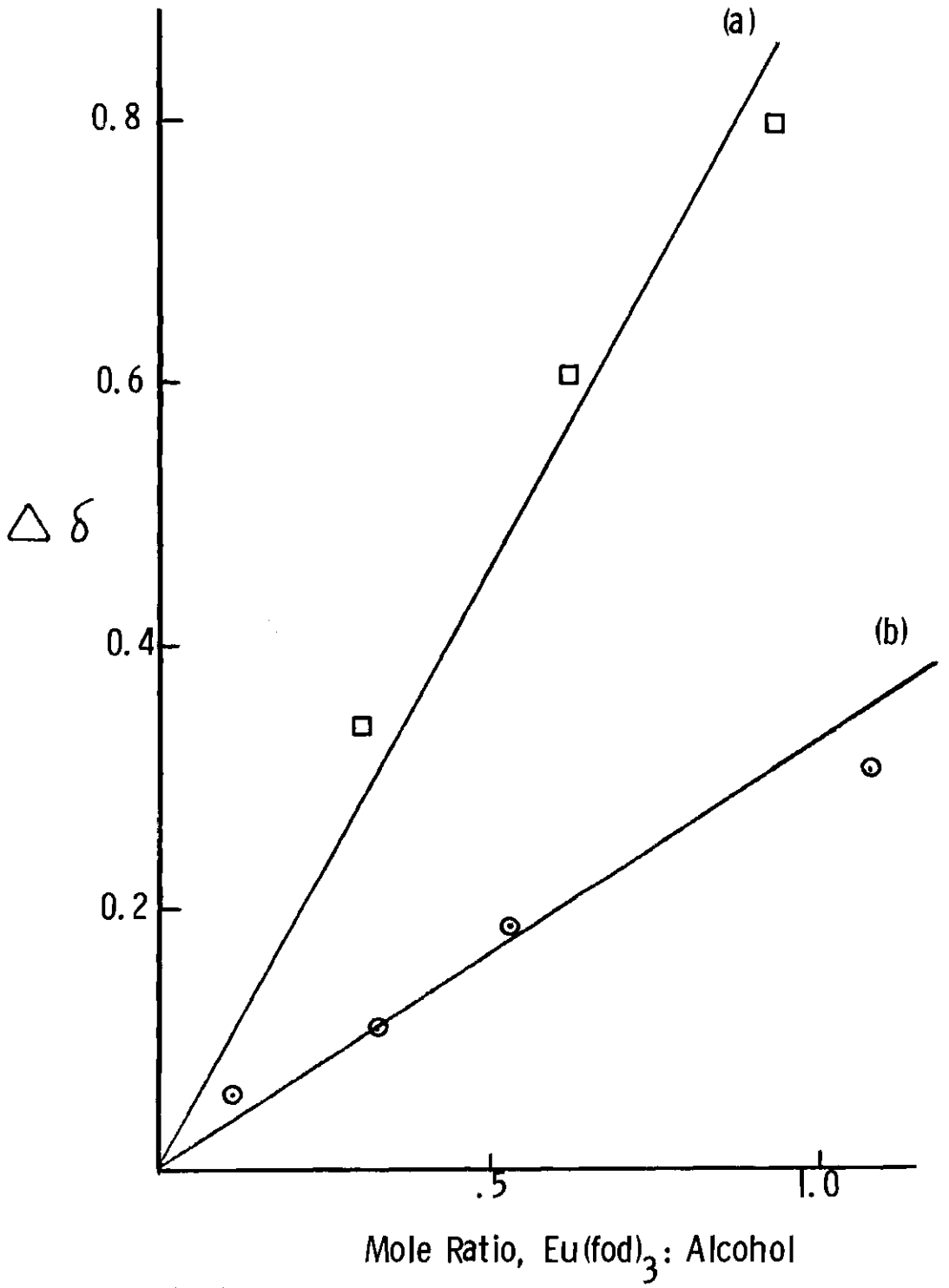

Figure 1. $Eu(fod)_3$ shift reagent study on <u>cis</u> and <u>trans</u> 1,2,2,6,6-pentamethyl-4-tert-butylcyclohexan-1-ols, (a) axial alcohol (b) equatorial alcohol.

CHAPTER III

RESULTS

The Amides

Dialkylamino (methyl) magnesium compounds,[8] CH_3MgNR_2 (where NR_2 = NPr^i_2, NPh_2, and 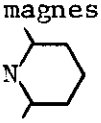), used in these studies were prepared conveniently and quantitatively by the reaction of dimethylmagnesium with an equal molar amount of the corresponding secondary amine at room temperature (eq. 1). Preparation and analysis data

$$CH_3MgCH_3 + HNPr^i_2 \xrightarrow{Et_2O} CH_3MgNPr^i_2 + CH_4 \qquad (1)$$

are summarized in Table 1.

The CH_3MgNR_2 compounds prepared by the above method were allowed to react with two representative ketones, i.e., 4-tert-butylcyclohexanone (I) representing a non-sterically hindered ketone and 2,2,6,6-tetramethyl-4-tert-butylcyclohexanone (II) representing a sterically hindered ketone. The results of these reactions are summarized in Tables 2 and 3.

The least hindered methylating agents among magnesium compounds of the type CH_3MgX are methyl Grignard and dimethylmagnesium. These compounds give 60% and 65% equatorial attack, respectively, with ketone II, in diethyl ether. It was reasoned that increasing the steric bulk of the alkylating reagent CH_3MgX would

Table 1

Preparation of Dialkylamino(methyl)magnesium Reagents[a]

Reactants		Product	Analysis (Ratio)
CH_3MgCH_3 (mmoles)	HNR_2 (mmoles)		$Mg:CH_3$
49.9	$HNPr^i_2$ 50.0	$CH_3MgNPr^i_2$	1.00:0.99
42.9	$HNPh_2$ 42.8	CH_3MgNPh_2	1.00:1.02
47.2	 47.5	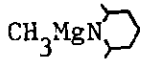	1.00:0.98

a. All reactions were carried out at room temperature in diethyl ether for one hour.

Table 2

Reactions of 4-tert-Butylcyclohexanone with Dialkylamino(methyl)magnesium Compounds[a]

Exp.	Reagent	Solvent	Additive	Relative Yield (%)[b] Axial-OH	Equatorial-OH	Yield of Alcohols (%)	Mass Balance[c] (%)
1	$CH_3MgNPr^i_2$	Et_2O	-	73	27	26.4	98.0
2	CH_3MgNPh_2	Et_2O	-	72	28	33.2	97.0
3	CH_3MgN 	Et_2O	-	71	29	10.4	57.1
4	$CH_3MgNPr^i_2$	Et_2O	$2Ph_3P$	95	5	7.5	43.2
5	CH_3MgNPh_2	Et_2O	$2Ph_3P$	100	0	3.6	33.6
6	CH_3MgN 	Et_2O	$2Ph_3P$	78	22	12.1	64.3
7	$CH_3MgNPr^i_2$	Et_2O	Ph_3P	73	27	21.9	11.7
8	CH_3MgBr	Et_2O	$2Ph_3P$	64	36	93.4	93.4
9	CH_3MgCH_3	Et_2O	$2Ph_3P$	70	30	25.0	52.2

Table 2 (contd)

Exp.	Reagent	Solvent	Additive	Relative Yield (%)[b] Axial-OH	Equatorial-OH	Yield of Alcohols (%)	Mass Balance[c] (%)
10	$CH_3MgNPr^i_2$	Et_2O	$LiClO_4$	79	21	9.7	56.4
11	CH_3MgNPh_2	Et_2O	$LiClO_4$	100	0	9.4	86.8
12	CH_3MgN 	Et_2O	$LiClO_4$	0	0	0	12.9
13	$CH_3MgNPr^i_2$	PhH	-	63	37	43.6	99.0
14	CH_3MgNPh_2	PhH	-	71	29	29.8	100
15	$CH_3MgNPr^i_2$	PhH	$2Ph_3P$	84	16	15.5	61.5
16	CH_3MgBr	Ph_2O	-	100	0	23.6	34.8
17	CH_3MgBr	Ph_2O	$2Ph_3P$	100	0	34.0	54.9
18	CH_3MgCH_3	Ph_2O	-	84	16	12.1	26.8

Table 2 (contd)

Exp.	Reagent	Solvent	Additive	Relative Yield (%)[b] Axial-OH	Equatorial-OH	Yield of Alcohols (%)	Mass Balance[c] (%)
19	CH_3MgCH_3	Ph_2O	$2Ph_3P$	91	9	15.3	31.2
20	$CH_3MgNPr^i_2$	Ph_2O	-	76	24	8.6	49.3
21	$CH_3MgNPr^i_2$	Ph_2O	$2Ph_3P$	88	12	6.0	35.7
22	CH_3MgNPh_2	Ph_2O	-	100	0	3.2	50.3
23	CH_3MgNPh_2	Ph_2O	$2Ph_3P$	100	0	3.1	57.8
24	CH_3MgN	Ph_2O	-	0	0	0	10.3
25	CH_3MgN	Ph_2O	$2Ph_3P$	0	0	0	11.2

a. The molar ratio of reagent to ketone is 1.0:1.0. Reactions were performed at room temperature.

b. Yields were determined by glpc using an internal standard.

c. The mass balance includes the yield of alcohols and recovered ketone.

Table 3

Reactions of 2,2,6,6-Tetramethyl-4-tert-butylcyclohexanone with Dialkylamino(methyl)magnesium Compounds[a]

Exp.	Reagent	Solvent	Additive	Relative Yield (%)[b] Axial-OH	Equatorial-OH	Yield of Alcohols (%)	Mass Balance[c] (%)
26	CH_3MgBr	Et_2O	-	71	29	81.0	104
27	CH_3MgCH_3	Et_2O	-	86	14	109	109
28	$CH_3MgNPr^i_2$	Et_2O	-	100	0	103	106
29	CH_3MgNPh_2	Et_2O	-	87	13	118	118
30	CH_3MgN 	Et_2O	-	97	3	95.8	103
31	CH_3MgBr	Et_2O	$2Ph_3P$	81	19	93.8	93.8
32	CH_3MgCH_3	Et_2O	$2Ph_3P$	95	5	92.1	92.1
33	$CH_3MgNPr^i_2$	Et_2O	$2Ph_3P$	100	0	80.0	89.0
34	CH_3MgNPh_2	Et_2O	$2Ph_3P$	88	12	108	108

Table 3 (contd)

Exp.	Reagent	Solvent	Additive	Relative Yield (%)[b] Axial-OH	Equatorial-OH	Yield of Alcohols (%)	Mass Balance[c] (%)
35	CH_3MgN	Et_2O	$2Ph_3P$	100	0	82.3	82.9
36	CH_3MgBr	Ph_2O	-	79	21	106	106
37	CH_3MgCH_3	Ph_2O	-	89	11	91.6	91.6
38	$CH_3MgNPr^i_2$	Ph_2O	-	100	0	98.6	98.6
39	CH_3MgNPh_2	Ph_2O	-	79	21	80.0	80.0
40	CH_3MgN	Ph_2O	-	100	0	95.2	103
41	CH_3MgBr	Ph_2O	$2Ph_3P$	90	10	104	104
42	CH_3MgCH_3	Ph_2O	$2Ph_3P$	80	20	104	104
43	$CH_3MgNPr^i_2$	Ph_2O	$2Ph_3P$	100	0	91.4	91.4

Table 3 (contd)

Exp.	Reagent	Solvent	Additive	Relative Yield (%)[b] Axial-OH	Equatorial-OH	Yield of Alcohols (%)	Mass Balance[c] (%)
44	CH_3MgNPh_2	Ph_2O	$2Ph_3P$	100	0	27.5	100
45	CH_3MgN 	Ph_2O	$2Ph_3P$	100	0	89.1	95.6

a. The molar ratio of reagent to ketone was 2.0:1.0. Reactions were performed at room temperature.

b. Yields were determined by glpc using an internal standard.

c. The mass balance includes the yield of alcohols and recovered ketone.

cause a corresponding increase in attack from the least hindered side of the ketone, namely from the equatorial side. Hence, the effect of replacing X with the bulkier dialkylamino group $R_2'N$ was studied. In the case of ketone I it was found that dialkylamino (methyl)-magnesium compounds give essentially the same results as methyl Grignard and dimethylmagnesium in diethyl ether (exp 1-3) and benzene (exp 13-14). It is apparent that the bulkiness of the dialkylamino group is too far removed from the reaction center to be effective. However, the discovery was made that the addition of two parts triphenylphosphine to one part reagent increased the steric bulk of the reagent by complexing the magnesium. For the reagents diisopropylamino (methyl) magnesium (exp 4) and diphenylamino (methyl) magnesium (exp 5) excellent stereochemical results were obtained (95 and 100% equatorial attack, respectively). For the 2,6-dimethyl-piperidine reagent (exp 6) there was only a small increase in the amount of equatorial attack with the addition of the triphenyl-phosphine indicating that the steric bulk of the reagent was only slightly affected. The 2,6-dimethyl groups probably decrease the degree of complexation by triphenylphosphine to the magnesium atom due to steric interference. When only one part triphenylphosphine was added per one part reagent, there was no increase in equatorial attack. Also, the addition of two parts triphenylphosphine to one part Grignard reagent (exp 8) or dimethylmagnesium (exp 9) had no effect on the stereochemical course of reaction. Excellent stereo-chemistry however was obtained for diphenylamino (methyl) magnesium when $LiClO_4$ was added (exp 11). The mechanism here, however, probably

involves complexation of the ketone by the lithium salt.[2]

Changing solvents from diethyl ether to benzene gives no increase in equatorial attack, but a change to diphenyl ether, a less basic and more sterically hindered ether than diethyl ether, does give more equatorial attack. For example, diphenylamino (methyl) magnesium gives 100% equatorial attack in diphenyl ether (exp 22) compared to 72% in diethyl ether (exp 2). The effect is less for diisopropylamino (methyl) magnesium (exp 20) and apparently the diphenyl ether even interferes with the ability of triphenylphosphine to complex the reagents (compare exps 21 and 4). The low yields and low mass balances obtained in all the reactions with ketone I are due to enolization followed by Aldol condensation reactions in many cases.

Clearly then, CH_3MgNPh_2 is the most stereoselective of the CH_3MgNR_2 compounds giving 100% equatorial attack when the solvent system is Et_2O- $2Ph_3P$ (exp 5), Et_2O-$LiClO_4$ (exp 11), and Ph_2O (exp 22); however, the yields are low (3.1 - 9.4%). On the other hand, CH_3MgBr in Ph_2O (exp 16) and Ph_2O-$2Ph_3P$ (exp 17) not only resulted in 100% equatorial attack, but produced much higher yields (23.6-34.0%) than the CH_3MgNR_2 compounds. Of course, less enolization is expected with the CH_3MgBr compound than for the more basic CH_3MgNR_2 reagents.

In order to study the reagents further and circumvent the problem of enolization, alkylation studies were conducted on ketone II, a nonenolizable ketone. The results are summarized in Table 3. The diisopropylamino (methyl) magnesium compound in ether

gives the best stereochemical results (exp 26 - 28, 100% axial alcohol), even without added triphenylphosphine. The addition of triphenylphosphine increases the amount of axial alcohol for the other reagents (exp 33 - 35 in ether and 43-45 in Ph_2O) including methyl Grignard and dimethylmagnesium (exp 31 - 32 and 41 - 42) as expected. In addition, changing solvent from diethyl ether to diphenyl ether also gave increased yields of axial alcohol with all reagents (exp 36-40).

Alkoxy(methyl)magnesium compounds,[10] CH_3MgOR (where OR = O— 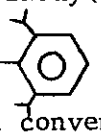 and O— 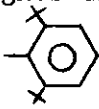), used in these studies were prepared conveniently and quantitatively by the reaction of dimethylmagnesium with an equal molar amount of the corresponding alcohol at room temperature (eq. 2, where R = Pr^i and Bu^t).

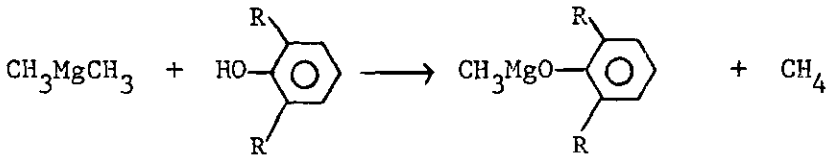

(2)

Preparation and analysis data are summarized in Table 4.

The CH_3MgOR compounds prepared as above were allowed to react with the two representative ketones, 4-tert-butylcyclohexanone (I) and 2,2,6,6-tetramethyl-4-tert-butylcyclohexanone (II). The results of these reactions are summarized in Tables 5 and 6.

The effect of replacing X in the general formula CH_3MgX with the bulkier alkoxy group OR was studied. In the case of ketone I it was found that reagent I (CH_3MgO— 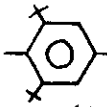) gave similar results to the methyl Grignard, and reagent II (CH_3MgO— 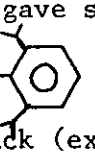) gave a modest increase in the amount of equatorial attack (exp 46-47). For

Table 4

Preparation of Methylmagnesium Alkoxides[a]

Reactants CH_3MgCH_3 (mmoles)	HOR' (mmoles)	Product		Analysis (Ratio) $Mg:CH_3$
16.0	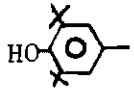 16.1	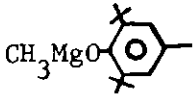	(I)	1.00:0.99
15.8	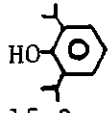 15.9	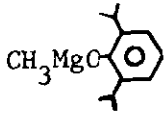	(II)	1.00:0.98

a. All reactions were carried out at room temperature in diethyl ether for one hour.

Table 5

Reactions of 4-tert-Butylcyclohexanone with Methylmagnesium Alkoxides[a]

Exp.	Reagent	Solvent	Additive	Relative Yield (%)[b] Axial-OH	Equatorial-OH	Yield of Alcohols (%)	Mass Balance[c] (%)
46	I	Et_2O	-	56	44	14.7	67.7
47	II	Et_2O	-	87	13	33.3	73.5
48	I	Et_2O	$2Ph_3P$	57	43	14.2	67.4
49	II	Et_2O	$2Ph_3P$	77	23	38.5	73.0
50	I	Ph_2O	-	0	0	0.0	0.0
51	II	Ph_2O	-	0	0	0.0	39.1
52	I	Ph_2O	$2Ph_3P$	0	0	0.0	0.0
53	II	Ph_2O	$2Ph_3P$	0	0	0.0	76.8

Table 5 (contd)

a. The molar ratio of reagent to ketone was 1.0:1.0. Reactions were performed at room temperature.

b. Yields were determined by glpc using an internal standard.

c. The mass balance includes the yield of alcohols and recovered ketone.

Table 6

Reactions of 2,2,6,6-Tetramethyl-4-tert-butylcyclohexanone with Methylmagnesium Alkoxides[a]

Exp.	Reagent	Solvent	Additive	Relative Yield (%)[b] Axial-OH	Equatorial-OH	Yield of Alcohols (%)	Mass Balance[c] (%)
54	I	Et_2O	-	94	6	94.9	94.9
55	II	Et_2O	-	100	0	88.5	95.6
56	I	Et_2O	$2Ph_3P$	89	11	107	107
57	II	Et_2O	$2Ph_3P$	100	0	98.6	98.6
58	I	Ph_2O	-	100	0	89.2	111
59	II	Ph_2O	-	100	0	71.2	89.4
60	I	Ph_2O	$2Ph_3P$	100	0	31.9	91.1
61	II	Ph_2O	$2Ph_3P$	100	0	18.5	71.8

Table 6 (contd)

a. The molar ratio of reagent to ketone was 2.0:1.0. Reactions were performed at room temperature.

b. Yields were determined by glpc using an internal standard.

c. The mass balance includes the yield of alcohols and recovered ketone.

both reagents the addition of two parts triphenylphosphine to one part reagent produced little change in the results. Previously the addition of triphenylphosphine to dialkylamino(methyl)magnesium compounds led to a substantial increase in the amount of equatorial attack presumably because the steric bulk of the reagent was increased by complexation of the magnesium by Ph_3P (exp 48-49). Changing solvent from diethyl ether to diphenyl ether (exp 50-51) resulted in the loss of all alcohol products unlike the advantageous effect found with the CH_3MgNR_2 compounds. Enolization, followed by Aldol condensation reactions, was responsible for the low yields and low mass balances.

The problem of enolization was removed by employing a nonenolizable substrate, ketone II. Excellent stereochemical results (100% axial alcohol) were obtained for reagent II in diethyl ether even without added triphenylphosphine (exp 55). Changing solvents from diethyl ether to diphenyl ether gave an increase in equatorial attack for reagent I (from 94 to 100% axial alcohol), and so both reagents I and II give 100% equatorial attack in Ph_2O. As in the case of alkylation with CH_3MgNR_2 compounds, addition of Ph_3P (exp 60-61) to ketones I and II in Ph_2O had a detrimental effect on the yield.

CHAPTER IV

DISCUSSION

It is evident from the data that the stereoselectivity of dialkylamino and alkoxy(methyl)magnesium compounds as alkylating agents depends on several factors. However, the steric requirement of the reagent seems to be the most important factor. Of course, the effectiveness of a reagent can be increased if the ketone contains a group close enough to the carbonyl group to supply some steric hindrance at the carbonyl site. Presumably for steric reasons the choice of solvent also has an influence. Diphenyl ether is a more effective solvent than diethyl ether, perhaps because the association of the reagent changes, being more associated in diphenyl ether than in diethyl ether. If indeed the degree of association of the reagent is nearly the same in both solvents or if indeed only the monomer reacts regardless of the concentration of associated species, Ph_2O solvated to the magnesium compounds would be expected to provide significantly greater steric hindrance than the reagent solvated to diethyl ether if the degree of solvation is the same. Past experience would indicate that it is the monomer that is reacting, and these results indicate that the degree of solvation of the magnesium compounds with Ph_2O and Et_2O is approximately the same.

CHAPTER V

CONCLUSIONS

The selectivity of dialkylamino(methyl)magnesium and alkoxy(methyl)magnesium compounds as alkylating agents depends on several factors. The steric requirement of the reagent is most important. However, the effectiveness of a reagent can be increased if the ketone contains a group close enough to the carbonyl group to supply some steric hindrance at the carbonyl site. A solvent effect is evident on changing from diethyl ether to diphenyl ether, a less basic and more sterically hindered ether. Diphenyl ether is a more effective solvent than diethyl ether because the association of the reagent changes, being more associated in diphenyl ether.

The ease of preparation of these alkylating reagents in addition to the excellent stereochemistry observed indicates that these dialkylamino(methyl)magnesium and alkoxy(methyl)magnesium compounds may have considerable potential as stereoselective alkylating agents. However, the reaction is limited to nonenolizable substrates.

CHAPTER VI

RECOMMENDATIONS FOR FURTHER RESEARCH

1. Preparation and characterization of dialkylphosphino-(methyl)magnesium compounds, CH_3MgPR_2.
2. Evaluation of dialkylphosphino(methyl)magnesium compounds as stereoselective alkylating reagents towards model cyclic ketones.

APPENDIX 1

GAS ANALYSIS APPARATUS

A special apparatus was designed for gas evolution analysis as shown in Figure 2.

The apparatus is an adaptation of the three-way stopcock. A number 2 T-bore stopcock is equipped with number nine O-ring joints to fit on a standard vacuum line and on standard vacuum analysis tubes. The apparatus is held together with a standard O-ring clamp. This apparatus allows solution samples to be syringed on the bench top under a nitrogen flush and then be transferred directly to the vacuum line.

The previous method involved syringing samples through a rubber septum into a vacuum analysis tube. It was then necessary to fill the vacuum line with nitrogen. The sample tube was transferred by removing the septum quickly and placing the tube on the vacuum line under a nitrogen flush.

Advantages of the new apparatus are obvious. It can also be used to take small quantities of solvent into the glove box under vacuum.

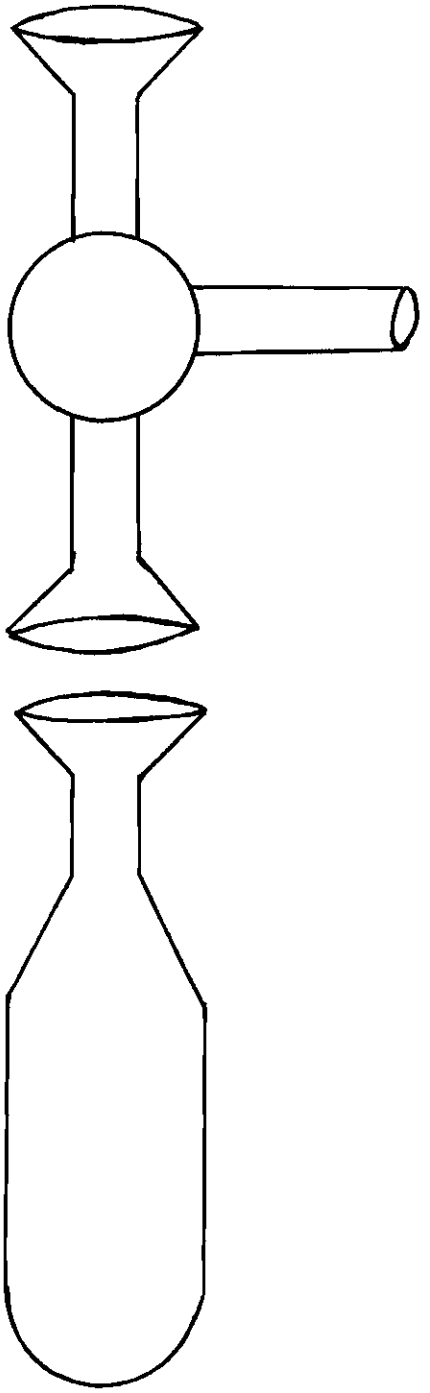

Figure 2. Gas Analysis Apparatus

APPENDIX 2

SHIFT REAGENT STUDY ON *cis* AND *trans* (AXIAL AND EQUATORIAL) 1,2,2,6,6-PENTAMETHYL-4-t-BUTYLCYCLOHEXAN-1-OL

Axial Alcohol

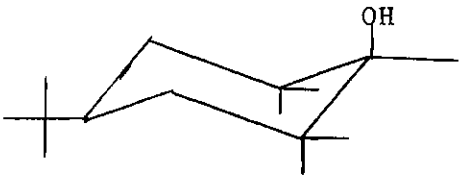

Run No.	Ratio mole $Eu(fod)_3$/mole Alcohol	Bu^t (δ)	Δδ
1	0	0.848	0
2	0.308	1.185	0.337
3	0.617	1.450	0.602
4	0.925	1.638	0.790

Equatorial Alcohol

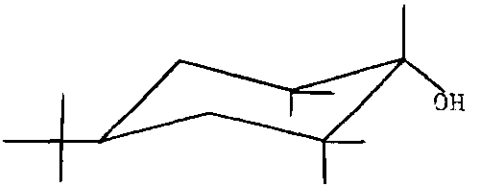

Run No.	Ratio mole $Eu(fod)_3$/mole Alcohol	Bu^t (δ)	Δδ
1	0	0.853	0
2	0.107	0.885	0.032
3	0.322	0.966	0.113
4	0.537	1.035	0.182
5	1.074	1.155	0.302

LITERATURE CITED*

1. E. C. Ashby and J. T. Laemmle, Chem. Rev., 75, 521 (1975).

2. E. C. Ashby, J. J. Lin and J. J. Watkins, Tetrahedron Letters, 20, 1709 (1977).

3. E. C. Ashby, J. J. Lin and A. B. Goel, J. Org. Chem., (in press).

4. D. R. Shriver, "The Manipulation of Air Sensitive Compounds," McGraw-Hill, New York, 1969.

5. C. N. Reilly, R. W. Schmid, and F. S. Sadek, J. Chem. Educ., 36, 619 (1959).

6. E. C. Ashby and R. Arnott, J. Organometal. Chem., 14, 1 (1968).

7. (a) P. V. Demarco, T. K. Elzey, R. B. Lewis, and E. Wenkert, J. Am. Chem. Soc., 92, 5734 (1970).

   (b) P. Belanger, C. Freppel, D. Tizane and J. C. Richer, Can. J. Chem., 49, 1985 (1971).

8. (a) G. E. Coates, M. L. H. Green and K. Wade, "Organometallic Compounds," Vol. 1, Meuthen and Co., London, 1967.

   (b) J. Nackashi, Ph.D. Thesis, Georgia Institute of Technology, 1974.

9. H. O. House and W. L. Respess, J. Org. Chem., 30, 201 (1965).

10. (a) G. E. Coates, M. L. H. Green, and K. Wade, "Organometallic Compounds," Vol. 1, Meuthen and Co., London, 1967.

    (b) J. P. Oliver, Ph.D. Thesis, Georgia Institute of Technology (in progress).

    (c) E. C. Ashby, J. Nackashi, and G. E. Parris, J. Am. Chem. Soc., 97, 3162 (1975).

*Journal title abbreviations used are listed in "List of Periodicals," Chemical Abstracts, (1961).

PART II

THERMAL DECOMPOSITION OF THE ALKOXIDES AND AMIDES OF MAGNESIUM, ZINC, AND ALUMINUM

CHAPTER I

INTRODUCTION

Background

In Part I the alkoxides and amides of magnesium were evaluated as stereoselective alkylating reagents. It was during this study that their thermal instability was observed quite by accident. Part II is concerned with the systematic DTA-TGA study of the thermal decomposition of the alkoxides and amides of magnesium, zinc, and aluminum. Emphasis is placed on kinetic and stereochemical data. This new thermal decomposition reaction is evaluated as a synthetic method for converting an alcohol or amine to an olefin.

Several methods are known for the dehydration of alcohols to olefins.[1] These methods include the pyrolysis of esters of carboxylic acids[2] and the pyrolysis of xanthates (the Chugaev reaction).[3] Both reactions involve a syn elimination to produce an olefin. The pyrolysis of esters occurs at 300-600°C, usually in the vapor phase. The yields are reasonable, but carbon skeleton rearrangements can occur due to the high temperature. The Chugaev reaction occurs at 100-250°C, but preparation of the xanthate may proceed in low yield. The pyrolysis product is often contaminated with sulfur containing impurities which are usually removed by distillation from sodium metal with an accompanying decrease in yield.

Part II concerns a new type of thermal decomposition reaction that compares favorably with the above mentioned reactions and offers an alternative method of dehydrating alcohols to olefins.

Several methods are known for the preparation of olefins from amines. These methods include the pyrolysis of quaternary ammonium hydroxides[4] (Hoffman elimination reaction) and the pyrolysis of amine oxides[5] (Cope elimination reaction). The Hoffman elimination reaction involves the thermal decomposition of a quaternary ammonium hydroxide to give an olefin, a tertiary amine, and water. The reaction usually occurs by an E_2 mechanism in an anti stereochemical manner. The yield is very dependent upon the particular compound being decomposed. An average yield might be in the range 50 to 75%. The disadvantages of the Hoffman elimination reaction include (1) the necessity of having a tertiary amine in order to convert it to the quaternary ammonium hydroxide, (2) separation of the olefin product from the tertiary amine and water by-products, and (3) a competing side reaction to produce an alcohol and tertiary amine due to a displacement reaction at the carbon atom.

The Cope elimination reaction involves the thermal decomposition of tertiary amine oxides to yield an olefin and a derivative of hydroxylamine in a syn stereochemical manner. The amine oxides are prepared by treating the tertiary amine with 35% aqueous hydrogen peroxide at room temperature or with stronger reagents as 40% peroxyacetic acid and monoperoxyphthalic acid. It is necessary to destroy excess peroxide before the pyrolysis is performed. The yields and disadvantages of this method of deaminating

amines to olefins are similar to those of the Hoffman eliminiation reaction.

Part II concerns a new type of deamination reaction that compares favorably with the above mentioned reactions and offers an alternative method of converting secondary amines to olefins.

The by-product from the decomposition of the magnesium amides is a yellow solid with empirical formula $(MgNR')_x$. Preliminary investigation indicated that this material potentially represents a new class of pseudo-aromatic compounds. The exact nature of this material is examined by spectroscopic methods.

Isothermal kinetic data was collected on the alkoxides and amides of magnesium by DTA-TGA. However, this procedure is tedious and requires a relatively large amount of material. The accuracy of the results could be questionable since the sample undergoes considerable reaction in being raised to the required temperature. In order to determine the accuracy of the isothermal kinetic data and to better understand the mechanism of the thermal decomposition of the magnesium alkoxides and amides in the solid state, a non-isothermal kinetic study of these decomposition reactions was undertaken in Part II also.

Purpose

There are several goals of the research described in Part II of this thesis. The primary purpose is to investigate the thermal decomposition of the alkoxides and amides of magnesium, zinc, and aluminum. This investigation involves a DTA-TGA study with emphasis

on stereochemical and kinetic data. Evaluation of the reaction as a synthetic method of converting an alcohol or secondary amine to an olefin is also studied. Determination of the nature of the residue $(MgNR')_x$ from the decomposition of the magnesium amides was another important goal. Finally, a non-isothermal kinetic study is performed in order to check the accuracy of activation parameters calculated using isothermal kinetic data and to provide additional information concerning the mechanism of the thermal decomposition reaction in the solid state.

CHAPTER II

EXPERIMENTAL

General

Apparatus

All operations were performed under a nitrogen atmosphere using either a nitrogen-filled glove box equipped with a special recirculating system to remove oxygen and moisture[6] or on the bench using Schlenk tube techniques.[7] Glassware was flash flamed and flushed with dry nitrogen prior to use. DTA-TGA analyses were performed on a Mettler thermoanalyzer II equipped to run under vacuum.[8] Powdered amide or alkoxide samples were loaded into a cylindrical aluminum crucible with fritted disk and cap (preheated to 250° and cooled to room temperature) in the glove box using a vibrator to insure uniform particle size when possible. Samples were transferred to the DTA-TGA machine under nitrogen and were heated at 4°C per minute at 10^{-6} mm Hg from 25° to 450°C and at a six inches per hour chart speed (Appendix 1). Infrared data was collected on a Perkin Elmer Model 621 Grating Infrared Spectrograph. Ultraviolet-visible spectra were obtained on a Cary Model 14 uv-visible spectrometer, and nmr spectra were obtained on a Varian A-60 nmr spectrometer. Ebuillioscopic molecular weight data was obtained by the method of Walker and Ashby.[9] Cryoscopic molecular weight data was collected by the method of Salzberg.[10]

Analyses

Gas analyses were carried out by hydrolyzing samples with

hydrochloric acid or methanol on a standard vacuum line equipped with a Toepler pump.[7] Magnesium and zinc were determined by EDTA titration at pH 10 using Eriochrome Black T as the indicator.[11] Aluminum was determined by reaction with excess EDTA and back titration with zinc acetate at pH 4 using dithiazone as an indicator. GLPC analyses were performed on an F and M Model 720 gas chromatograph.

Materials

Diethyl ether (Fisher Anhydrous Reagent Grade) was distilled from $LiAlH_4$ (Ventron) prior to use. Tetrahydrofuran and benzene (Fisher Certified Reagent Grade) were distilled from $NaAlH_4$ (Ventron). n-Dodecane (Eastman) was predried over NaOH and fractionally distilled. Toluene (Fisher) was distilled from CaH_2. Dimethylmercury, diphenylmercury, and dibenzylmercury were obtained commercially (Orgmet). Magnesium (Ventron chips), zinc (Baker Analyzed Reagent, granular), and aluminum (Alcoa Grade 101 Atomized Powder) were dried by flash flaming under vacuum before use.

Cyclohexanol (Fisher), cyclohexyl methyl ketone (Chemical Samples), cyclohexanone (Matheson, Coleman, and Bell), 1-octanol (Fisher), phenol (Baker), diisopropylamine (Aldrich), and N,N-dimethylaniline (Columbia Organic Chemicals) were distilled prior to use. Ethanol (Fisher) was dried via a benzene azeotrope, and isopropanol (Baker) was distilled from triisopropoxyaluminum. 2-Phenyl-1-ethanol (Eastman) was distilled from CaH_2 at reduced pressure, and benzophenone (Fisher) was sublimed under vacuum. 1,1-Diphenyl-1-ethanol (Eastman), t-butanol (Fisher), trans-2-phenylcyclohexanol (Aldrich), cis-2-methylcyclohexanol (Aldrich), triphenylphosphine (Eastman) and d_6-ethanol

(Pfaltz and Bauer) were used without further purification.

Diethylamine (Baker), di-n-propylamine, isopropylbenzylamine, p-anisidine, methylphenethylamine (Aldrich), di-n-butylamine, dicyclohexylamine, N-ethylaniline (Eastman), t-butylamine, piperdine (Fisher), N-ethyl-1-naphthylamine (Eastman), and di-sec-butylamine (Pfaltz and Bauer) were predried over NaOH and fractionally distilled. Diphenylamine (Fisher) and 1-adamantanamine (Aldrich) were used without further purification.

Preparation of Dialkyl and Diarylmagnesium Compounds

Dimethylmagnesium. Magnesium chips (20 g., 0.833 mole) were rinsed with diethyl ether and placed in a 1-liter flask with a three-way stopcock and egg-shaped stirring bar. The magnesium and apparatus were evacuated, flame heated, and purged with dry nitrogen. Dimethylmercury (30 ml, 0.400 mole) was added and the reaction mixture was allowed to stir at 25°C for 48 hours until the magnesium became white and powder-like. The flask was placed under vacuum for fifteen minutes to remove any unreacted dimethylmercury. The dimethylmagnesium was extracted with diethyl ether and filtered through a fritted filter funnel in the glove box. The active methyl to magnesium ratio = 2.02:1.00.

Diphenylmagnesium. Diphenylmagnesium was prepared from diphenylmercury in a similar manner to the dimethylmagnesium preparation except that the solid-solid reaction mixture was heated at 140°C. Ratio phenyl to magnesium = 2.04:1.00.

Dibenzylmagnesium.[12] To a dry 1-liter flask equipped with a three-way stopcock and stirring bar was added magnesium (19.5 g.,

0.882 mole,flame dried under vacuum), dibenzylmercury (25.0 g., 0.065 mole),and diethyl ether (400 ml). The reaction mixture was stirred for 26 hours under a nitrogen atmosphere. Ratio benzyl to magnesium = 1.98:1.00.

Preparation of Active Magnesium Hydride in THF

When 15.0 mmoles of $LiAlH_4$ solution in diethyl ether (30 ml) was added dropwise to a magnetically well-stirred solution of Et_2Mg (15.0 mmoles) in diethyl ether (35 ml), an exothermic reaction occurred and an immediate precipitate appeared. This reaction mixture was allowed to stir for one hour at room temperature followed by centrifugation of the insoluble white solid. The supernatant solution was separated by syringe and the insoluble white solid was washed with diethyl ether three to four times and finally made a slurry in THF. The analysis of this slurry showed that it contained a magnesium to hydrogen ratio = 1.00:2.02.

Preparation of Dimethyl and Diphenyl Zinc

Dimethylzinc. Dimethylzinc was prepared by the procedure of Noller.[13] Methyl iodide (Fisher) was dried over anhydrous $MgSO_4$ and distilled prior to use. Zinc-copper couple was obtained from Alfa Inorganics. The reaction of zinc-copper couple with methyl iodide was allowed to proceed overnight, and the dimethylzinc was distilled from the reaction mixture at atmospheric pressure under nitrogen. The neat dimethylzinc was diluted with diethyl ether to facilitate handling. Ratio methyl to zinc = 2.10:1.00.

Diphenylzinc.[14] To a 500-ml flask equipped with a reflux condenser and three-way stopcock sidearm was added granular zinc

(23.2 g.,0.355 mole, dried by flaming under vacuum), diphenylmercury (20.0 g.,0.056 mole), and toluene (100 ml). The reaction mixture was refluxed 39 hours. The solution was cooled and analyzed. Ratio phenyl to zinc = 2.03:1.00.

Preparation of Trimethyl- and Triphenylaluminum

Trimethylaluminum is commercially available (Ethyl Corp.) and was diluted with diethyl ether to facilitate handling. The ratio of methane: aluminum = 2.97:1.00.

Triphenylaluminum.[15] To a 500 ml flask equipped with a reflux condenser and a three-way stopcock sidearm was added powdered aluminum (12.3 g.,0.456 mole, dried by flaming under vacuum), diphenylmercury (21.9 g.,0.062 mole), and toluene (120 ml). The reaction mixture was refluxed 39 hours. The supernatant solution gave a phenyl:aluminum ratio = 3.05:1.00.

Preparation of Zinc Hydride

The method of Schlesinger[16] was used to prepare zinc hydride. $(CH_3)_2Zn$ was added to $LiAlH_4$ in 1:2 ratio in diethyl ether solution. The resultant precipitate of zinc hydride was removed by filtration. The ratio of hydrogen:zinc = 1.95:1.00.

Preparation of Alane and Bisdiisopropylaminoalane

Alane (AlH_3) was prepared from $LiAlH_4$ and 100% sulfuric acid in THF according to the procedure of Brown.[17] Bisdiisopropylaminoalane, $HAl(NPr^i_2)_2$, was prepared from AlH_3 and diisopropylamine in 1:2 ratio. Alane in THF was cooled to -78°, and the amine added. The reaction mixture was allowed to warm to room temperature with stirring. The THF was removed by vacuum distillation, and benzene added. The ratio

of hydrogen: aluminum = 1.00:1.00.

The Alkoxides

Preparation of threo 1,2-Diphenyl-1-propanol[18]

Threo-1,2-diphenyl-1-propanol was prepared by the reaction of phenyl magnesium bromide with 2-phenylpropanol (Aldrich).

A three-neck 500 ml flask was equipped with a reflux condenser, an addition funnel, a stirring bar, and a three-way stopcock. Magnesium (15.2 g., 0.626 moles) was added and the apparatus flamed under vacuum. The apparatus was purged with dry nitrogen, and diethyl ether (250 ml) added. Bromobenzene (Aldrich) (98.0 g., 0.624 mole) was then added dropwise to prepare the corresponding Grignard reagent. 2-Phenylpropanol (67.0 g., 0.550 mole) was diluted with diethyl ether (100 ml) and added dropwise to the phenylmagnesium bromide cooled in an ice bath. The reaction was quenched by hydrolysis with saturated ammonium chloride solution followed by diethyl ether extraction of the aqueous layer. The diethyl ether was dried over $MgSO_4$ and distilled at reduced pressure to yield an oily residue. The oil distilled at 137-139°C at 4 mm Hg to give 79.7 g. (75.2% yield) of crude threo-1,2-diphenyl-1-propanol (17% erythro isomer present).

The crude threo alcohol (79.7 g.,0.376 mole) and freshly prepared p-nitrobenzoylchloride (70.0 g.,0.377 mole) were dissolved in pyridine (150 ml) and heated on a steam bath for two hours. A precipitate formed. The slurry was poured onto ice and 20% H_2SO_4. The solid material was separated from the aqueous layer. The solid p-nitrobenzoyl ester was dissolved in ethyl acetate and dried over $MgSO_4$.

The p-nitrobenzyl ester was crystallized from the ethyl acetate to give 52.4 g. (0.145 mole, 38.6% yield), mp = 143-144°C (Lit. 143-144°C).[18]

The purified p-nitrobenzoyl ester (52.4 g., 0.145 mole), KOH (8.1 g.), NaOH (5.8 g.), methanol (104 ml), and H_2O (104 ml) were refluxed for 12 hours. The aqueous layer was extracted with diethyl ether. The diethyl ether was dried over $MgSO_4$ and distilled under vacuum to give an oil. The oil was distilled at 139-142° at 6 mm Hg (Lit. 136-137°C at 1-2 mm[18]) to give 27.1 g. (89.9% yield) threo-1,2-diphenyl-1-propanol. Analysis: nmr ($CDCl_3$): 1.22δ (d, 3H, CH_3), 2.25δ (d, 1H, OH), 3.00δ (p, 1H), 4.62δ (d, 1H), 7.08δ (d, 10H, Ph); mass spec: 212 (M^+), 107, 106, 77 m/e.

Preparation of Erythro - 1,2-Diphenyl-1-propanol[19]

Erythro-1,2-Diphenyl-1-propanol was prepared in three steps from d,l-benzoin.

A 1-liter three-neck flask was equipped with a solid addition tube, stirring bar, a reflux condenser, and a three-way stopcock. d,l-Benzoin (Aldrich, 38.6 g.,0.181 mole) was added slowly to CH_3MgI (100 g. MeI, 18.0 g. Mg,0.704 mole) in diethyl ether (500 ml) cooled in an ice bath. Then the mixture was refluxed three hours, cooled to 25°C, and quenched with NH_4Cl saturated solution. The diethyl ether layer was decanted and the aqueous layer washed with diethyl ether. The diethyl ether extracts were combined, dried over $MgSO_4$, filtered, and the ether removed under vacuum to give a yellow solid. The crude glycol product, $Ph(CH_3)COHCH(OH)Ph$, was crystallized from CS_2 (33.6 g., 80.9% yield), mp = 103-104°C; ir: strong obs. at 3400 cm^{-1}. The glycol (32.0 g.,0.140 mole) was added to H_2SO_4 (200 ml) at 0°C over

a period of one hour with constant stirring and then at 25°C for two hours. The material was poured onto 1000 g. ice and then extracted with diethyl ether. The diethyl ether was dried over $MgSO_4$ and reduced under vacuum to give an oil which slowly crystallized (26.6 g., 90.0% yield). The solid ketone product, $PhC(H)CH_3COPh$, was crystallized from cold ethanol to give white, fluffy crystals (4.0 g., 13.5% yield, mp = 49-50°C; Lit. 49-51°C).[19b]

A 500-ml three-neck flask was equipped with an addition funnel, stirring bar, reflux condenser, and three-way stopcock. To the pot was added $LiAlH_4$ (0.094 mole) in diethyl ether. The ketone, $PhC(H)CH_3COPh$, (0.298 mole) in diethyl ether was added dropwise, and the solution refluxed for 30 minutes. The reaction was quenched with a saturated solution of NH_4Cl. The aqueous layer was extracted with diethyl ether which was then dried over $MgSO_4$, filtered, and distilled under vacuum to give an oil. The oil was crystallized from pentane to give white needles (30.2 g., 47.8% yield), mp = 50-52°C (Lit. 50-51°C[18]); nmr ($CDCl_3$): 1.05δ (d, 3H, CH_3), 1.87δ (s, 1H, OH), 2.01δ (p, 1H), 4.62δ (d, 1H), and 7.27δ (d, 10H, Ph); mass spec: 212 (M^+), 197, 77 m/e.

Preparation of d_6-Isopropanol

d_6-Acetone (Fisher, 10.0 g.,0.190 mole) was placed in a 50-ml flask and $LiAlH_4$ (0.0474 mole) in 95 ml diethyl ether was added at room temperature. The reaction mixture was stirred for one hour, quenched with a minimum amount of water, and filtered. The filtrate was dried over $MgSO_4$ and the ether removed by distillation. The d_6-isopropanol was distilled at 80-82° under nitrogen to give 3.91 g (34.3% yield).

General Preparation of an Alkoxide

The general method for the preparation of an alkoxide is illustrated for methylmagnesium cyclohexyloxide.

A dry, weighed 100-ml flask was fitted with a rubber septum cap, purged with dry nitrogen and fitted with a needle connected to a nitrogen bubbler. A measured quantity of cyclohexanol was added to the flask via syringe and the flask reweighed (0.498 g.,4.98 mmoles). Then the flask was cooled to -78°C, and the calculated amount of dimethylmagnesium diethyl ether solution (5.02 mmole) added via syringe. The flask was warmed to 25°C and a solid formed with corresponding evolution of methane. The septum was replaced with a three-way stopcock, and the diethyl ether distilled under vacuum. The solid methylmagnesium cyclohexyloxide was transferred to the glove box for further manipulation and analysis. The ratio of magnesium: methane:cyclohexanol = 1.00:1.00:0.96.

General Methods of Decomposition

(a) Decomposition in the Solid State

The decomposition of diphenylaluminum 1,1-diphenyl-1-ethoxide illustrates the method of decomposing a solid alkoxide. In the glove box a 50 mg sample of the alkoxide is loaded into a 10-ml flask connected to an apparatus consisting of a dry ice cold finger and three-way stopcock. The apparatus is removed from the glove box and evacuated. The flask is immersed in a Woods' metal bath preheated to 270-275° for five minutes. The olefin, 1,1-diphenylethene, distills onto the dry ice cold finger from which it is washed with diethyl ether for glpc analysis after the addition of a suitable

internal standard.

(b) Decomposition in n-dodecane diluent

The decomposition of methylmagnesium 1,1-diphenyl-1-ethoxide represents the general method for the decomposition of an alkoxide in n-dodecane diluent. In the glove box a 100 mg sample of alkoxide is transferred to a 25-ml flask equipped with a reflux condenser and rubber septum. On the bench n-dodecane (10 ml) is added via syringe and the reaction mixture refluxed for 24 hours. The reaction mixture is then quenched with a saturated solution of NH_4Cl and extracted with ether. The ether layer is dried over $MgSO_4$ and analyzed by glpc. The aqueous layer is analyzed for magnesium to determine the yield.

Decomposition of 1,1-Diphenyl-1-ethoxy Magnesium Bromide

1,1-Diphenyl-1-ethanol (2.19 g., 0.0111 mmole) was placed in a 50-ml flask equipped with a stirring bar, reflux condenser, and three-way stopcock. Methyl magnesium bromide (0.0111 mole) in diethyl ether was added slowly. The solution was stirred 30 minutes, the diethyl ether removed under vacuum, and n-dodecane (4 ml) and N, N-dimethylaniline (1 ml) were added. The solution was refluxed 24 hours, quenched with a saturated solution of NH_4Cl and extracted with diethyl ether. The diethyl ether was washed with NaOH solution, dried over $MgSO_4$ and analyzed by glpc. The aqueous layer was analyzed for magnesium to determine the yield (89.6%).

Decomposition of Methylmagnesium threo and erythro-1,2-Diphenyl-1-propoxide

Methylmagnesium threo-1,2-diphenyl-1-propoxide (50 mg) and excess triphenylphosphine (200 mg) were placed in a dry 10-ml flask

equipped with a dry ice cold finger and three-way stopcock. The apparatus was evacuated, and the flask placed in a Woods' metal bath preheated to 270-275°C. The cis-1,2-diphenyl-1-propene product distilled onto the cold finger and was rinsed off with diethyl ether for glpc analysis after addition of the internal standard.

A similar experiment was performed on the methylmagnesium erythro-1,2-diphenyl-1-propoxide to produce trans-1,2-diphenyl-1-propene.

The Amides

Preparation of Threo-1,2-Diphenyl-1-Propylaniline

Threo-1,2-diphenyl-1-propylaniline was prepared in two steps from erythro-1,2-diphenyl-1-propanol.

The erythro alcohol $PhCHCH_3CHPhOH$[19] was converted to the brosylate by the following procedure. A solution of the erythro alcohol (8.8 g.) in 150 ml dry pyridine was cooled to -3°C, and 12.5 g. p-bromobenzenesulfonyl chloride was added such that the temperature was kept below 0°C. The solution was stored at 0°C for six days. At that time the mixture was poured onto ice and water. The solid that separated was filtered and combined with the benzene extract of the aqueous layer. The benzene solution was washed with water, ice-cold 10% H_2SO_4, water again, $NaHCO_3$ solution, and then water again. The benzene solution was dried over anhydrous $MgSO_4$ and reduced in volume. Pentane was added to give a solid (4.7 g., 26.5% yield, mp = 71-72°C; Lit. 80-81°C).[19d]

The erythro brosylate[19] (12.4 g.) and freshly distilled aniline (2.60 ml aniline, 10:1 excess) were dissolved in 300 ml benzene and refluxed for 20 hours. The benzene solution was filtered to remove the white solid and then concentrated under vacuum. HCl was bubbled through the solution to form a white solid which was removed by filtration. The benzene solution was treated with HCl gas again and the resultant solid collected. The HCl salt was dissolved in water, made basic, and diethyl ether extracted. The ether layer was dried over anhydrous $MgSO_4$ and reduced in volume. The threo-$PhCHCH_3CHPhNHPh$ was crystallized three times from ether to give 0.6 g. material (7.2% yield), mp 118-119° (Decomposition). Anal. Calcd. for $C_{21}H_{21}N$: C, 87.76; H, 7.37; N, 4.87; Found: C, 87.54; H, 7.45; N, 4.81; nmr in $CDCl_3$: 1.20δ (d, 3H, CH_3), 3.07δ (m, 1H), 4.38δ (d, 1H), 7.27δ (m, 15H); ir in nujol: 3400 cm^{-1} (NH), 1600, 750, 695 cm^{-1} (Ph); mass spec: 287 (M^+), 182, 105, 77 m/e. A mixture of threo and erythro anilines gave a methyl doublet at 1.23δ (threo) as well as a methyl doublet at 1.10δ (erythro).

This mixture of anilines was prepared in two steps from a mixture of erythro and threo-1,2-diphenyl-1-propanols.

The method of Shetty[20a] was used to convert the alcohols to the corresponding formamides. Typically, 9.4 g. (145 mmole) KCN was added slowly to 13.5 ml HOAc at 0°C with stirring. Then 14.5 ml H_2SO_4 in 13.5 ml HOAc was added, and the ice bath was removed. Over a period of 10 minutes 26.5 g. of a mixture of erythro and threo-1,2-diphenyl-1-propanols was added. The mixture was stirred 15 minutes, cooled, and diluted with 100 ml water. The aqueous layer was made

basic and diethyl ether extracted. The ether layer was dried over $MgSO_4$, filtered, and reduced under vacuum to give an oil which later solidified (22.9 g., crude yield = 77%). The formamide mixture was treated with pentane to remove unreacted alcohols and olefin by-products. The resultant insoluble material $PhCHCH_3CHPhNHCHO$ was crystallized from $EtOAc/Et_2O$ mixtures to give a white solid. Analysis gave: mp 122-132°C; mass spec: 239 (M^+), 134, 105, 77 m/e; nmr in $CDCl_3$: erythro methyl doublet at 1.15δ and threo methyl doublet at 1.35δ, ratio 2:1.

By repeated crystallizations from $EtOAc/Et_2O$ mixtures pure erythro-$PhCHCH_3CHPhNHCHO$ was isolated (5% yield). Analysis gave: mp 148-149°C; Calcd. for $C_{16}H_{17}NO$: C, 80.30; H, 7.16; N, 5.85. Found: C, 80.18; H, 7.20; N, 5.80; mass spec: 239 (M^+), 134, 105, 77 m/e; ir in nujol: 3220 (NH), 1660 (CO), 760, 700 (Ph) cm^{-1}; nmr in $CDCl_3$: 1.15δ (d, 3H, CH_3), 3.15δ (m, 1H), 5.20δ (t, 1H), 7.22δ (m, 10H). Base catalyzed hydrolysis of the pure erythro formamide gave erythro-1,2-diphenyl-1-propylamine. Analysis gave: mp 123-124°C (lit. 127°C)[20b] mass spec: 106, 105, 77 m/e; nmr in $CDCl_3$: methyl doublet at 1.02δ.

A sample of erythro and threo formamides (3.2 g., 13.5 mmole), 2.3 g. K_2CO_3, 2.0 ml PhBr, and a trace of CuI were refluxed in 10 ml nitrobenzene for 18 hours.[21] Excess solvent was then steam distilled out, and the residue was fractionally distilled under vacuum. The first fraction (0.3 g., 7.7% yield, bp 155-165°C) consists of a mixture of erythro and threo-1,2-diphenyl-1-propylanilines contaminated with cis and trans-1,2-diphenylpropene. Analysis gave: mass spec: 194 (M^+, olefin), 182, 105, 77 m/e; nmr in $CDCl_3$: erythro methyl

doublet at 1.10δ and threo methyl doublet at 1.23δ.

Thus, the assignment of the stereochemistry of threo-$PhCHCH_3CHPhNHPh$ could be questioned since it was based on comparisons of the nmr spectrum of a mixture of isomers to that for one pure isomer.

Preparation of Isopropylaniline[22]

Sodium borohydride (10 g., excess) was added to a mixture of 4.7 ml aniline (50 mmole), 13.5 g. sodium acetate trihydrate, 42 ml acetic acid, 125 ml water, 30 ml ethanol, and 10 ml (excess) acetone, at 0°C with stirring. The solution was made basic with NaOH, and the aqueous layer was extracted with diethyl ether. The ether extract was dried over anhydrous $MgSO_4$ and reduced under vacuum to give 5.7 g. oil (crude yield = 84.4%). The oil was distilled under nitrogen (bp = 199-200°C; lit. 198-207[23]). Anal. Calcd. for $C_9H_{13}N$: C, 79.96; H. 9.69; N, 10.35. Found: C, 79.80; H, 9.71; N, 10.31; nmr in $CDCl_3$: 1.18δ (d, 6H, CH_3), 3.47δ (m, 2H, NH + CH) and 6.88δ (m, 5H, Ph), ir (neat): 3410 cm^{-1} (NH), 1600, 1505, 750, 690 cm^{-1} (Ph); n_D^{25} = 1.5458 (lit. 1.5298, 1.5331[24]); mass spec: 135 (M^+), 120 (M^+-CH_3), 93, 77, 42 m/e.

Preparation of d_6-Isopropylaniline

The procedure for the preparation of isopropylaniline was repeated substituting d_6-acetone for acetone. The resultant oil (yield = 76.8%) was distilled under nitrogen (bp = 199-201°). The per cent isotopic purity was determined by mass spectroscopy comparison to the deuterated isopropylaniline and was found to be 99 atom %. Anal. Calcd. for $C_9H_7D_6N$: C, 77.03. Found: C, 76.55; nmr in $CDCl_3$:

3.35δ (s, 1H, NH), 3.49δ (s, 1H, CH), and 6.85δ (m, 5H, Ph); ir (neat): 3200 cm^{-1} (NH), 1510, 655, 595 cm^{-1} (Ph); n_D^{25} = 1.5390; mass spec: 141 (M^+), 123 (M^+ $-CD_3$), 94, 77 m/e.

Preparation of d_6-Isopropylbenzylamine

The procedure for the preparation of isopropylaniline was repeated substituting d_6-acetone and 5.46 ml (50 mmole) benzylamine. The resultant oil (crude yield = 66.1%) was distilled under nitrogen (bp = 193-194°C). The percent isotopic purity was determined by mass spectroscopy comparison to the nondeuterated isopropylbenzylamine and was found to be 93.6 atom %. Anal. Calcd. for $C_9H_7D_6H$: C, 76.99. Found: C, 77.38; nmr in $CDCl_3$: 1.28δ (s, 2H, CH_2), 3.75δ (s, 1H, NH), 3.82δ (s, 1H, CH), and 7.27δ (s, 5H, Ph); ir (neat): 3300 cm^{-1} (NH), 2120 cm^{-1} (CD), 1665, 1605, 1495, 735, 700 cm^{-1} (Ph), n_D^{25} = 1.5269; mass spec: 155 (M^+), 137 (M^+ $-CD_3$), 108, 91, 77 m/e.

General Preparation of an Amide

The general method for the preparation of an amide is illustrated for diisopropylamino(phenyl)magnesium.

A dry, weighed 100-ml flask is fitted with a rubber septum cap, purged with dry nitrogen and fitted with a needle connected to a nitrogen bubbler. A measured quantity of diisopropylamine is added to the flask via syringe and the flask is reweighed (0.402 g., 3.98 mmoles). Then the flask is cooled to -78°C and the calculated amount of diphenylmagnesium diethyl ether solution (4.00 mmole) is added via syringe. The flask is warmed to 25°C and a solid forms with corresponding formation of benzene. The septum is replaced with a three-way stopcock and the solvent is distilled out under

vacuum. The solid diisopropylamino(phenyl)magnesium is transferred to the glove box for further manipulation and analysis. Ratio magnesium:benzene:diisopropylamine:diethyl ether = 1.00:1.03:0.93:0.89.

General Methods of Decomposition

(a) Decomposition in the Solid State. The method of decomposing amides in the solid state is illustrated for the thermal decomposition of threo-1,2-diphenyl-1-propylanilino(methyl) magnesium.

Threo-1,2-diphenyl-1-propylanilino(methyl)magnesium and excess triphenylphosphine were placed in a dry 10-ml flask equipped with a dry ice cold finger and three-way stopcock. The apparatus was evacuated, and the flask was placed in a Woods' metal bath preheated to 270-275°C. The cis-1,2-diphenylpropene product distilled onto the cold finger and was removed by rinsing with diethyl ether for glpc analysis after addition of the internal standard. The pot was analyzed for magnesium to determine the yield (75%).

(b) Decomposition in n-Dodecane Diluent. The decomposition of an amide in n-dodecane diluent is illustrated for diethylamino (methyl)magnesium.

The reagent (4.3 mmole) is prepared in the usual manner in a 100-ml flask equipped with a Teflon sidearm stopcock, magnetic stirring bar, and reflux condenser with a three-way stopcock. The diethyl ether solvent is removed under vacuum, and 25 ml n-dodecane is added via syringe. The apparatus is connected via the three-way stopcock to a gas evolution apparatus designed to collect evolved gases at atmospheric pressure. The n-dodecane solution is refluxed with stirring for three hours, and the evolved gases measured. The

quantitative yield is 8.6 mmoles gases identified as a mixture of methane and ethylene by mass spectroscopy.

The Magnazines

The general method for the preparation of an N-substituted magnazine is illustrated for N,N',N''-tricyclohexylmagnazine. A 250-ml flask equipped with a Teflon three-way sidearm stopcock, a stirring bar, a reflux condenser, and a nitrogen bubbler is flash flamed under vacuum and filled with dry nitrogen. A measured quantity of dicyclohexylamine is added to the flask via syringe (15.0 ml, 76.5 mmole). Then the flask is cooled to -78°C, and the calculated amount of dimethylmagnesium in diethyl ether solution (76.5 mmole) is added via syringe. The flask is warmed to 25° and a white solid forms with corresponding evolution of methane. A sample of the slurry is now removed for analysis. Ratio magnesium to methane to dicyclohexylamine = 1.00:0.97:1.02.

The diethyl ether is now removed under vacuum, and 50 ml n-dodecane is added. The slurry is refluxed 24 hours to produce an insoluble yellow solid. The solid is collected by filtration and washed with diethyl ether in the glove box. Analysis gave % Mg = 20.2 (TH = 20.0) and a $Mg/H_2N\text{-}C_6H_{11}$ ratio equal to 1.00:1.04.

CHAPTER III

RESULTS

The Alkoxides

Magnesium, zinc, and aluminum alkoxides[25] are prepared quantitatively by the reaction of a suitable alkyl or aryl metal compound with an alcohol. This general reaction is illustrated by equations 1 - 3.

$$(CH_3)_2Mg + Ph_2\text{-}\overset{\overset{CH_3}{|}}{C}OH \longrightarrow CH_3MgO\overset{\overset{CH_3}{|}}{C}Ph_2 + CH_4 \qquad (1)$$

$$Ph_2Zn + i\text{-}PrOH \longrightarrow PhZnOPr^i + PhH \qquad (2)$$

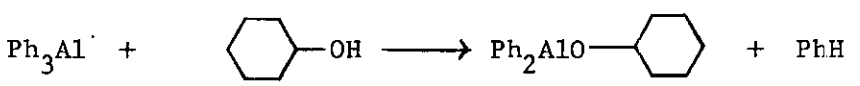

$$Ph_3Al + \bigcirc\!\!-OH \longrightarrow Ph_2AlO\!\!-\!\!\bigcirc + PhH \qquad (3)$$

Details of the preparation are given in the experimental section and are summarized in Tables 1 - 3. Then, in a second step, the alkoxide is thermally decomposed as illustrated in reactions 4 - 6.

$$CH_3MgO\overset{\overset{CH_3}{|}}{C}Ph_2 \xrightarrow{\Delta} CH_4 + Ph_2C = CH_2 + MgO \qquad (4)$$

Table 1. Preparation of Magnesium Alkoxides

Reactants (mmole)		Reaction	Analysis (%)				Analysis (Ratio)				Product
MgR_2	R'OH	Time (h.)	Mg :	R :	R'O :	Solvent	Mg :	R :	R'O :	Solvent	
MgH_2 (5.00)	i-PrOH (4.97)	16	22.8	0.92	56.0	20.3	1.00 :	0.98 :	1.01 :	0.30	$HMgOPr^i \cdot 0.30$ THF
(4.52)	t-BuOH (4.55)	20	18.3	0.73	56.6	24.4	1.00 :	0.97 :	1.03 :	0.45	$HMgOBu^t \cdot 0.45$ THF
(5.45)	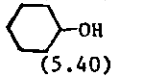 (5.40)	24	19.1	0.82	77.2	2.84	1.00 :	1.04 :	6.95 :	0.05	HMgO- 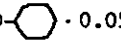 · 0.05 THF
(4.76)	$PhCH_2CH_2OH$ (4.75)	20	11.0	0.46	54.3	34.3	1.00 :	1.02 :	0.99 :	1.03	$HMgOCH_2CH_2Ph \cdot 1.03$ THF
$Mg(CH_3)_2$ (5.00)	EtOH (4.95)	1	28.8	17.8	53.4	0.0	Mg 1.00 :	CH_3 1.11 :	OEt 0.95 :	Et_2O 0.00	CH_3MgOEt
(5.01)	i-PrOH (4.95)	0.5	25.7	14.9	59.4	0.0	1.00 :	0.94 :	0.95 :	0.00	CH_3MgOPr^i
(5.00)	t-BuOH (5.00)	0.5	21.3	13.3	65.3	0.0	1.00 :	1.01 :	1.02 :	0.00	CH_3MgOBu^t
(5.00)	Octyl-OH (5.09)	1	13.8	8.5	73.5	4.2	1.00 :	0.98 :	1.02 :	0.10	$CH_3MgOOct \cdot 0.10\ Et_2O$
(5.02)	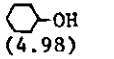 (4.98)	0.5	18.1	11.2	70.8	0.0	1.00 :	1.00 :	0.96 :	0.00	CH_3MgO- 
(5.00)	$PhCH_2CH_2OH$ (5.05)	0.5	15.1	6.95	76.6	0.0	1.00 :	0.89 :	1.02 :	0.00	$CH_3MgOCH_2CH_2Ph$
(4.98)	$Ph_2C{=}O$ (5.00)	0.5	7.84	4.89	62.9	24.4	1.00 :	1.01 :	0.99 :	1.02	$CH_3MgO-C(CH_3)Ph_2 \cdot 1.0\ Et_2O$
(5.00)	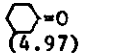 (4.97)	0.5	16.2	9.73	74.0	0.0	1.00 :	0.97 :	0.98 :	0.00	CH_3MgO- 

Table 1. Preparation of Magnesium Alkoxides (Continued)

(24.5)	threo $PhCHCH_3CHPhOH$ (24.6)	0.5	8.15	4.43	75.0	12.4	1.00 : 0.88 : 1.06 : 0.50	threo $PhCHCH_3CHPhOMgCH_3 \cdot 0.50\ Et_2O$
(11.3)	erythro $PhCHCH_3CHPhOH$ (11.2)	0.5	8.48	5.87	72.2	13.4	1.00 : 1.12 : 0.98 : 0.52	erythro $PhCHCH_3CHPhOMgCH_3 \cdot 0.52\ Et_2O$
(5.00)	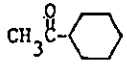 (5.02)	0.5	12.1	7.5	70.6	9.8	1.00 : 0.98 : 0.99 : 0.27	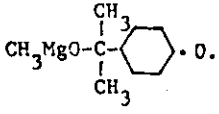 $\cdot 0.27\ Et_2O$
(6.79)	trans 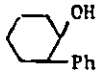 (6.78)	1	8.9	5.5	64.4	21.2	1.00 : 0.69 : 0.95 : 0.78	trans 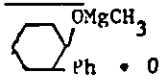 $\cdot 0.78\ Et_2O$
(3.00)	cis 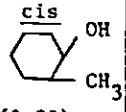 (3.02)	1	17.8	11.0	71.2	0.0	1.00 : 0.95 : 0.99 : 0.00	cis 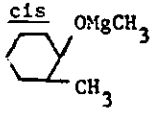
(5.07)	 (10.02)	24(60°)	10.9	0.0	89.1	0.0	1.00 : 0.00 : 1.95 : 0.00	$Mg(O$ 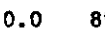 $)_2$
(14.92)	PhOH 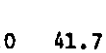 (14.90) (14.92)	12(66°)	10.2	0.0	41.7	39.1 9.0	1.00 : 0 : 1.00 : .99 : .30	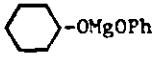 $\cdot 0.30$ THF
Ph_2Mg (5.00)	EtOH (5.05)	1	16.1	51.1	29.9	3.9	1.00 : 0.99 : 1.02 : 0.06	$PhMgOEt \cdot 0.06\ Et_2O$
(4.02)	i-PrOH (4.02)	1	14.1	44.7	34.3	6.9	1.00 : 1.02 : 1.02 : 0.16	$PhMgOPr^i \cdot 0.16\ Et_2O$
(9.70)	$PhCH_2CH_2OH$ (9.65)	2	10.9	35.1	54.1	0.0	1.00 : 1.02 : 1.00 : 0.00	$PhMgOCH_2CH_2Ph$

Table 1. Preparation of Magnesium Alkoxides (Continued)

(4.64)	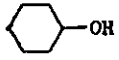 (4.62)	1	6.4	20.4	26.3	46.9	1.00 : 0.97 : 1.01 : 2.39	PhMgO- 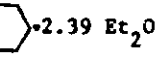 ·2.39 Et_2O
(3.07)	$Ph_2\overset{CH_3}{\overset{\vert}{C}}OH$ (3.09)	1	6.4	20.1	51.5	22.0	1.00 : 0.94 : 0.99 : 1.14	$PhMgO-\overset{CH_3}{\overset{\vert}{C}}Ph_2 \cdot 1.14\ Et_2O$
$Mg(CH_2Ph)_2$ (1.74)	EtOH (1.75)	1	12.4	46.5	23.0	18.1	1.00 : 0.95 : 0.97 : 0.48	$PhCH_2MgOEt \cdot 0.48\ Et_2O$
(3.17)	i-PrOH (3.19)	1	11.3	42.2	27.3	19.2	1.00 : 0.99 : 1.01 : 0.56	$PhCH_2MgOPr^i \cdot 0.56\ Et_2O$
(3.30)	 (3.25)	1	8.7	32.6	35.4	23.3	1.00 : 0.95 : 0.98 : 0.88	$PhCH_2MgO$-  ·0.88 Et_2O
(2.85)	$Ph_2\overset{CH_3}{\overset{\vert}{C}}OH$ (2.89)	1	6.0	22.5	48.7	22.8	1.00 : 1.16 : 1.05 : 1.25	$PhCH_2MgO-\overset{CH_3}{\overset{\vert}{C}}Ph_2 \cdot 1.25\ Et_2O$
$Ph_2\overset{CH_3}{\overset{\vert}{C}}OMgCH_3$ (10.0)	$HNPr^i_2$ (39.0)	48(66°)	5.8	23.7	46.6	23.9	1.00 : 0.95 : 0.97 : 1.00	$Ph_2\overset{CH_3}{\overset{\vert}{C}}OMgNPr^i_2 \cdot 1.00\ HNPr^i_2$
$(CH_3)_2Mg$ (5.24)	$(CD_3)_2CHOH$ (5.24)	1	24.7	15.3	60.0	0.0	1.00 : 1.02 : 0.99 : 0.00	$CH_3MgOCH(CD_3)_2$
Ph_2Mg (8.41)	$(CD_3)_2CHOH$ (8.43)	1	12.5	39.5	41.5	6.5	1.00 : 0.98 : 1.04 : 0.17	$PhMgOCH(CD_3)_2 \cdot 0.17\ Et_2O$
$(PhCH_2)Mg$ (3.77)	$(CD_3)_2CHOH$ (3.77)	1	10.8	40.5	36.2	12.5	1.00 : 0.98 : 1.03 : 0.38	$PhCH_2MgOCH(CD_3)_2 \cdot 0.38\ Et_2O$

Table 2. Preparation of Zinc Alkoxides

Reactants (mmoles) R_2Zn	R'OH	Reaction Time (h.)	Analysis (%) Zn	R	R'O	Solvent	Analysis (Ratio) Zn	R	R'O	Solvent	Product
ZnH_2 (4.03)	 (4.00)	24	33.4	0.5	50.6	15.5	1.00	0.94	1.00	0.42	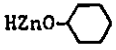 · 0.42 THF
Me_2Zn (4.50)	i-PrOH (4.48)	2	43.3	9.9	39.1	7.7	1.00	0.99	1.01	0.16	CH_3ZnOPr^i · 0.16 THF
(5.72)	 (5.82)	24 (40°)	31.5	7.2	47.7	13.6	1.00	0.71	0.95	0.39	CH_3ZnO-  · 0.39 THF
(6.21)	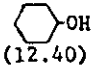 (12.40)		24.8	0.0	75.2	0.0	1.00	0.00	2.02	0.00	$Zn(O$-  $)_2$
(4.25)	$Ph_2\overset{CH_3}{\overset{\vert}{C}}OH$ (4.20)	2	23.6	4.0	72.2	0.0	1.00	0.77	1.02	0.00	$CH_3ZnO-\overset{CH_3}{\overset{\vert}{C}}Ph_2$
Ph_2Zn (4.35)	EtOH (4.30)	3	34.9	41.1	24.0	0.0	1.00	1.05	0.95	0.00	PhZnO-Et
(3.70)	i-PrOH (3.70)	2	32.5	38.2	29.3	0.0	1.00	1.01	0.99	0.00	$PhZnOPr^i$
(3.68)	t-BuOH (3.65)	3	30.4	35.7	33.9	0.0	1.00	1.02	0.99	0.00	$PhZnOBu^t$
(5.15)	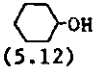 (5.12)	24	27.1	31.9	41.0	0.0	1.00	0.95	0.97	0.00	PhZnO- 
(3.52)	$Ph_2\overset{CH_3}{\overset{\vert}{C}}OH$ (3.50)	2	16.9	19.9	51.0	12.2	1.00	1.03	1.01	0.65	$PhZnO-\overset{CH_3}{\overset{\vert}{C}}Ph_2$ · 0.65 THF
(4.37)	$(CD_3)_2CHOH$ (4.38)	1	29.3	34.5	36.2	0.0	1.00	0.98	0.99	0.00	$PhZnOCH(CD_3)_2$
	CD_3CD_2OH										

Table 3. Preparation of Aluminum Alkoxides

Exp. No.	Reactants (mmoles) R_3Al	R'OH	Reaction time (h.)	Analysis (%) Al : R : R'O : Solvent	Analysis (ratio) Al : R : R'O : Solvent	Product
1	Me_3Al (4.25)	HO-⬡ (4.20)	2	15.5 17.2 56.7 10.6	1.00 : 1.70 : 1.05 : 0.25	Me_2AlO-⬡ · 0.25 Et_2O
2	Ph_3Al (2.36)	$HoPr^i$ (2.32)	3	10.2 58.1 22.3 9.4	1.00 : 2.04 : 1.04 : 0.34	Ph_2AlOPr^i · 0.34 Et_2O
3	(3.12)	HO-⬡ (3.10)	10	8.5 48.6 31.2 11.7	1.00 : 2.02 : 0.95 : 0.50	Ph_2AlO-⬡ · 0.50 Et_2O
4	(2.75)	$HOC(CH_3)Ph_2$ (2.72)	3	5.2 29.8 38.2 26.8	1.00 : 2.10 : 1.02 : 1.87	Ph_2AlO-$C(CH_3)Ph_2$ · 1.87 Et_2O
5	$HAl(NPr^i_2)_2$ (4.04)	$Ph_2C(CH_3)OH$ (4.05)	1	5.4 40.0 39.5 15.1	1.00 : 1.92 : 0.98 : 0.97	$Ph_2C(CH_3)OAl(NPr^i_2)_2$ · 0.97 PhH

$$PhZnOPr^{i} \xrightarrow{\Delta} PhH + CH_3-\overset{H}{\overset{|}{C}}=CH_2 + ZnO \qquad (5)$$

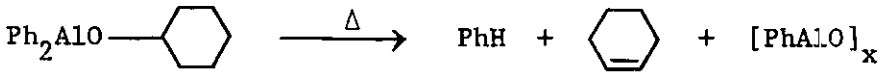

(6)

The products are hydrocarbon, olefin, and metal oxide.

DTA- TGA Data[26]

The decomposition reaction was studied by DTA - TGA (differential thermal analysis - thermogravimetric analysis). These data are summarized in Tables 4 - 6. Samples of alkoxides were decomposed under vacuum at 4°C per minute from 25° to 450°C. Typical DTA - TGA curves are shown in Figures 1 - 3. The DTA - TGA curves have several common characteristics i.e., the decomposition is endothermic, coordinated solvent is lost first, and then the main decomposition occurs in one step with no apparent intermediate formed. Both condensable and non-condensable evolved gases are detected and analysis of the product after decomposition indicates that the residue is the corresponding metal oxide.

Some of the compounds studied were volatile. Sublimation of the alkoxides was especially predominant for the dimethylaluminum alkoxides and some of the alkoxides of magnesium and zinc (mainly the isopropoxides and tert-butoxides). An additional problem encountered was the disproportionation of methylzinc alkoxides during preparation (30% disproportionation for methylzinc cyclohexyloxide).

Table 4. Thermal Decomposition of Magnesium Alkoxides

Compound (sample wt., mg)	Thermometric Change	Range of Transition (peak max.), °C	wt. loss mg (%)	Evolved Gas
CH_3MgOEt (18.9)	Endo	165 - 200 (185)	14.0 (74.1)	$CH_4 + CH_2 = CH_2$ sublimation
$PhMgOEt \cdot 0.06\ Et_2O$	Endo	60 - 140 (100)	1.5 (3.3)	Et_2O
(45.1)	Endo	260 - 440 (315)	30.0 (66.5)	$PhH + CH_2 = CH_2$
$PhCH_2MgOEt \cdot 0.48\ Et_2O$	Endo	65 - 175 (140)	8.2 (18.1)	Et_2O
(45.4)	Endo	190 - 355 (270)	28.3 (62.3)	$PhCH_3 + CH_2 = CH_2$
$HMgOPr^i \cdot 0.30\ THF$	Endo	60 - 140 (90)	3.3 (10.6)	THF
(31.1)	Endo	140 - 275	3.9 (12.5)	THF + some H_2
	Endo	275 - 366 (340)	11.9 (38.3)	$H_2 + CH_3CH = CH_2$
CH_3MgOPr^i (27.5)	Endo	200 - 280 (215)	25.0 (90.9)	$CH_4 + CH_3CH = CH_2$ sublimation
$PhMgOPr^i \cdot 0.16\ Et_2O$	Endo	50 - 140 (95)	3.9 (6.7)	Et_2O
(58.1)	Endo	225 - 425 (310)	38.6 (66.4)	$PhH + CH_3CH = CH_2$
$PhCH_2MgOPr^i \cdot 0.56\ Et_2O$	Endo	45 - 157 (95)	16.0 (20.3)	Et_2O
(79.0)	Endo	205 - 350 (290)	44.5 (56.3)	$PhCH_3 + CH_3CH = CH_2$
$HMgOBu^t \cdot 0.45\ THF$	Endo	50 - 180 (115)	10.2 (21.2)	THF
(48.2)	Endo	180 - 275	4.2 (8.7)	THF + H_2
	Endo	275 - 365 (335)	18.9 (39.2)	$H_2 + (CH_3)_2C = CH_2$
CH_3MgOBu^t (96.7)	Endo	110 - 235 (195)	91.8 (94.9)	$CH_4 + (CH_3)_2C = CH_2$ sublimation

Table 4. Thermal Decomposition of Magnesium Alkoxides (Continued)

$CH_3MgOOct^n \cdot 0.10\ Et_2O$ (97.2)	Endo	220	82.0 (84.4)	sublimation only
HMgO-⬡ · 0.05 THF (62.3)	Endo	60 - 170 (105)	1.8 (2.9)	THF
	Endo	255 - 430 (375)	42.0 (67.4)	H_2 + ⬡
CH_3MgO-⬡ (39.2)	Endo	225 - 380 (340)	28.5 (72.7)	CH_4 + ⬡
PhMgO-⬡ · 2.39 Et_2O (66.2)	Endo	50 - 200 (105)	25.0 (37.8)	Et_2O
	Endo	200 - 395 (345)	28.0 (42.3)	PhH + ⬡
$PhCH_2MgO$-⬡ · 0.88 Et_2O (90.2)	Endo	55 - 190 (120)	21.0 (23.3)	Et_2O
	Endo	245 - 400 (335)	53.0 (58.8)	$PhCH_3$ + ⬡
$HMgOCH_2CH_2Ph$ · 1.03 THF (46.9)	Endo	45 - 160 (95)	13.7 (29.2)	THF
	Endo	205 - 290 (270)	0.5 (10.7)	H_2
	Endo	290 - 385 (315)	22.0 (46.9)	$PhCH = CH_2$
$CH_3MgOCH_2CH_2Ph$ (54.6)	Endo	90 - 335 (270)	41.2 (75.5)	CH_4 + $PhCH = CH_2$
$PhMgOCH_2CH_2Ph$ (51.0)	Endo	35 - 180 (105)	15.0 (29.4)	PhH
	Endo	190 - 330 (255)	23.3 (45.7)	$PhCH = CH_2$
$CH_3MgOCPh_2 \cdot 1.0\ Et_2O$ (54.2)	Endo	100 - 185 (160)	12.5 (23.1)	Et_2O
	Endo	185 - 345 (270)	33.7 (62.2)	$CH_4 + Ph_2C = CH_2$
$(i\text{-}Pr)_2N(CH_3)MgOCPh_2 \cdot 1.0\ HNPr^i_2$ (51.1)	Endo	140 - 215 (205)	15.5 (30.3)	$HNPr^i_2$
	Endo	215 - 340 (270)	31.0 (60.7)	$HNPr^i_2 + Ph_2C = CH_2$
$PhMgO-C(CH_3)Ph_2 \cdot 1.14\ Et_2O$ (78.1)	Endo	40 - 170 (85)	17.5 (22.4)	Et_2O
	Endo	170 - 435 (270)	60.6 (77.6)	$PhH + Ph_2C = CH_2$

Table 4. Thermal Decomposition of Magnesium Alkoxides (Continued)

$PhCH_2MgOC(CH_3)Ph_2 \cdot 1.25\ Et_2O$ (100.6)	Endo	55 - 180 (105)	23.0 (22.9)	Et_2O
	Endo	180 - 360 (260)	65.0 (64.6)	$PhCH_3 + Ph_2C = CH_2$
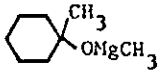 (58.6)	Endo	230 - 340 (300)	44.0 (75.1)	CH_4 + 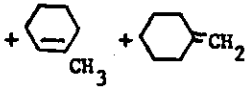
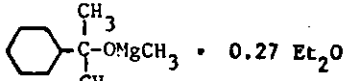 (45.0)	Endo	50 - 175 (105)	4.5 (10.0)	Et_2O
	Endo	175 - 360 (290)	32.5 (72.2)	CH_4 + 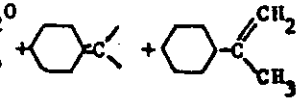
trans 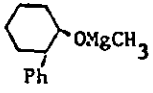 $\cdot$ 0.78 THF (74.4)	Endo	50 - 195 (125)	15.5 (20.8)	THF
	Endo	230 - 405 (330)	49.0 (65.9)	CH_4 + 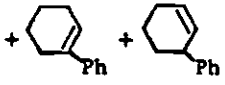
cis 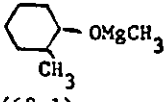 (68.1)	Endo	260 - 405 (305,345)	50.2 (73.7)	CH_4 + 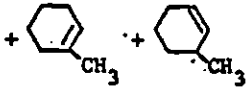
threo $PhCHCH_3CHPhOMgCH_3 \cdot 0.5\ Et_2O$ (40.8)	Endo	50 - 145 (95)	2.0 (5.0)	Et_2O
	Endo	185 - 260 (235)	8.2 (20.0)	CH_4
	Endo	260 - 400 (350)	24.7 (60.6)	cis 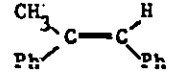
erythro $PhCHCH_3CHPhOMgCH_3 \cdot 0.5\ Et_2O$ (36.9)	Endo	45 - 135 (85)	4.8 (13.0)	Et_2O
	Endo	205 - 310 (240)	26.9 (72.9)	CH_4 + trans 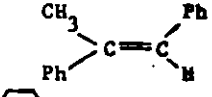
$Mg(O-C_6H_{11})_2$ (48.1)	Endo	40 - 400 (340)	41.1 (85.4)	H_2 + 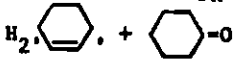

Table 4. Thermal Decomposition of Magnesium Alkoxides (Continued)

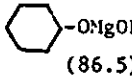 -OMgOPh · 0.30 THF (86.5)	Endo	50 - 190 (95)	7.8 (9.0)	THF
	Endo	190 - 370 (315)	38.4 (44.4)	 =O
	Endo	370 - 465	16.8 (19.4)	H_2 plus unknown product
$PhMgOCH(CD_3)_2$ · 0.17 Et_2O (91.0)	Endo	50 - 165 (100)	6.5 (7.1)	Et_2O
	Endo	165 - 390 (310)	58.0 (63.7)	$PhD + CD_2CH = CD_3$
$PhCH_2MgOCH(CD_3)_2$·0.38 Et_2O (88.3)	Endo	40 - 160 (85)	11.0 (12.5)	Et_2O
	Endo	160 - 390 (290)	58.0 (65.7)	$PhD + CD_2 = CHCD_3$
$CH_3MgOCH(CH_3)_2$[a] (38.0)	Endo	200 - 485 (305)	22.5 (59.2)	$CH_4 + CH_2 = CHCH_3$
$CH_3MgOCH(CD_3)_2$[a] (49.1)	Endo	245 - 480 (350)	29.0 (59.1)	$CH_3D + CD_2CHCD_3$

a - under static Argon atmosphere

Table 5. Thermal Decomposition of Zinc Alkoxides

Compound (sample wt., mg)	Thermometric Change	Range of Transition (Peak Max.), °C	wt. loss mg (%)	Evolved Gas
PhZnOEt (51.2)	Endo	160 - 430 (255)	20.5 (40.0)	PhH
$CH_3ZnOPr^i \cdot 0.16$ THF (66.2)	Endo	50°	54.0 (81.6)	Sublimation only
$PhZnOPr^i$ (32.7)	Endo	110 - 340 (230°)	19.5 (59.6)	PhH + $CH_2 = CHCH_3$
$PhZnOBu^t$ (64.2)	Endo	60 - 278 (200)	26.2 (40.8)	PhH
	Endo	278 - 465	4.6 (7.2)	$CH_2 = C(CH_3)_2$
HZnO-⬡ · 0.42 THF (47.8)	Endo	35 - 105 (75)	4.5 (9.4)	THF
	Endo	105 - 205 (150)	0.5 (1.0)	H_2
	Endo	205 - 380 (290)	23.0 (48.1)	⬡
$7\,CH_3ZnO$-⬡ · 0.39 THF + 0.3 Zn(O-⬡)$_2$ (58.4)	Endo	50 - 215 (150)	11.0 (18.8)	THF
	Endo	215 - 325 (295)	9.0 (15.4)	CH_4 + ⬡
	Endo	325 - 415 (385)	23.0 (39.4)	H_2, ⬡, ⬡=O
PhZnO-⬡ (100.3)	Endo	195 - 340 (310)	64.5 (64.3)	PhH + ⬡
$CH_3ZnO-C(CH_3)-Ph_2$ (71.2)	Endo	55 - 360 (265)	49.0 (68.8)	$CH_4 + Ph_2CCH_2$

Table 5. Thermal Decomposition of Zinc Alkoxides (Continued)

$PhZnOC(CH_3)Ph_2$ (49.6)	Endo	45 - 125 (75)	6.0 (12.1)	THF
	Endo	198 - 340 (260)	33.1 (66.7)	$PhH + Ph_2C = CH_2$
$Zn(O-C_6H_{11})_2$ (42.3)	Endo	310 - 408 (382)	28.9 (68.3)	H_2, 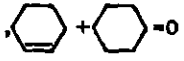
$PhZnOCH(CD_3)_2$[a] (45.2)	Endo	115 - 485 (265)	27.5 (60.8)	$PhD + CD_2 = CHCD_3$
$PhZnOCD_2CD_3$ (45.3)	Endo	180 - 340 (220)	25.5 (56.3)	$PhD + CD_2 = CD_2$

a - under static Argon atmosphere

Table 6. Thermal Decomposition of Aluminum Alkoxides

Compound (sample wt., mg)	Thermometric Change	Range of Transition (peak max.), °C	Wt. loss mg (%)	Evolved gas
$(CH_3)_2AlO$-⬡ (68.7)	Endo	80°	68.7 (100)	Sublimation only
$Ph_2AlOPr^i \cdot 0.34\ Et_2O$ (31.1)	Endo	60 - 102 (90°)	3.0 (9.7)	Et_2O
	Endo	145	25.0 (80.4)	Sublimation only
Ph_2AlO-⬡ $\cdot 0.50\ Et_2O$ (69.6)	Endo	50 - 165 (110)	8.1 (11.6)	Et_2O
	Endo	195 - 375 (285)	35.7 (51.3)	PhH + ⬡
$Ph_2AlOC(CH_3)Ph_2 \cdot 1.87\ Et_2O$ (108.1)	Endo	55°	94.0 (87.0)	sublimation only
$Ph_2C(CH_3)$-$OAl(NPr^i_2) \cdot 0.97$ PhH (92.8)	Endo	55 - 100 (85)	14.0 (15.1)	PhH
	Endo	110 - 460 (225)	61.5 (66.3)	$NHPr^i_2 + Ph_2C = CH_2$

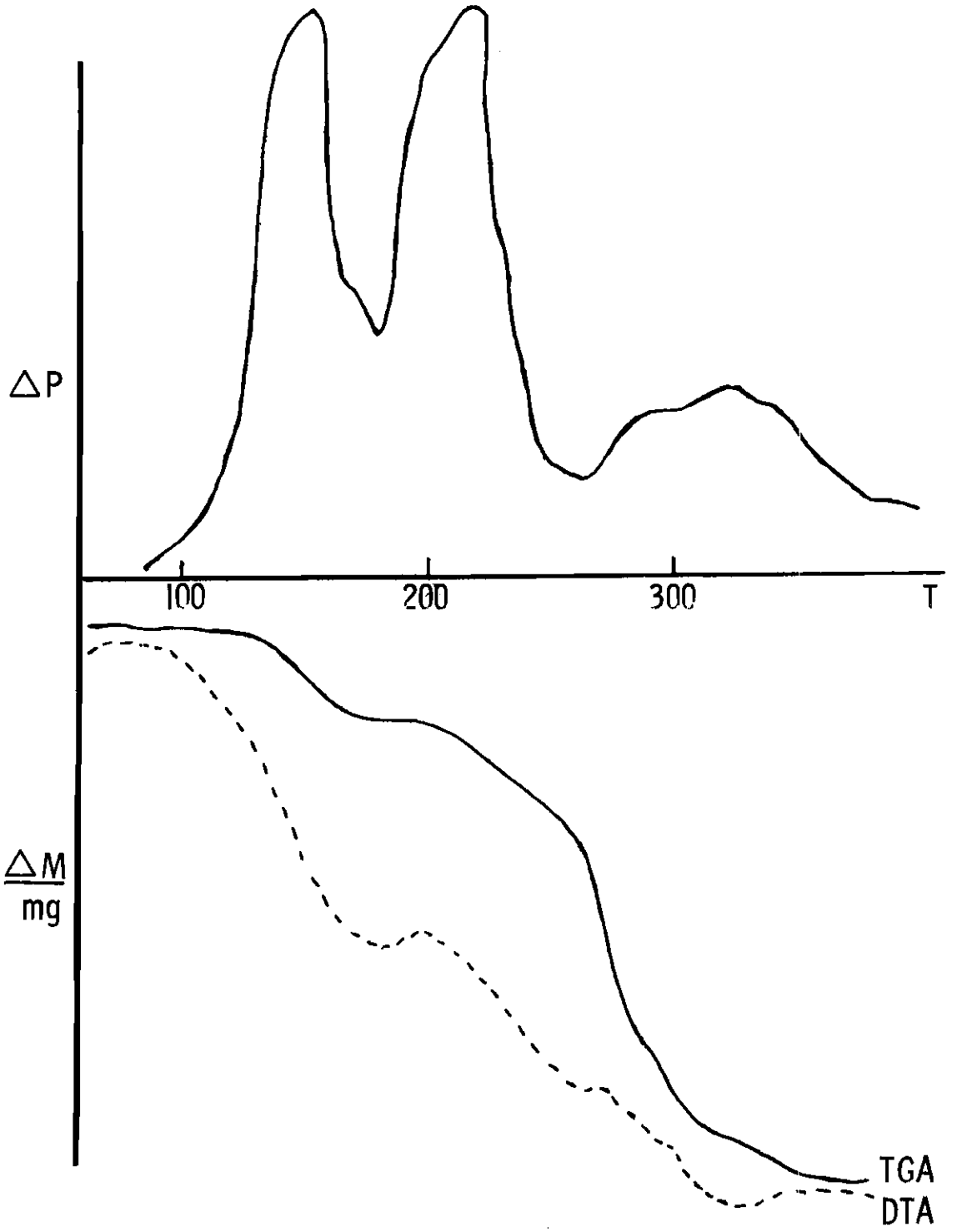

Figure 1. Vacuum DTA-TGA of $CH_3MgOC(CH_3)Ph_2 \cdot 1.0\ Et_2O$

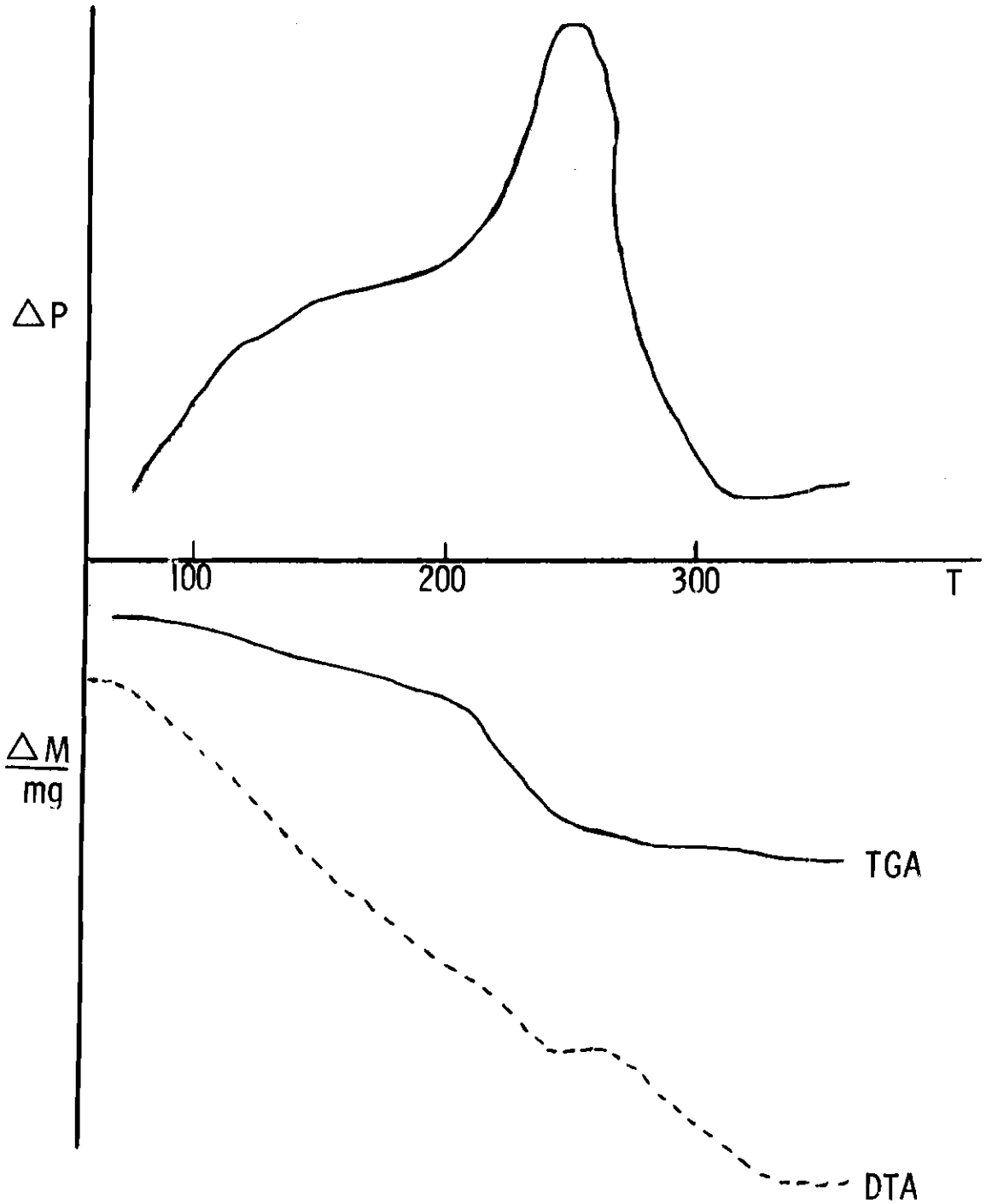

Figure 2. Vacuum DTA-TGA of $PhZnOPr^i$

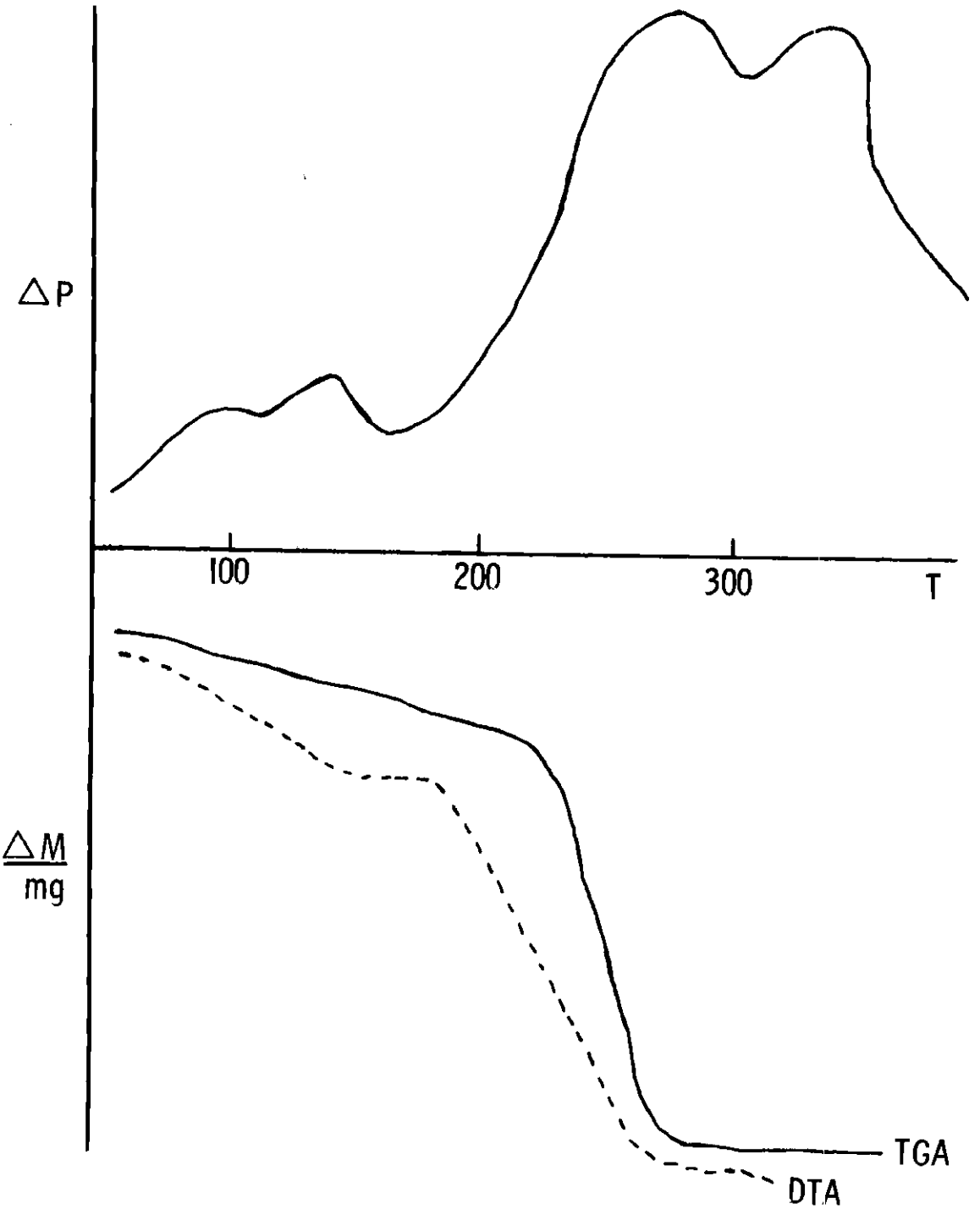

Figure 3. Vacuum DTA-TGA of Ph_2AlO—⬡ · 0.50 Et_2O

Comparisons among alkoxides having the same alkoxy group and metal, but different alkyl groups indicates certain trends. For the isopropoxy magnesium compounds the order of increasing decomposition temperature was CH_3 (215°) < $PhCH_2$ (290°) < Ph (310°) < H (340°). The order for the cyclohexyloxyzinc compounds ($RZnOC_6H_{11}$) was CH_3 (295°) < Ph (310°) and the 1,1-diphenylethoxy magnesium and cyclohexyloxy magnesium compounds decomposed at the same temperature (270°). Insufficient data was available to determine a trend for the aluminum compounds due to the problem of sublimation. A comparison of phenylcyclohexyloxy metal compounds in which only the identity of the metal changes exhibited an increase in decomposition temperature in the order Al < Zn < Mg.

For alkoxides with the same alkyl group and metal there are apparently conflicting trends in the decomposition temperatures. In the case of the methyl magnesium alkoxides, the order of increasing decomposition temperature parallels an approximate increase in the stability of the olefin product. However, for the phenyl magnesium alkoxides the decomposition temperature follows an approximate decrease with the stability of the olefinic product. The cyclohexyloxy group appears to be out of order in both comparisons. The benzyl magnesium alkoxides show the order: $OC(CH_3)PH_2$ < OEt < OPr^i < O-  , and the phenyl zinc alkoxides decompose in the order: OPr^i < OEt < $OCPh_2$ < O-  . Obviously, the order of decomposition is dependent not only on the type of alkyl or aryl groups on the metal but also on the type of metal and alkoxy group.

The dialkoxy magnesium and zinc compounds were found to decompose in two steps. The first step involves an α-elimination to yield a ketone and the intermediate alkoxy metal hydride. This intermediate then decomposes to give hydrogen and an olefin. These reactions are illustrated in Equations 7 and 8 for dicyclohexyloxy magnesium.

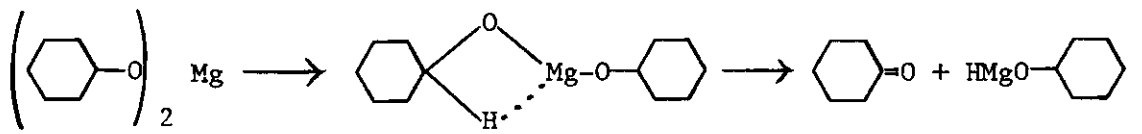

(7)

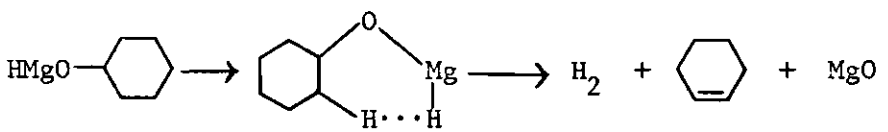

(8)

In general, there is no evidence to support the formation of an intermediate in the decomposition of the alkoxides. Most DTA-TGA traces show no break in the TGA curve. One compound fails to decompose completely i.e., phenylzinc ethoxide. This compound eliminates benzene and gives a product of empirical formula $[ZnOCH_2CH_2]_x$ as determined by hydrolysis of the material remaining in the crucible after the DTA-TGA determination. The compound is not soluble in typical organic solvents and is only slowly decomposed with dilute sulfuric acid. Such behavior is typical of a polymeric material. Another compound, phenylzinc t-butoxide, apparently decomposes to an

intermediate $[ZnOCH_2C(CH_3)_2]_x$ which cannot be isolated due to further decomposition to evolve isobutylene. The $(ZnOCH_2CH_2)_x$ material does not decompose further since the incipient olefin product is ethylene, a nonsubstituted and hence less stable olefin.

Stereochemistry

Our postulated mechanism for the decomposition of alkyl metal alkoxides involves the formation of a cyclic six-center transition state. This concept is illustrated for methylmagnesium threo-1,2-diphenyl-1-propoxide in Figure 4. An incipient methyl carbanion

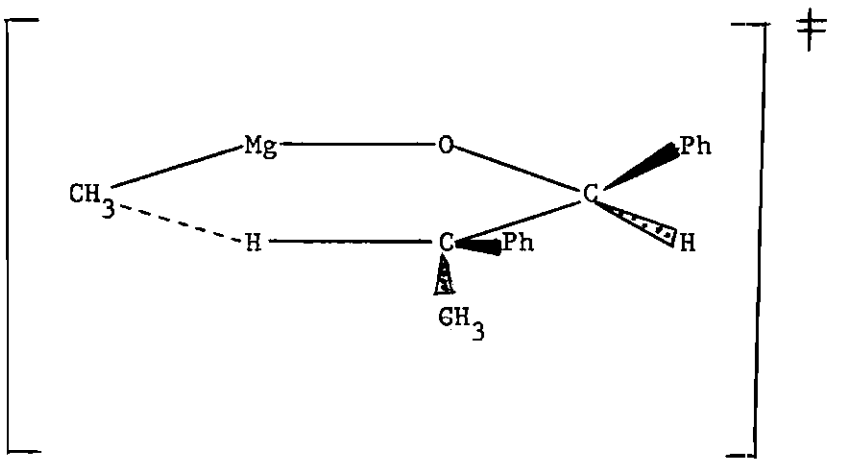

Figure 4. Transition State for the Decomposition of an Alkoxide

abstracts a β-hydrogen from the alkoxy group to give methane, cis-1,2-diphenylpropene, and magnesium oxide. In the actual experiment it was necessary to use triphenylphosphine to prevent isomerization of the cis olefin product by the magnesium oxide by-product which acts as a Lewis acid catalyst. The result of the reaction is the formation of 100% cis-1,2-diphenylpropene in about 70% yield. The corresponding

methylmagnesium erythro-1,2-diphenylpropoxide gives 100% trans-1,2-diphenylpropene in about 65% yield.

Kinetics

(a) Kinetic Isotope Effect. Several alkoxides were prepared in which the alkoxy portion was deuterated in the β positions. The deuterated and nondeuterated alkoxides were decomposed via DTA-TGA at a constant temperature (235°C). First-order rate constants were determined by following the loss in weight of a tared sample of the alkoxide due to the formation of volatile reaction products. A linear least squares plot of the natural logarithm of moles alkoxide versus time in minutes gives the first-order rate constants summarized in Table 7. Kinetic isotope effects (kH/kD) were calculated by taking the ratio of the rate of the decomposition of the nondeuterated alkoxide to the rate of the decomposition of the deuterated alkoxide.

(b) Determination of Activation Parameters. Constant temperature kinetics were conducted on several alkoxides via DTA-TGA. The rate constants were determined as before and are summarized in Table 8 for several alkoxides. The frequency factor (A) and experimental activation energy (E_a) were calculated from the Arrhenius theory $k = Ae^{-E_a/RT}$ with the aid of a least squares plot of ln k versus $^1/T$, where T is absolute temperature. The energies of activation were obtained by use of the equation $E_a = -R \times \text{slope}$, and the frequency factors were calculated from the Arrhenius equation where intercept = ln A. Having calculated the E_a and A values for a given compound, it was then possible to calculate an entropy of activation ($\Delta S^{\neq}$) at a specific temperature using the equation of O'Connor and Nace,[28]

Table 7. Kinetic Isotope Effects for Alkoxides

Compound	k at 235° (min^{-1})	R	Atmosphere	kH/kD
$CH_3MgOCH(CH_3)_2$	9.18×10^{-3}	0.999	Ar	0.675
$CH_3MgOCH(CD_3)_2$	1.36×10^{-2}	0.999	Ar	
$PhMgOCH(CH_3)_2$	2.10×10^{-3}	0.990	Vac	0.712
$PhMgOCH(CD_3)_2$	2.95×10^{-3}	0.994	Vac	
$PhZnOCH(CH_3)_2$	1.33×10^{-3}	0.987	Ar	0.226
$PhZnOCH(CD_3)_2$	5.89×10^{-3}	0.999	Ar	
$PhCH_2MgOCH(CH_3)_2$	4.60×10^{-3}	0.980	Vac	1.300
$PhCH_2MgOCH(CD_3)_2$	3.55×10^{-3}	0.990	Vac	
$PhZnOCH_2CH_3$[a]	1.79×10^{-3}	0.967	Vac	0.626
$PhZnOCD_2CD_3$[a]	2.86×10^{-3}	0.967	Vac	

[a] The temperature was 220° and the evolution of hydrocarbon was followed.

Table 8. First-Order Rate Constants for the Thermal Decomposition of Alkoxides

Compound	$k(min^{-1})$	Temp(°C)	R
threo $Ph(CH_3)CHCH(Ph)OMgCH_3$	7.50×10^{-4}	200	0.985
	3.18×10^{-3}	235	0.976
	1.75×10^{-2}	285	0.954
erythro $Ph(CH_3)CHCH(Ph)OMgCH_3$	5.38×10^{-3}	200	0.982
	7.79×10^{-3}	210	0.934
	1.64×10^{-2}	235	0.988
$PhMgOPr^i \cdot 0.16\ Et_2O$	6.00×10^{-4}	200	0.982
	2.10×10^{-3}	235	0.990
	4.21×10^{-3}	285	0.988
$PhCH_2MgOPr^i$	6.33×10^{-4}	200	0.983
	4.60×10^{-3}	235	0.980
	3.04×10^{-2}	282	0.993
PhZnO- 	1.24×10^{-3}	215	0.988
	3.60×10^{-3}	235	0.999
	1.08×10^{-2}	278	0.976
PhZnOEt	1.50×10^{-3}	200	0.993
	1.79×10^{-3}	220	0.967
	3.43×10^{-3}	235	0.982

$\Delta S^{\neq} = 2.303\ R \log A - 2.303\ R \log (K\ e\ \frac{k'T}{h})$, where k' is the Boltzman constant, h is Planck's constant, and K is the transmission coefficient which is assumed to be unity. The activation parameters are listed in Table 9. The R value is a measure of the fit of the experimental data to a straight line. Ideally the R value would be unity (Appendix 2).

Product Distributions and Yields

The alkoxides were decomposed under vacuum at 270-275° using a Woods' metal bath and a dry ice condenser. The olefinic products distilled out from the reaction mixture and product ratios and yields were determined by glpc and nmr comparisons of authentic samples. An alternative method of decomposition involved reflux of the compounds in a diluent such as n-dodecane. The data are contained in Table 10.

Several alkoxides possessed more than one type of β-hydrogen leading to mixtures of olefins. These compounds were the methyl magnesium alkoxide of 1-methyl-1-cyclohexanol, dimethylcyclohexylcarbinol, cis-2-methyl-1-cyclohexanol, and trans-2-phenyl-1-cyclohexanol. The alkoxide methylmagnesium 1-methyl-cyclohexyloxide decomposed in 43.2% yield to give a 41 to 59 ratio of methylenecyclohexane and 1-methyl-1-cyclohexene, respectively. This ratio represents a statistical yield of products based upon the number of available β-hydrogens. Similar statistical yields of olefins were produced for the alkoxides methylmagnesium dimethylcyclohexylcarbyloxide and methylmagnesium cis-2-methyl-1-cyclohexyloxide. However, methylmagnesium trans-2-phenyl-1-cyclohexyloxide produced an 88 to 12 ratio of 1-phenyl-1-cyclohexene and 3-phenyl-1-cyclohexene. A statistical

Table 9. Activation Parameters for the Decomposition of Alkoxides

Compound	E_a (Kcal/mole)	A (sec^{-1})	R	$\Delta S^{\ddagger}$ (eu) at 200°C
threo $Ph(CH_3)CHCH(Ph)OMgCH_3$	19.4	1.15×10^4	0.999	-42.6
erythro $Ph(CH_3)CHCH(Ph)OMgCH_3$	15.5	1.26×10^3	0.999	-47.0
$PhMgOPr^i$	11.8	3.25	0.946	-58.9
$PhCH_2MgOPr^i$	24.7	2.83×10^6	0.998	-31.6
PhZnO 	17.3	1.32×10^3	0.982	-46.9
PhZnOEt	11.4	3.91	0.912	-58.5
$PhMgOCH(CD_3)_2$	12.7	15.2	0.978	-55.8
$PHCH_2MgOCH(CD_3)_2$	16.9	9.81×10^2	0.991	-47.5

Table 10. Thermal Decomposition of Alkoxides: Yields and Product Ratios

Compound	Olefin	Yield[a] Ratio	Yield[a] Total	Method	Yield[e] Chugaev Ratio	Yield[e] Reaction Total	Yield[e] Acetate Ratio	Yield[e] Pyrolysis Total	Reference
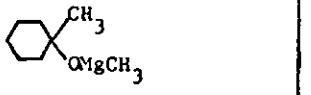	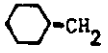	41	43.2	a	21	49.0	24	61.6	12, 13
	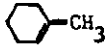	59			79		76		
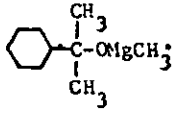	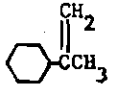	84	84.9	a	88	29.1			12
	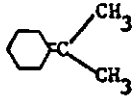	16			22				
cis 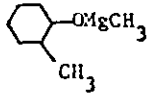	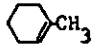	34	69.3	a			25	62.5	14
	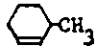	66					75		
trans 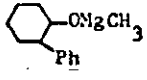	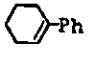	88	68.5	a	88	f	87	53.0	15
	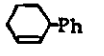	12			12		13		
threo $PhCH(CH_3)CH(Ph)OMgCH_3$	$PhCH{=}C(CH_3)Ph$ cis	100	49.4	a	100	46.2			10
	trans	0			0				

Table 10. Thermal Decomposition of Alkoxides: Yields and Product Ratios (Continued)

erythro	$PhCH{=}C(CH_3)Ph$							
$PhCH(CH_3)CH(Ph)OMgCH_3$	trans	100	47.8	a	100	53.9		10
	cis	0			0			
$CH_3MgOC(CH_3)Ph_2 \cdot 1.0\ Et_2O$	$Ph_2C = CH_2$		81.3	a				
			81.3	b				
$(i\text{-}Pr)_2NMgOC(CH_3)Ph_2$	$Ph_2C = CH_2$		70.1	a				
$BrMgOC(CH_3)Ph_2$	$Ph_2C = CH_2$		102	c				
			89.6	d				
			40.3	b				
$Mg(O\text{-}C_6H_{11})_2$	$C_6H_{11}{=}O$		87.7	a				
	C_6H_{10}		57.9					
$(i\text{-}Pr)_2NAlOC(CH_3)Ph_2$	$Ph_2C = CH_2$		101	a				
$Ph_2AlOC(CH_3)Ph_2$	$Ph_2C = CH_2$		103	a				
$PhZnOC(CH_3)Ph_2$	$Ph_2C = CH_2$		76.2	a				
$PhMgOC(CH_3)Ph_2$	$Ph_2C = CH_2$		41.6	a				

Table 10. Thermal Decomposition of Alkoxides: Yields and Product Ratios (Continued)

(a) Solid decomposed using Woods' metal bath.

(b) n-dodecane reflux for 24 hours.

(c) n-dodecane reflux for 24 hours, excess Ph_3P added.

(d) n-dodecane reflux for 24 hours, excess $(CH_3)_2NPh$ added.

(e) Yield based on alcohol.

(f) No yield given; the crude methyl xanthate was decomposed to give a product which was distilled twice to remove the odor of mercaptans.

yield would have been 67 to 33. The increase in the amount of the 1-phenyl-1-cyclohexene is due to the stabilizing effect of the phenyl group to produce a conjugated olefin. The products of the Chugaev and Acetate Pyrolysis reactions involving the counterpart of the alkoxide also gives the two cyclohexenes in about the same ratio due to the influence of the phenyl in forming the more thermodynamically stable olefin.

The yields from the thermal decomposition of alkoxides are comparable to those from the Chugaev and Acetate Pyrolysis reactions. In the Chugaev reaction the preparation of the methyl xanthate can be a low yield reaction. The preparation of the acetate ester is not quantitative either. However, the preparation of the alkoxide is a quantitative reaction, and the alkoxides do not have to be isolated or purified. There are several methods for the preparation of alkoxides. Usually dimethylmagnesium, diphenylzinc or triphenylaluminum is allowed to react with the appropriate alcohol in a one to one mole ratio. In addition, Grignard reagents can react directly with ketones, aldehydes or alcohols to produce alkoxides. For example, benzophenone, or 1,1-diphenyl-1-propanol reacts with methylmagnesium bromide to produce 1,1-diphenyl-1-propoxymagnesium bromide. The thermal decomposition of this compound is best conducted in a diluent such as n-dodecane using an amine or triphenylphosphine as a trap for the HBr generated.

The Amides

Magnesium, zinc, and aluminum amides[33] are prepared quantitatively by reacting a suitable hydrido, alkyl, or aryl metal compound directly with a secondary amine. This general reaction is illustrated in equations 9 - 11. Details of the preparation are given

$$(CH_3)_2Mg + HN(C_6H_{11})_2 \longrightarrow CH_3MgN(C_6H_{11})_2 + CH_4 \quad (9)$$

$$(Ph)_2Zn + HNPr^i_2 \longrightarrow PhZnNPr^i_2 + PhH \quad (10)$$

$$Ph_3Al + HNEt_2 \longrightarrow Ph_2AlNEt_2 + PhH \quad (11)$$

in the experimental section and are summarized in Tables 11 - 13. Then, in a second step the amide is thermally decomposed as illustrated in reactions 12 - 14. The products are hydrocarbon, an olefin, and a residue of empirical formula $(MNR')_x$.

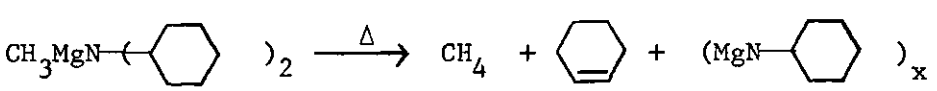

$$CH_3MgN(C_6H_{11})_2 \xrightarrow{\Delta} CH_4 + C_6H_{10} + (MgN(C_6H_{11}))_x \quad (12)$$

Table 11. Preparation of Magnesium Amides

Reactants (mmoles) R_2Mg	R'_2NH	Reaction time (h.)	Analysis (%) Mg	R	R'_2N	Solvent	Analysis (Ratio) Mg	R	R'_2N	Solvent	Probable Product
MgH_2 (3.58)	$Mg(NPr^n_2)_2$ (3.50)	5	16.5	0.66	71.2	11.7	1.00	0.97	1.05	0.24	$HMgNPr^n_2 \cdot 0.24$ THF
(3.70)	$Mg(NBu^s_2)_2$ (3.70)	4	12.1	0.48	64.0	23.4	1.00	0.96	1.00	0.65	$HMgNBu^s_2 \cdot 0.65$ THF
(4.00)	$Mg[N(-\bigcirc)_2]_2$ (4.00)	6	8.63	0.35	63.9	27.1	1.00	0.98	1.01	1.06	$HMgN(\bigcirc)_2 \cdot 1.06$ THF
$(CH_3)_2Mg$ (53.2)	Et_2NH (53.4)	1	22.7	13.6	63.8	00.0	1.00	0.97	0.95	0.00	CH_3MgNEt_2
(75.0)	Pr^n_2NH (75.2)	1	17.7	10.4	71.9	00.0	1.00	0.98	0.99	0.00	$CH_3MgNPr^n_2$
(18.0)	Pr^i_2NH (18.1)	0.5	18.9	10.9	70.2	00.0	1.00	0.95	0.90	0.00	$CH_3MgNPr^i_2$
(50.0)	Bu^n_2NH (50.3)	0.5	16.1	9.20	74.6	00.0	1.00	0.93	0.88	0.00	$CH_3MgNBu^n_2$
(75.0)	Bu^s_2NH (75.5)	0.5	15.7	9.90	74.4	00.0	1.00	1.02	0.90	0.00	$CH_3MgNBu^s_2$
(51.8)	$\bigcirc NH$ (52.0)	1	19.9	11.9	68.2	00.0	1.00	0.97	0.99	0.00	$CH_3MgN\bigcirc$
(76.5)	$(-\bigcirc)_2NH$ (76.5)	1	10.9	6.54	82.5	00.0	1.00	0.97	1.02	0.00	$CH_3MgN(-\bigcirc)_2$
(46.5)	Ph(Et)NH (46.8)	0.5	14.4	9.27	76.3	00.0	1.00	1.04	1.07	0.00	$CH_3MgN(Et)Ph$
(6.60)	$PhCH_2CH_2(CH_3)NH$ (6.61)	0.5	14.3	8.47	77.2	00.0	1.00	0.95	0.98	0.00	$CH_3MgN(CH_3)(CH_2CH_2Ph)$

Table 11. Preparation of Magnesium Amides (Continued)

	$HNPh_2$							
(4.36)	(4.39)	1	8.6	5.3	59.3	26.8	1.00 : 0.85 : 1.21 : 1.03	$CH_3MgNPh_2 \cdot 1.03\ Et_2O$
Ph_2Mg	$HNEt_2$							
(4.00)	(4.01)	1	12.3	39.0	36.3	12.4	1.00 : 1.03 : 0.98 : 0.33	$PhMgNEt_2 \cdot 0.33\ Et_2O$
	$HNPr^i_2$							
(4.00)	(3.98)	1	9.1	28.8	37.4	24.7	1.00 : 1.03 : 0.93 : 0.89	$PhMgNPr^i_2 \cdot 0.98\ Et_2O$
	$HNBu^n_2$							
(4.01)	(4.05)	1	8.4	26.6	44.1	20.9	1.00 : 1.05 : 0.93 : 0.82	$PhMgNBu^n_2 \cdot 0.82\ Et_2O$
	$HNBu^s_2$							
(3.99)	(4.03)	1	7.1	22.5	37.5	32.9	1.00 : 1.02 : 0.96 : 1.52	$PhMgNBu^s_2 \cdot 1.52\ Et_2O$
	HN⟨⬡⟩$_2$							
(4.93)	(4.94)	1	6.9	21.7	50.7	20.7	1.00 : 1.05 : 1.08 : 0.94	PhMgH-⟨⬡⟩$_2$ · 0.94 PhH
$(PhCH_2)_2Mg$	$HNEt_2$							
(2.95)	(2.91)	1	9.9	37.3	29.5	23.3	1.00 : 1.10 : 1.05 : 0.77	$PhCH_2MgNEt_2 \cdot 0.77\ Et_2O$
	$HNPr^i_2$							
(2.30)	(2.32)	1	8.0	30.1	33.2	28.7	1.00 : 1.27 : 1.02 : 1.17	$PhCH_2MgNPr^i_2 \cdot 1.17\ Et_2O$
	$HNBu^n_2$							
(3.00)	(2.96)	1	8.0	29.9	42.1	20.0	1.00 : 0.80 : 0.95 : 0.82	$PhCH_2MgNBu^n_2 \cdot 0.82\ Et_2O$
	$HNBu^s_2$							
(1.60)	(1.57)	1	7.7	28.7	40.5	23.1	1.00 : 0.85 : 0.93 : 0.99	$PhCH_2MgNBu^s_2 \cdot 0.99\ Et_2O$
	HN⟨⬡⟩$_2$							
(2.80)	(2.78)	1	5.3	19.7	39.0	36.0	1.00 : 0.80 : 0.94 : 2.25	$PhCH_2MgN$-⟨⬡⟩$_2$ · 2.25 Et_2O
$(CH_3)_2Mg$	$(CH_3)_2CHNHPh$							
(4.23)	(4.23)	1	11.2	6.9	61.8	20.1	1.00 : 0.89 : 1.10 : 0.59	$(CH_3)_2CH(MgCH_3)NPh \cdot 0.59\ Et_2O$
	$(CD_3)_2CHNHPh$							
(5.68)	(5.70)	1	11.4	7.0	65.7	15.9	1.00 : 1.10 : 0.95 : 0.46	$(CD_3)_2CH(MgCH_3)NPh \cdot 0.46\ Et_2O$

Table 11. Preparation of Magnesium Amides (Continued)

(4.13)	$(CH_3)_2CHNHCH_2Ph$ (4.12)	1	11.6	7.2	70.6	10.6	1.00 : 0.93 : 0.97 : 0.30	$(CH_3)_2CHN(MgCH_3)CH_2Ph \cdot 0.30\ Et_2O$
(4.60)	$(CD_3)_2CHNHCH_2Ph$ (4.62)	1	11.9	7.4	75.6	5.1	1.00 : 0.80 : 1.05 : 0.14	$(CD_3)_2CHN(MgCH_3)CH_2Ph \cdot 0.14\ Et_2O$
(4.59)	<u>threo</u> $PhCH_3CHCHPhNHPh$ (4.61)	0.5	7.53	4.88	87.6	0.00	1.00 : 1.05 : 1.02 : 0.00	<u>threo</u> $PhN(MgCH_3)CHPhCHCH_3Ph$
(30.0)	H_2NBu^t (30.0)	1	18.2	11.2	52.4	18.3	1.00 : 0.92 : 0.95 : 0.33	$CH_3MgNHBu^t \cdot 0.33\ Et_2O$
(31.7)	HNEt(Naph-1) (31.8)	1	13.4	8.3	78.3	0.00	1.00 : 0.69 : 0.95 : 0.00	CH_3MgNH(Naph-1)

Table 12. Preparation of Zinc Amides

Ser. No.	Reactants (mmoles) R_2Zn	R'_2NH	Reaction Time (h.)	Analysis (%) Zn	R	R'_2N	Solvent	Analysis (Ratio) Zn	R	R'_2N	Solvent	Probable Product
1.	Ph_2Zn (2.55)	$HNEt_2$ (2.60)	1	25.2	29.7	27.7	17.4	1.00	0.95	1.05	0.49	$PhZnNEt_2 \cdot 0.49\ PhCH_3$
2.	(2.65)	$HNPr^i_2$ (2.64)	1	22.8	26.9	34.9	15.4	1.00	0.98	1.10	0.48	$PhZnNPr^i_2 \cdot 0.48\ PhCH_3$
3.	(2.81)	$HNBu^n_2$ (2.79)	1	20.1	23.6	39.3	17.0	1.00	0.97	1.02	0.60	$PhZnNBu^n_2 \cdot 0.60\ PhCH_3$
4.	(5.09)	$HN(C_6H_{11})_2$ (5.14)	1	16.9	20.0	46.6	16.5	1.00	0.97	0.96	0.69	$PhZnN(C_6H_{11})_2 \cdot 0.69\ PhCH_3$

Table 13. Preparation of Aluminum Amides

Ser. No.	Reactants (mmoles) R_3Al	R'_2NH	Reaction Time (h.)	Analysis (%) Al	R	R'_2N	Solvent	Analysis (Ratio) Al	R	R'_2N	Solvent	Probable Product
1.	Ph_3Al (1.44)	$HNEt_2$ (1.44)	1	8.3	47.4	22.2	22.1	1.00	1.90	0.95	0.78	$Ph_2AlNEt_2 \cdot 0.78\ PhCH_3$
2.	(1.64)	$HNPr^i_2$ (1.63)	1	8.1	46.3	30.1	15.5	1.00	1.85	0.97	0.56	$Ph_2AlNPr^i_2 \cdot 0.56\ PhCH_3$
3.	(1.70)	$HNBu^n_2$ (1.72)	1	7.0	40.0	33.2	19.8	1.00	1.97	1.02	0.83	$Ph_2AlNBu^n_2 \cdot 0.83\ PhCH_3$
4.	(2.45)	$HN(C_6H_{11})_2$ (2.42)	1	4.1	23.3	27.2	45.4	1.00	1.98	1.05	3.26	$Ph_2AlN(C_6H_{11})_2 \cdot 3.26\ PhCH_3$

$$PhZnNPr^i_2 \xrightarrow{\Delta} PhH + CH_2 = CHCH_3 + (ZnNPr^i)_x \quad (13)$$

$$Ph_2AlNEt_2 \xrightarrow{\Delta} PhH + CH_2 = CH_2 + (PhAlNEt)_x \quad (14)$$

DTA-TGA Data[26]

The decomposition reaction was studied by DTA-TGA (differential thermal analysis-thermogravimetric analysis).[6] This data is summarized in Tables 14 - 16. Samples of amides were decomposed under vacuum at 4° per minute from 25° to 450°C. Typical DTA-TGA curves are shown in Figures 5 - 7. The DTA-TGA curves have several common characteristics e.g., all decompositions are endothermic. In general, the coordinated solvent is lost first, and then the main decomposition occurs in one step with no apparent intermediate. Both condensable and non-condensable evolved gases can be identified and measured quantitatively. Further decomposition of the residue $(MgNR')_x$ occurs at higher temperatures.

Some of the compounds studied were volatile e.g., complete sublimation occurred for diethylamino(phenyl)zinc and di-n-butylamino-(diphenyl)aluminum. The decomposition of diphenylamino(methyl)-magnesium resulted in 8.7% sublimation. All methylzinc amides and dimethylaluminum amides sublimed.

Comparisons among amides having the same amide group and metal but different alkyl groups indicate a particular decomposition trend. For both di-n-butylaminomagnesium and diisopropylaminomagnesium

Table 14. Thermal Decomposition of Magnesium Amides

Compound (sample wt., mg)	Therm-icity	Range of Transition (peak max.), °C	wt. loss mg	(%)	Evolved Gas
CH_3MgNEt_2	Endo	70 - 208 (190)	11.4	(14.4)	CH_4
(79.1)	Endo	220 - 272 (262)	29.7	(37.5)	$CH_2{=}CH_2$
$PhMgNEt_2 \cdot 0.33\ Et_2O$	Endo	55 - 115 (85)	2.4	(12.1)	Et_2O
(19.9)	Endo	185 - 330 (220)	7.9	(39.7)	PhH
	Endo	330 - 462 (400)	2.8	(14.1)	$CH_2{=}CH_2$
$PhCH_2MgNEt_2 \cdot 0.77\ Et_2O$	Endo	50 - 150 (95)	14.0	(23.3)	Et_2O
(60.2)	Endo	150 - 445 (240)	26.2	(43.5)	$PhCH_3 + CH_2{=}CH_2$
$HMgNPr^n_2 \cdot 0.24\ THF$	Endo	50 - 190 (120)	10.0	(11.8)	THF
(84.7)	Endo	190 - 265	5.3	(6.3)	THF Cleavage Product
	Endo	265 - 450 (340, 396)	17.6	(20.8)	$H_2 + CH_3CH{=}CH_2$
$CH_3MgNPr^n_2$	Endo	160 - 230 (215)	10.2	(11.4)	CH_4
(89.1)	Endo	230 - 365 (325)	27.0	(30.3)	$CH_3CH{=}CH_2$
$CH_3MgNPr^i_2$	Endo	80 - 160 (125)	22.8	(42.0)	$CH_4 + CH_3CH{=}CH_2$
(54.4)					
$PhMgNPr^i_2 \cdot 0.89\ ET_2O$	Endo	65 - 140 (110)	14.5	(24.7)	Et_2O
(58.7)	Endo	140 - 445 (250)	26.7	(45.5)	$PhH + CH_3CH{=}CH_2$
$PhCH_2MgNPr^i_2 \cdot 1.17\ Et_2O$	Endo	45 - 150 (90)	20.0	(28.7)	Et_2O
(69.7)	Endo	150 - 345 (210)	33.0	(47.3)	$PhCH_3 + CH_3CH{=}CH_2$
$CH_3MgNBu^n_2$	Endo	125 - 265 (200)	26.8	(41.7)	$CH_4 + CH_3CH_2CH{=}CH_2$
(42.0)					
$PhMgNBu^n_2 \cdot 0.82\ Et_2O$	Endo	105 - 175 (155)	9.0	(20.7)	Et_2O
(43.5)	Endo	175 - 462 (235°)	20.0	(46.0)	$PhH + CH_3CH_2CH{=}CH_2$

Table 14. Thermal Decomposition of Magnesium Amides (Continued)

$PhCH_2MgNBu^n_2 \cdot 0.82\ Et_2O$ (90.2)	Endo	50 - 135 (90)	18.0	(20.0)	Et_2O
	Endo	135 - 455 (215)	42.5	(47.1)	$PhCH_3 + CH_3CH_2CH{=}CH_2$
$HMgNBu^s_2 \cdot 0.65\ THF$ (29.7)	Endo	50 - 145 (90)	6.0	(20.2)	THF
	Endo	145 - 260	2.6	(8.8)	$THF + H_2$
	Endo	260 - 390 (335)	7.0	(23.6)	$H_2 + CH_3CH_2CH{=}CH_2 + CH_3CH{=}CHCH_3$
$CH_3MgNBu^s_2$ (52.0)	Endo	80 - 175 (115)	23.0	(44.2)	$CH_4 + CH_3CH_2CHCH_2 + CH_3CHCHCH_3$
$PhMgNBu^s_2 \cdot 1.52\ Et_2O$ (86.6)	Endo	40 - 145 (130)	28.5	(32.9)	Et_2O
	Endo	145 - 450 (285)	34.5	(39.8)	$PhH + CH_2{=}CHCH_2CH_3 + CH_3CH{=}CHCH_3$
$PhCH_2MgNBu^s \cdot 0.99\ Et_2O$ (47.7)	Endo	40 - 140 (75)	11.0	(23.1)	Et_2O
	Endo	140 - 395 (205)	24.5	(51.4)	$PhCH_3 + CH_2{=}CHCH_2CH_3 + CH_3CH{=}CHCH_3$
$HMgN{-}(C_6H_{11})_2 \cdot 1.06\ THF$ (97.1)	Endo	50 - 180 (100)	26.0	(26.8)	THF
	Endo	200 - 390 (280)	29.2	(30.1)	H_2 + 
$CH_3MgN{-}(C_6H_{11})_2$ (28.2)	Endo	130 - 280 (200)	11.9	(42.1)	CH_4 + 
$PhMgN(C_6H_{11})_2 \cdot 0.94\ PhH$ (60.3)	Endo	55 - 140 (100)	15.7	(26.0)	PhH
	Endo	140 - 455 (295)	25.4	(42.1)	PhH + 
$PhCH_2MgN(C_6H_{11})_2 \cdot 2.25\ Et_2O$ (58.3)	Endo	85 - 210 (185)	21.0	(36.0)	Et_2O
	Endo	210 - 460 (295)	20.5	(35.2)	$PhCH_3$ + 
$CH_3MgN(CH_3){-}CH_2CH_2Ph$ (62.9)	Endo	140 - 440 (275)	33.3	(52.9)	$CH_4 + PhCH{=}CH_2$
$CH_3MgNEtPh$ (37.2)	Endo	180 - 320 (215, 270)	10.4	(28.0)	$CH_4 + CH_2{=}CH_2$
$CH_3MgNPh_2 \cdot 1.03$ (84.4)	Endo	45 - 235 (145)	22.7	(26.9)	Et_2O
	Endo	355 - 465 (415)	7.0	(8.3)	CH_4 + 8.7% Sublimation

Table 14. Thermal Decomposition of Magnesium Amides (Continued)

CH_3MgN  (50.8)	Endo	60 - 230 (185)	6.8	(13.4)	CH_4
$CH_3MgNEt(Naph\text{-}1)$ (26.3)	Endo	65 - 140 (85)	5.6	(21.3)	$CH_4 + CH_2{=}CH_2$
$CH_3MgNHBu^t \cdot 0.33\ Et_2O$ (43.3)	Endo	60 - 160 (105)	9.0	(20.8)	Et_2O
	Endo	200 - 275 (250)	5.0	(11.5)	CH_4
$(CH_3)_2CH(MgCH_3)NPh$ (19.8)	Endo	50 - 160 (100)	4.5	(22.7)	Et_2O
	Endo	160 - 305 (210)	5.5	(27.8)	$CH_4 + CH_2{=}CHCH_3$
$(CD_3)_2CH(MgCH_3)NPh$ (55.2)	Endo	55 - 160 (95)	8.8	(15.9)	Et_2O
	Endo	160 - 395 (215)	16.0	(30.0)	$CH_3D + CD_2{=}CHCD_3$
$(CH_3)_2CH(MgCH_3)NCH_2Ph$ (61.6)	Endo	50 - 150 (115)	6.5	(10.6)	Et_2O
	Endo	150 - 375 (240)	18.5	(30.0)	$CH_4 + CH_2{=}CHCH_3$
$(CD_3)_2CH(MgCH_3)NCH_2Ph$ (86.9)	Endo	50 - 140 (100)	4.5	(5.2)	Et_2O
	Endo	140 - 400 (195)	27.5	(31.6)	$CH_3D + CD_2{=}CHCD_3$
<u>threo</u> $CH_3MgNPhCHPhCHCH_3Ph$ (23.9)	Endo	100 - 155 (120)	15.8	(66.1)	CH_4 + <u>cis</u> $PhC(CH_3){=}CHPh$

Table 15. Thermal Decomposition of Zinc Amides

Compound (sample wt., mg)	Thermicity	Range of Transition (peak max.), °C	wt. loss mg	wt. loss (%)	Evolved Gas
$PhZnNEt_2 \cdot 0.49\ PhCH_3$ (100.6	Endo	70	77.0	(76.5)	Sublimation only
$PhZnNPr^i_2 \cdot 0.48\ PhCH_3$ (80.3)	Endo	35 - 70 (60)	12.4	(15.4)	$PhCH_3$
	Endo	70 - 170 (120)	33.6	(41.8)	$PhH + CH_2{=}CHCH_3$
$PhZnNBu^n_2 \cdot 0.60\ PhCH_3$ (83.1)	Endo	70 - 205 (175)	53.0	(63.8)	$PhCH_3$, PhH, + $CH_2{=}CHCH_2CH_3$
PhZnN-⬡$_2$ · 0.69 $PhCH_3$ (78.0)	Endo	45 - 105 (95)	15.0	(19.2)	$PhCH_3$
	Endo	105 - 170 (145)	39.0	(50.0)	PhH + ⬡

Table 16. Thermal Decomposition of Aluminum Amides

Compound (sample wt., mg)	Therm-icity	Range of Transition (peak max.), °C	wt. loss mg	wt. loss (%)	Evolved Gas
$Ph_2AlNEt_2 \cdot 0.78\ PhCH_3$	Endo	60 - 120 (90)	12.7	(21.9)	$PhCH_3$
(57.9)	Endo	120 - 240 (205)	24.3	(42.0)	$PhH + CH_2{=}CH_2$
$Ph_2AlNPr^i_2 \cdot 0.56\ PhCH_3$	Endo	40 - 90 (80)	6.5	(16.3)	$PhCH_3$
(40.0)	Endo	90 - 230 (180)	15.5	(38.8)	$PhH + CH_2{=}CHCH_3$
$Ph_2AlNBu^n_2 \cdot 0.83\ PhCH_3$	Endo	90 - 200 (180)	14.5	(20.3)	$PhCH_3$
(71.5)	Endo	200	50.5	(70.6)	Sublimation only
Ph_2AlN-  $_2 \cdot 3.26\ PhCH_3$	Endo	70 - 250 (195)	48.8	(72.0)	$PhCH_3$, PhH, + 
(67.8)					

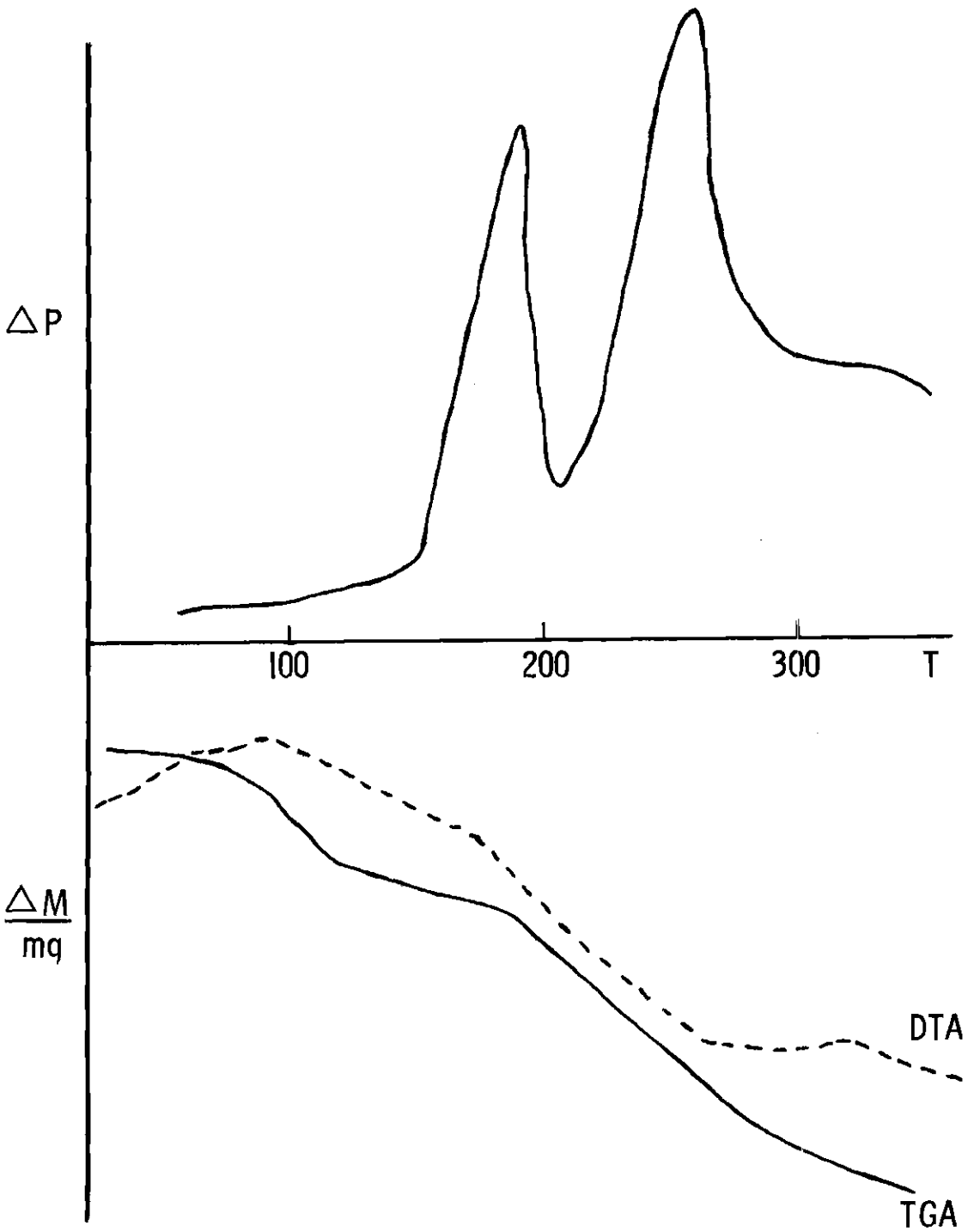

Figure 5. Vacuum DTA-TGA of CH_3MgN-⬡$_2$

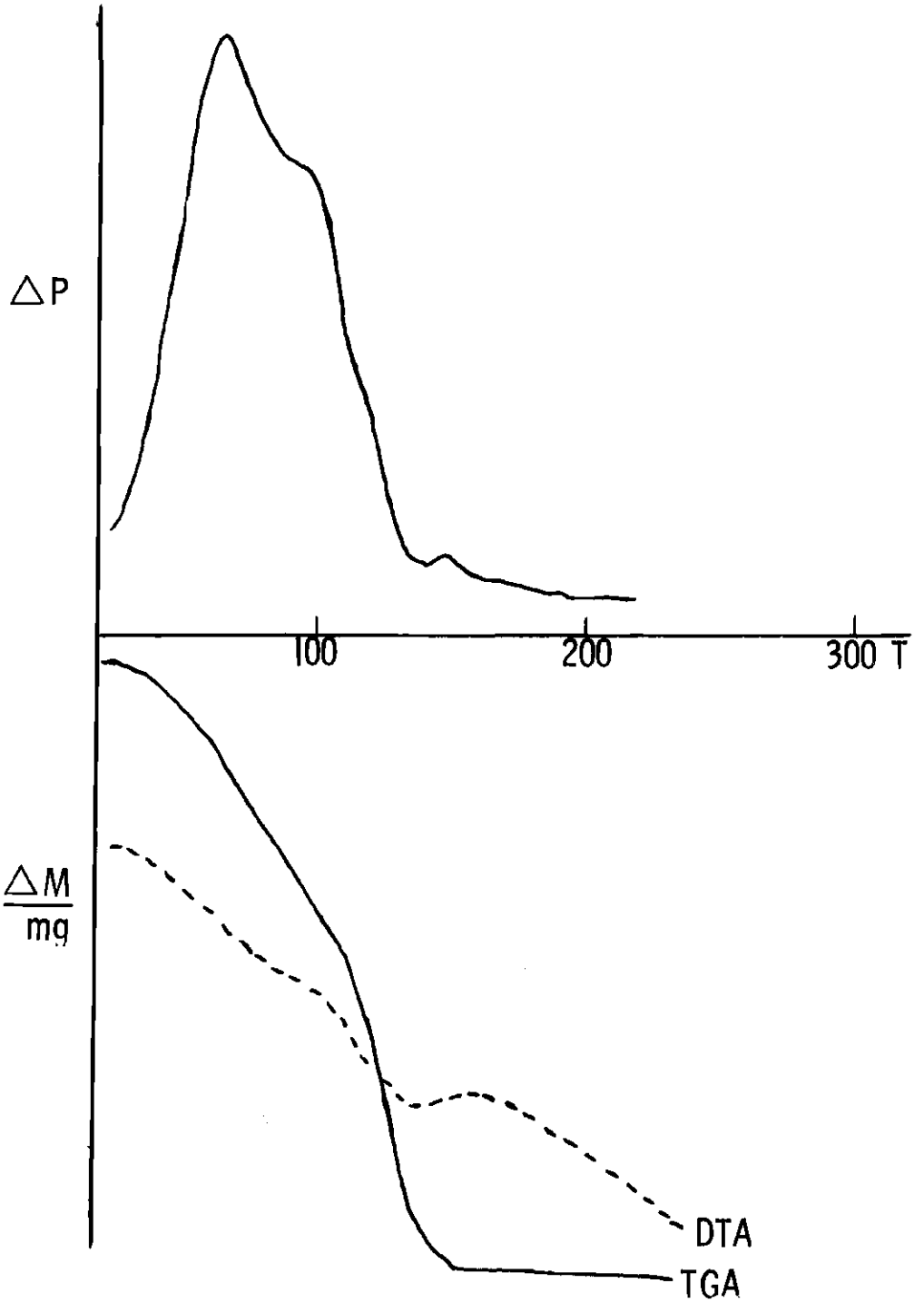

Figure 6. Vacuum DTA-TGA of $PhZnNPr^{i}_{2} \cdot 0.48\ PhCH_3$

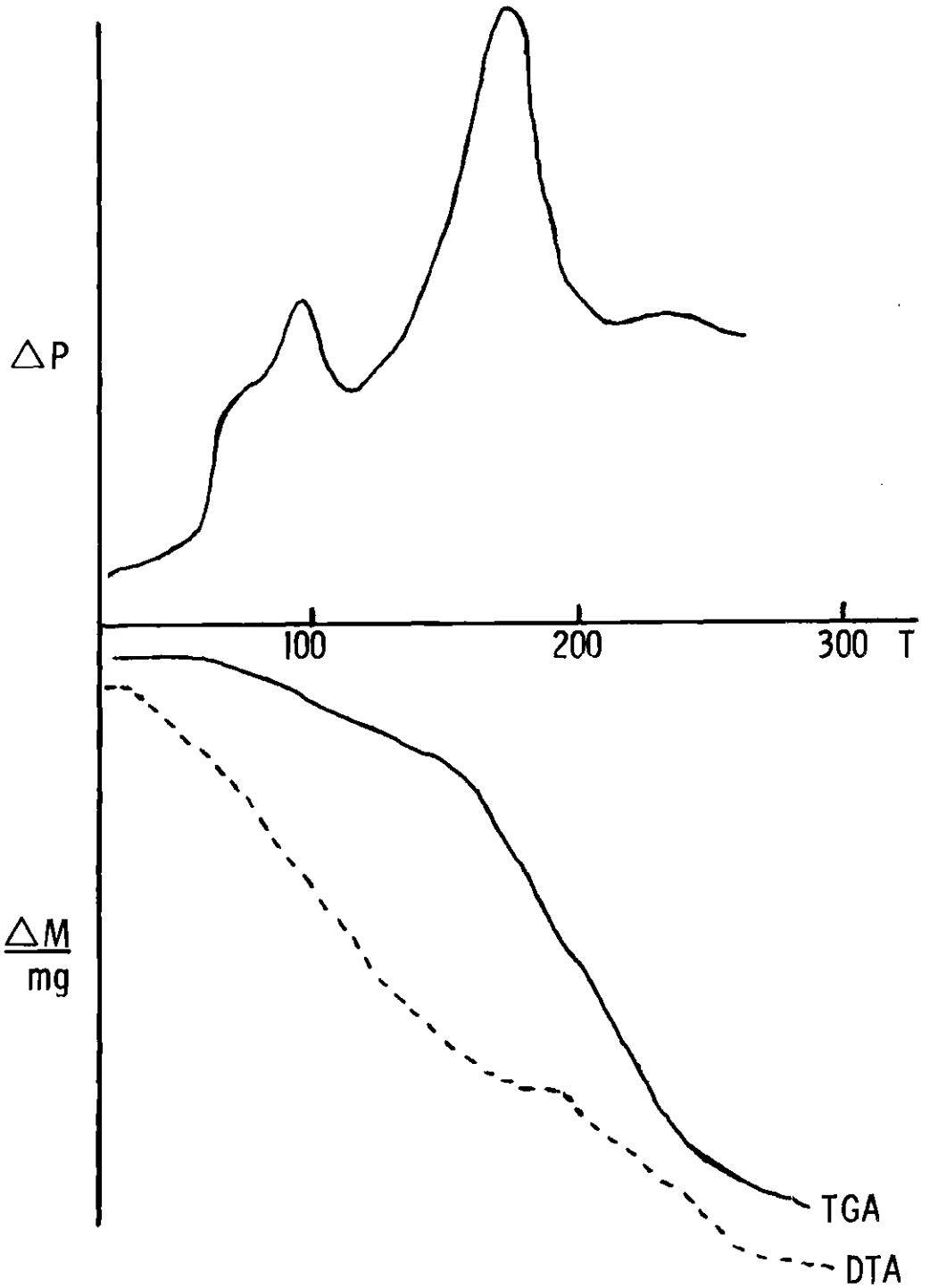

Figure 7. Vacuum DTA-TGA of $Ph_2AlNEt_2 \cdot 0.78\ PhCH_3$

compounds, the order of increasing decomposition temperature is: $CH_3 < PhCH_2 < Ph$. However, the order for the dicyclohexylamino-magnesium compounds is: $CH_3 < PhCH_2 = Ph$. This order is not exactly what is expected for increasing stability of an incipient carbanion ($CH_3 < Ph < PhCH_2$).[27] A comparison of dicyclohexyl-(phenyl)- and diisopropyl(phenyl)amides in which only the identity of the metal changes gives an order of increasing decomposition temperature: Zn < Al < Mg.

There is a recurring trend for amides with the same alkyl group and metal but different amino groups. For methyl, phenyl, and benzyl magnesium amides the order of increasing decomposition temperatures parallels an approximate decrease in the stability of the olefin product. Obviously, the order of decomposition is dependent not only on the type of alkyl or aryl group on the metal but also on the type of metal and amide group.

In general, there is no evidence to support the formation of an intermediate in the decomposition of the amides. Most DTA-TGA traces show no break in the TGA curve. One compound fails to follow this general rule, N-ethylanilino(methyl)magnesium ($CH_3MgNEtPh$). This compound apparently eliminates methane at an early stage (215°) and then ethylene at a later stage (270°). A sample was refluxed in n-dodecane for 24 hours and quenched with deuterium oxide followed by acidic workup. Mass spectral analysis on the hydrolysis product gave a 54:46 ratio of CH_3CH_2NHPh to CDH_2CH_2NHPh as well as a large quantity of aniline. The deuterated N-ethylaniline is due to hydrolysis of an intermediate. Two possible structures for the

intermediate are represented by A and B below. The structure A represents a cyclic species whereas structure B represents a polymeric material. The aniline product is due to hydrolysis of the residue $(MgNPh)_x$ formed in the decomposition reaction. The DTA-TGA

A B

curves for diethylamino(methyl)magnesium and di-n-propylamino(methyl)-magnesium indicate the formation of an intermediate. However, these intermediates were not isolated. The apparent break in the TGA curve of Figure 5 is due to a "buoyancy effect" caused by a sudden evolution of product gases.

Stereochemistry

Our postulated mechanism for the decomposition of alkyl metal amides involves the formation of a cyclic six-center transition state. This concept is illustrated for threo-1,2-diphenyl-1-propylanilino(methyl)magnesium in Figure 8. An incipient methyl carbanion

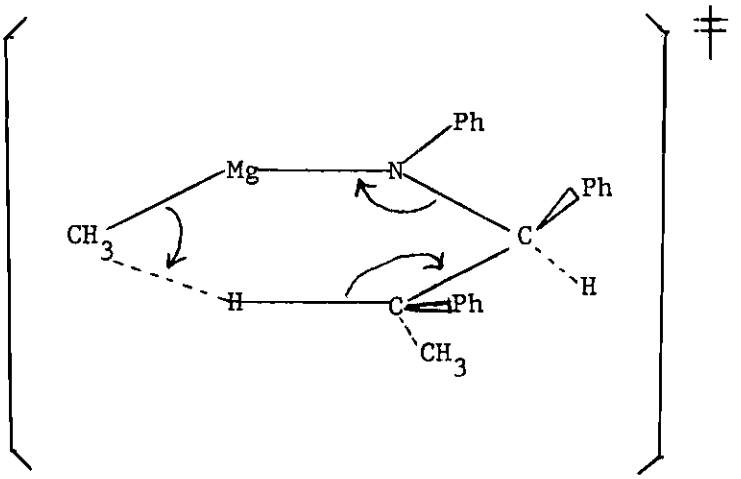

Figure 8. Transition State for the Decomposition of an Amide

abstracts a β-hydrogen from the amide group to give methane, cis-1,2-diphenylpropene, and a residue $(MgNPh)_x$. In the actual experiment it was necessary to use triphenylphosphine to prevent isomerization of the cis olefin product since the by-product, $(MgNPH)_x$, acts as a Lewis acid isomerization catalyst. The result was 100% cis-1,2-diphenylpropene in about 75% yield.

Kinetics

(a) Kinetic Isotope Effect. Two amides were prepared in which the amino portion was deuterated in the β positions. The deuterated and nondeuterated amides were decomposed via DTA-TGA at a constant temperature (223°C). First-order rate constants were determined by following the loss in weight of a tared sample of the amide due to the formation of volatile reaction products. A linear least squares plot of the natural logarithm of moles of amide versus

time in minutes gives the first-order rate constants summarized in Table 17. Kinetic isotope effects (kH/kD) were calculated by taking the ratio of the rate of the decomposition of the nondeuterated amide to the rate of the decomposition of the deuterated amide.

(b) Determination of Activation Parameters. Constant temperature kinetics were conducted on several amides via DTA-TGA. The rate constants were determined as before and are summarized in Table 18 for several amides. The frequency factor (A) and experimental activation energy (E_a) were calculated from the Arrhenius equation, $k = Ae^{-E_a/RT}$ with the aid of a linear least squares plot of ln k versis 1/T, where T is the absolute temperature. The energies of activation were obtained by use of the equation $E_a = -R \times \text{slope}$, and the frequency factors were calculated from the Arrhenius equation where the intercept = ln A. Having calculated the E_a and A values for a given compound, it was then possible to calculate an entropy of activation ($S^{\neq}$) at a specific temperature (200°C) using the equation of O'Connor and Nace,[28] $S^{\neq} = 2.303R \log A - 2.303 R \log (\frac{KeK'T}{h})$, where K' is the Boltzman constant, h is Planck's constant, and K is the transmission coefficient which is assumed to be unity. The activation parameters are listed in Table 19. The R value is a measure of the fit of the experimental data to a straight line. Ideally the R value would be unity (Appendix 2).

Table 17. Kinetic Isotope Effects for Amides

Compound	k at 223° (min^{-1})	R	Atmosphere	kH/kD
$CH_3MgN(Ph)CH(CH_3)_2$	3.58×10^{-3}	0.985	Vac.	2.47
$CH_3MgN(Ph)CH(CD_3)_2$	1.45×10^{-3}	0.989	Vac.	
$CH_3MgN(CH_2Ph)CH(CH_3)_2$	4.65×10^{-3}	0.945	Vac.	3.60
$CH_3MgN(CH_2Ph)CH(CD_3)_2$	1.29×10^{-3}	0.986	Vac.	

Table 18. First-Order Rate Constants for Amides

Compound	$k(min^{-1})$	Temp(°C)	R
$CH_3MgN(C_6H_{11})_2$	2.43×10^{-3}	170	0.984
	4.48×10^{-3}	200	0.999
	3.47×10^{-2}	235	0.987
$PhMgN(C_6H_{11})_2$	1.67×10^{-3}	160	0.982
	1.86×10^{-3}	182	0.996
	2.72×10^{-3}	210	0.993
$CH_3MgNPr^i_2$	3.40×10^{-3}	85	0.999
	4.16×10^{-2}	95	0.968
	1.40×10^{-1}	110	0.958
$PhMgNPr^i_2$	1.04×10^{-3}	200	0.984
	1.87×10^{-3}	235	0.991
	1.08×10^{-2}	285	0.945
$PhCH_2MgNPr^i_2$	5.05×10^{-4}	70	0.968
	1.51×10^{-3}	90	0.992
	1.64×10^{-2}	155	0.996
$(CH_3)_2CH(MgCH_3)NCH_2Ph$	2.33×10^{-3}	175	0.997
	3.35×10^{-3}	200	0.999
	4.65×10^{-3}	223	0.945
$(CD_3)_2CH(MgCH_3)NCH_2Ph$	6.74×10^{-4}	200	0.987
	1.29×10^{-3}	223	0.986
	4.88×10^{-3}	252	0.995

Table 19. Activation Parameters for Amides

Compound	Ea (Kcal/mole)	A(sec^{-1})	R	$\Delta S^{\neq}$(eu) at 200°C
CH_3MgN- 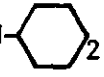 $_2$	18.1	2.55×10^{4}	0.947	-41.0
PhMgN-  $_2$	4.1	2.96×10^{-3}	0.970	-72.8
$CH_3MgNPr^i_2$	39.4	8.75×10^{19}	0.947	+30.2
$PhMgNPr^i_2$	14.7	8.61×10^{1}	0.978	-52.3
$PhCH_2MgNPr^i_2$	11.9	3.10×10^{2}	0.985	-49.8
$(CH_3)_2CHN(MgCH_3)CH_2Ph$	6.5	5.79×10^{-2}	0.999	-66.9
$(CD_3)_2CHN(MgCH_3)CH_2Ph$	19.0	5.54×10^{3}	0.993	-44.0
$(CH_3)_2CHN(MgCH_3)Ph$	6.5	3.70×10^{2}	0.999	-49.4
$(CD_3)_2CHN(MgCH_3)Ph$	11.0	3.2	0.967	-58.9

The Magnazines

The preparation and subsequent thermal decomposition of magnesium amides are illustrated in equations 15 and 16 for diisopropylamino(methyl)magnesium. Typically, a dialkyl or diarylmagnesium compound is allowed to react with a secondary amine containing a β-hydrogen in a one-to-one mole ratio in diethyl ether. The diethyl

$$(CH_3)_2Mg + HNPr^i_2 \longrightarrow CH_3MgNPr^i_2 + CH_4 \qquad (15)$$

$$CH_3MgNPr^i_2 \xrightarrow{\Delta} CH_4 + CH_2{=}CHCH_3 + (MgNPr^i)_x \qquad (16)$$

ether is removed under vacuum, and the amide is decomposed neat or in n-dodecane diluent. Detailed preparation data are given in the Experimental. The residue is usually a yellow solid with empirical formula $(MgNR')_x$.

Compounds of empirical formula $(MgNR')_x$ can also be prepared from primary amines as shown in equations 17 and 18. It is necessary to heat the intermediate amide to effect the abstraction of the second

$$(CH_3)_2Mg + H_2NBu^t \longrightarrow CH_3MgHNBu^t + CH_4 \qquad (17)$$

$$CH_3MgNHBu^t \xrightarrow{\Delta} CH_4 + (MgNBu^t)_x \qquad (18)$$

amino hydrogen.

A series of $(MgNR')_x$ compounds was prepared and analyzed by spectroscopic methods. The data is presented in Table 20, and typical ir and uv spectra are illustrated in Figure 9 for $(MgNPr^i)_x$.

The compound $(MgNPr^i)_x$ was studied in detail due to its ease of isolation and purification. This compound was crystallized twice from tetrahydrofuran (THF). Ebullioscopic molecular weight data on $(MgNPr^i)_x$ in THF exhibits an i-value of three over a wide concentration range (0.01 - 0.1 M) (Figure 10). Nmr data in d_8-THF and d_4-HOAc (Table 21) indicate that two types of isopropyl groups are present. Other compounds are included for reference.

Studies on the n-butyl compound $(MgNBu^n)_x$ gave similar results to the $(MgNPr^i)_x$ compound. This compound also gave an i-value equal to three at all concontrations in THF (Figure 11); however, the nmr spectra in d_8-THF and d_4-HOAc were complex indicating more than one type of n-butyl group. Since $(MgNBu^n)_x$ was also soluble in benzene, molecular weight data was collected both cryoscopically and ebullioscopically in that solvent (Figure 11).

The phenyl compound $(MgNPh)_x$ was studied ebullioscopically in tetrahydrofuran. An i-value of 3.4 was observed at all concentrations (Figure 12) (Appendices 3 and 4).

When $(MgNPr^i)_x$ was heated in acetic acid a new type of isopropyl group appeared at 1.16 (d) and 3.97 (m) δ (Ratio 5.8) at the expense of

Table 20. Analysis Data for $(MgNR')_x$ Compounds

RR[1]	Decomposition Temp. (°C)	Color	% Mg Found[a]	% Mg Calcd.	IR (Mg - N) in Nujol	UV in THF λ_{max} (nm)	ε[b]
Et	262	yellow	29.2	(36.1)	1840 1565	307	7200
n-Pr	325	dark yellow	18.4	(29.9)	1915 1560	insol.	
i-Pr	125	bright yellow	28.5	(29.9)	1855 1690	303 365	2160 sh
n-Bu	200	dark yellow	21.5	(25.5)	1875 1550	270	6530
s-Bu	115	yellow orange	23.6	(25.5)	1850 1650	insol.	
C_6H_{11}	200	yellow	20.2	(20.0)	1580 1500	238 309	10000 7700
Et, Ph	215, 217	yellow brown	17.1	(21.1)	----	240 290	28500 6690
H, Bu^t	250	yellow	19.5	(25.5)	1870 1665	insol.	
H, C_6H_4OMe	---	red brown	17.0	(16.7)	----	insol.	
H, 1-Ada	---	bright yellow	13.4	(14.0)	1580	insol.	

a) A low % Mg is due to coordinated diethyl ether solvent.

b) The extinction coefficient is based on the trimeric compound.

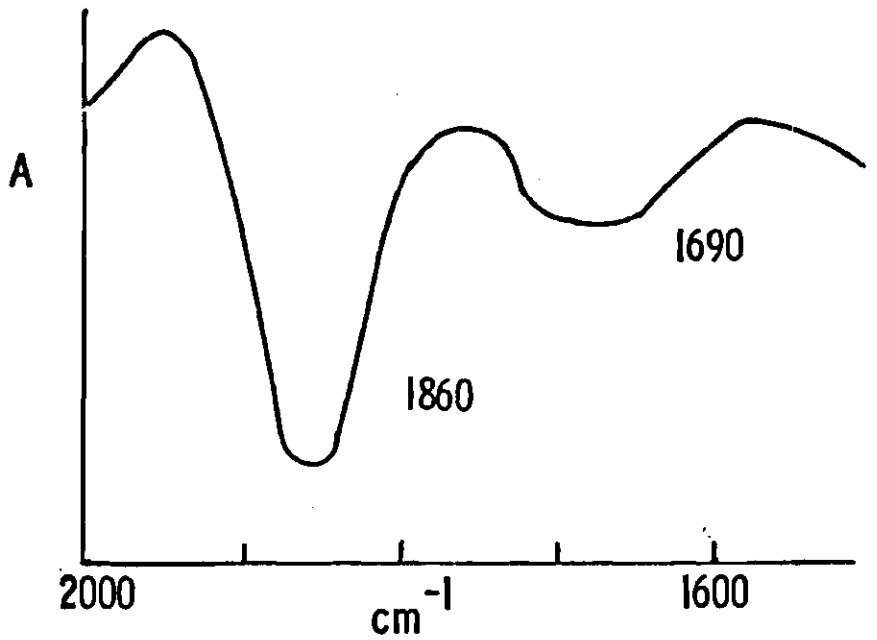

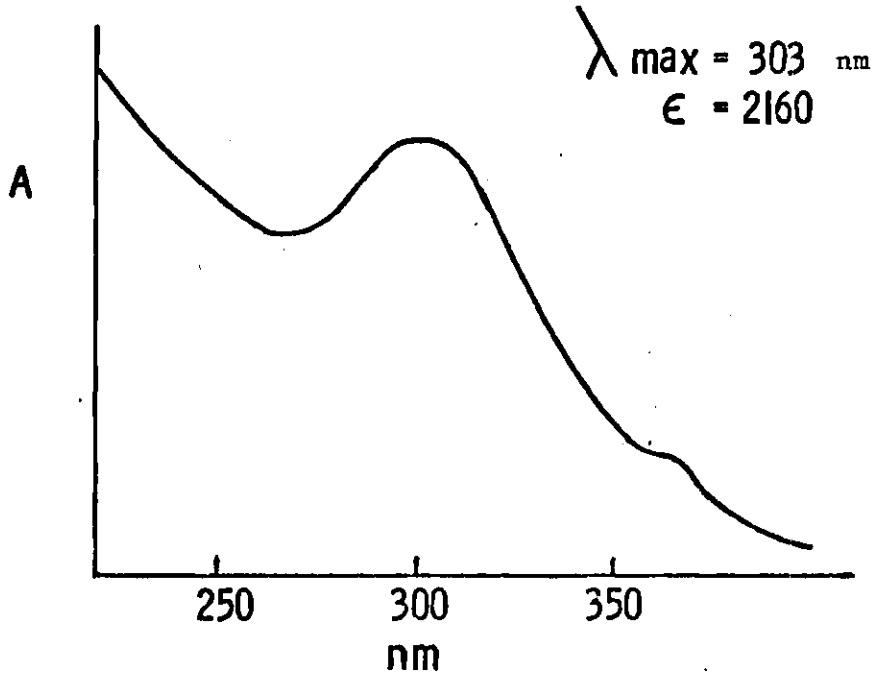

Figure 9. IR and UV Spectra of $(MgNPr^{i})_{x}$ in THF

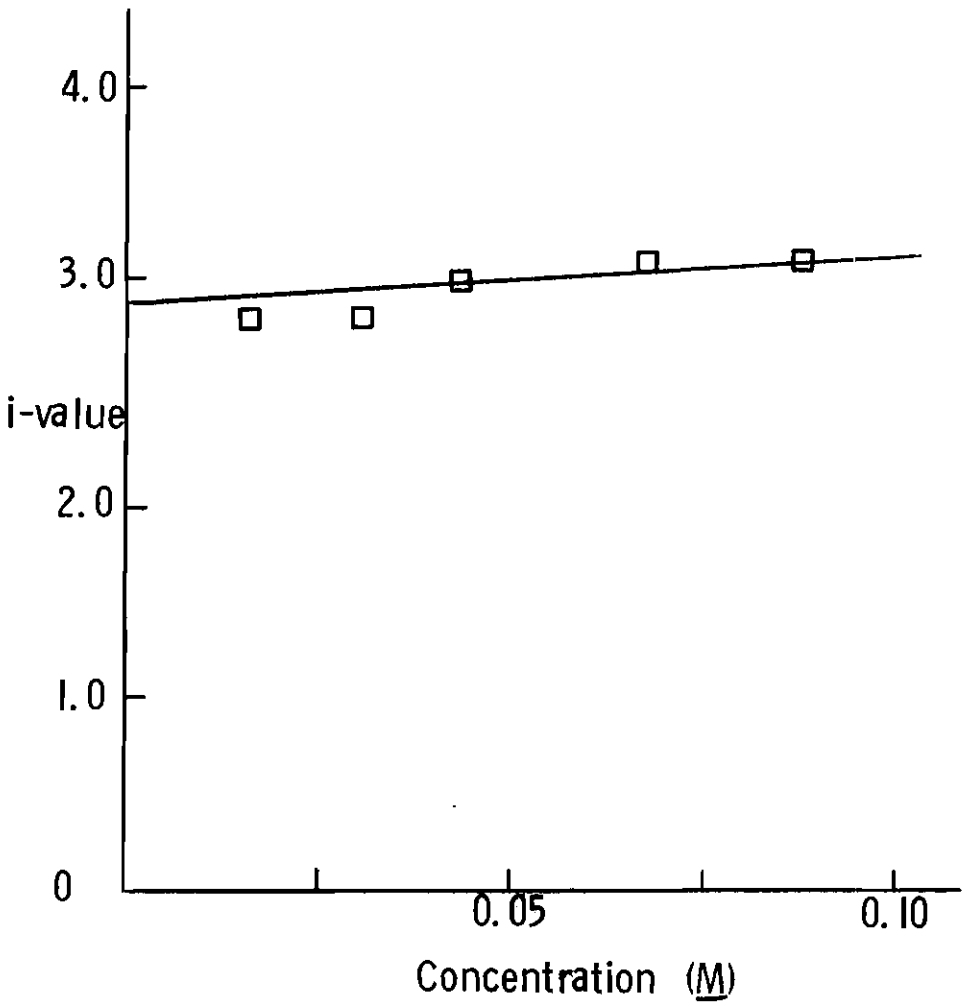

Figure 10. Ebullioscopic Molecular Weight Data for $(MgNPr^{i})_{x}$ in THF

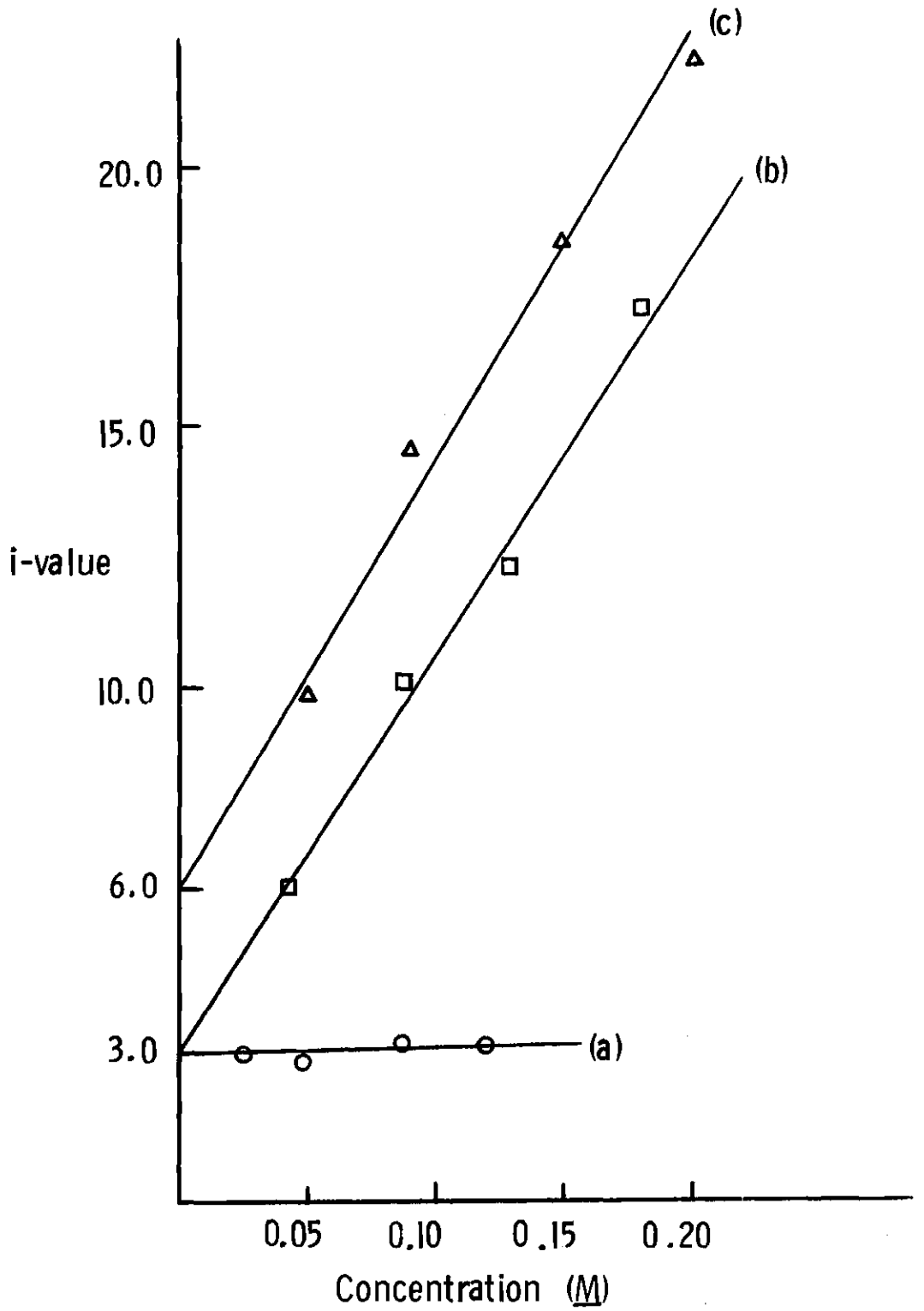

Figure 11. Molecular Weight Data for $(MgNBu^n)_x$

(a) ebullioscopically in THF, (b) ebullioscopically in benzene, and (c) cryoscopically in benzene.

Table 21. NMR Data for $(MgNPr^i)_x$ and Related Compounds

Compound	Solvent	Methyl Protons (δ)	Methine Proton (δ)
$(MgNPr^i)_x$	d_4-HOAc	1.34 d 1.42 d	3.59 m 4.29 m
	d_8-THF	0.97 d 1.03 d	3.45 m ---a
H_2NPr^i	THF	1.02 d	3.02 m
	HOAc	1.32 d	3.52 m
$Mg(NPr^i_2)_2$	THF	1.17 d	---a
	HOAc	1.36 d	3.56 m

[a] Signal obscured by solvent.

[b] The ratio of methyl to methine protons is 6:1.

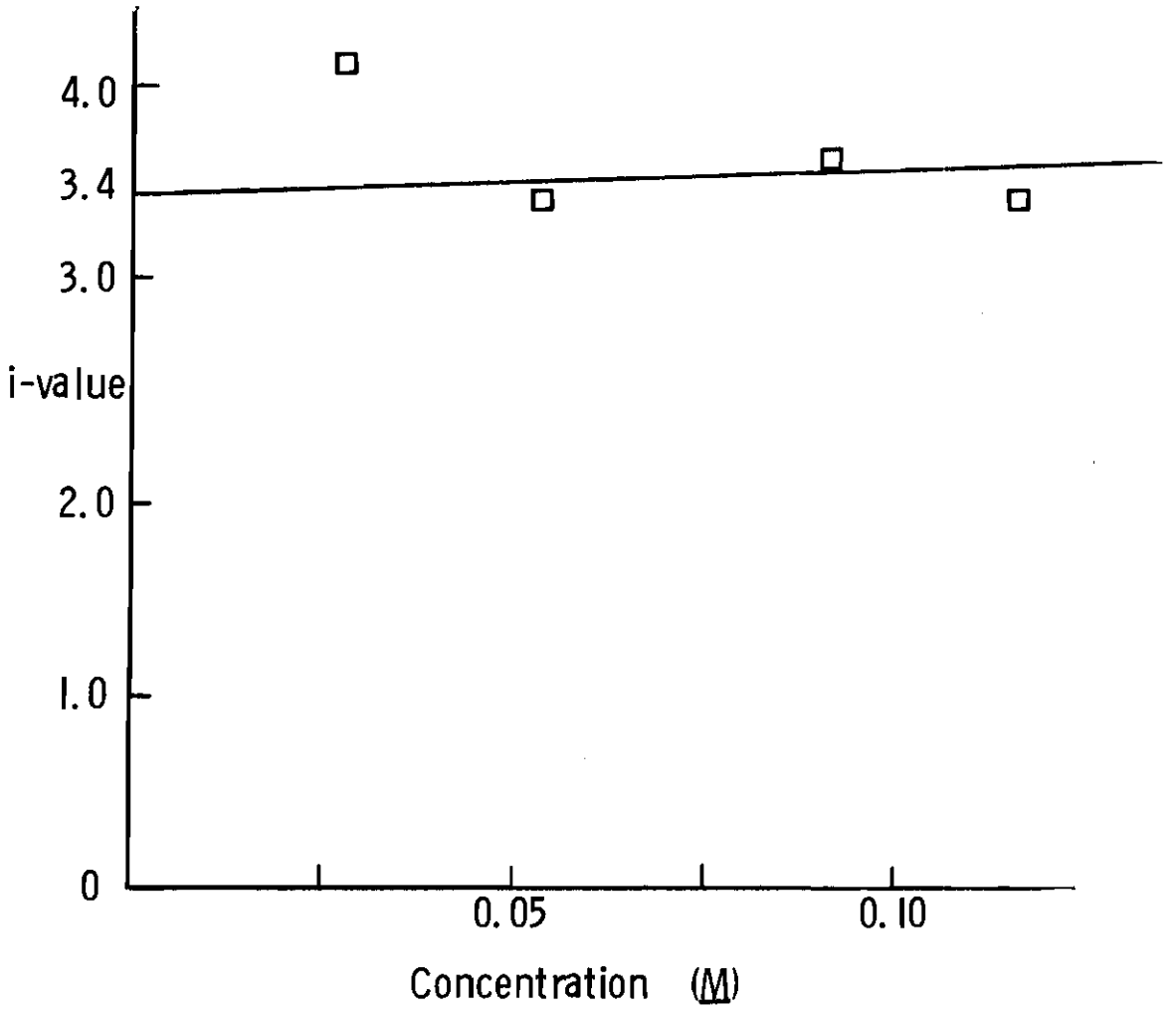

Figure 12. Ebullioscopic Molecular Weight Data for $(MgNPh)_x$ in THF

the original two isopropyl groups. Cryoscopic molecular weight data in acetic acid indicated the monomeric compound having the formula $AcOMgNHPr^i$ (Appendices 3 and 4). Isolation of this reaction product

$$(MgNPr^i)_x + x(HOAc) \longrightarrow x(AcOMg{-}\overset{H}{\overset{|}{N}}Pr^i) \qquad (19)$$

as the monoacetic acid salt gave a Mg/HOAc ratio equal to 0.945. Infrared analysis indicated no bands in the 2000 to 1650 cm^{-1} range.

Treatment of $(MgNPr^i)_x$ with methanol resulted in its conversion to a white solid (29.3% Mg; calcd. for $MgNPr^i$ = 29.9). Infrared analyses of this material in nujol and fluorolube exhibit absorption bands at 2850 (m), 1380 (m), 1160 (w), 1090 (s), 500 (m) and 350 (m) cm^{-1}. An acetic acid salt of the material exhibits a neutralization equivalent of 222 and a molecular ion in the mass spectrum at 222 m/e indicates the formation of the monoacetic acid salt of the dimer (molecular weight calcd. for $(MgNPr^i)_2 \cdot HOAc$ = 222).

The $(MgNR')_x$ compounds, in general, can be hydrolyzed to the corresponding primary amine. Equations 20 to 22 illustrate a method of converting 2° amines to 1° amines. The yield of cyclohexene was 87%, and hydrolysis gave a quantitative yield of cyclohexylamine. It should

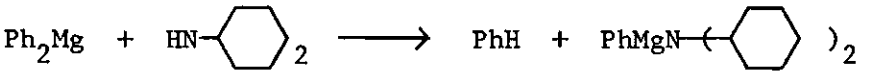

(20)

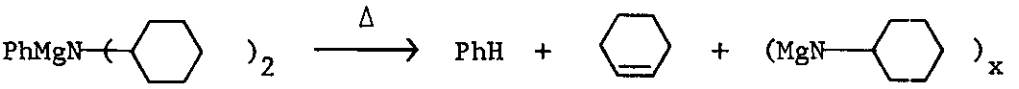

(21)

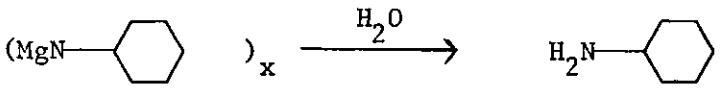

(22)

also be noted that the yellow residue prepared in equation 21 was identical to that material prepared by the thermal decomposition of dicyclohexylamino(methyl)magnesium (CH_3MgN–(⬡)$_2$).

Non-isothermal Kinetics

Constant temperature kinetics were conducted on several alkoxides and amides of magnesium via thermogravimetric analysis (TGA). First-order rate constants were determined by following the loss in weight of a tared sample of the alkoxide or amide due to the formation of volatile reaction products. A linear least squares plot of the natural logarithm of moles alkoxide or amide versus time in minutes gives first-order rate constants. The frequency factor (A) and experimental activation energy (E_a) were calculated from the Arrhenius theory $k = Ae^{-E_a/RT}$ with the aid of a least squares plot of ln k versus 1/T, where T is absolute temperature. The energies of activation were obtained by use of the equation $E_a = -R \times \text{slope}$, and the frequency factors were calculated from the Arrhenius equation where intercept = ln A. Having calcualted the E_a and A values for a given compound, it was then possible to calculate an entropy of activation ($\Delta S^{\neq}$) at a specific temperature using the equation of O'Connor and Nace,[28] $\Delta S^{\neq} = 2.303\ R \log (A) - 2.303\ R \log (K\ e\frac{k'T}{h})$, where k' is the Boltzman constant, h is Planck's constant, and K is the transmission coefficient

which is assumed to be unity.

Several methods exist for studying the kinetics of thermal decomposition reactions by dynamic thermogravimetry.[26] The methods of Freeman and Carroll[34] and Coats and Redfern[35] were applied to the thermal decomposition of magnesium alkoxides and amides. However, the correlations were very poor leading to a large scattering of data points. A better fit of the experimental data was obtained by the method of Achar.[36] This method applies to all reaction mechanisms, provided that the correct mechanism is known.

The Achar method is based on the equation $\ln(\frac{1}{f(\alpha)} \cdot \frac{d\alpha}{dT}) = \ln(A/B) - \frac{E_a}{RT}$, where R is the gas constant, α is the fraction of sample reacted in time t, and B is the heating rate. When the left-hand side of the equation is plotted against 1/T, a straight line is obtained from which E_a and A can be determined. The energy of activation is calculated from the equation $E_a = -R \times \text{slope}$, and A (the Arrhenius preexponential factor) is calculated from the equation $\ln(A/B) = \text{intercept}$. The form of $f(\alpha)$ depends on the nature of the reaction and must be determined prior to the application of the Achar equation.

Application of the procedure of Satava[37] led to the determination of the correct form of $f(\alpha)$. The most commonly used mechanisms were considered, and the experimental data gave the best straight line, as determined by the correlation coefficient (R), from a linear least squares plot of log g (α) versus 1/T, for the equation $-\ln(1 - \alpha) = kt$. Therefore, the form of $f(\alpha)$ as applied to the Achar equation was $f(\alpha) = (1 - \alpha)$, and the revised Achar equation becomes $\ln(\frac{1}{1-\alpha} \cdot \frac{d\alpha}{dT}) = \ln(A/B) - \frac{E_a}{RT}$ where $g(\alpha)$ is $\frac{1}{1-\alpha} \cdot \frac{d\alpha}{dT}$.

A typical DTA-TGA curve is illustrated in Figure 13 for diisopropylamino(phenyl)mangesium. Coordinated solvent (diethyl ether) was lost first and then the main decomposition occurs in one step with no apparent intermediate. Data for the Achar equation were taken from the steep portion of the curve.

Isothermal and non-isothermal calculations of E_a and A are summarized in Table 22. The average agreement between the E_a values calculated by the two methods was $\pm$ 20%. Only two compounds, dicyclohexylamino(methyl)magnesium and dicyclohexylamine(phenyl)-magnesium, lie significantly outside of this range ($\pm$ 38%). The best estimate of the "true" E_a is probably the average number obtained by the two methods. As expected, the agreement between the A values is not as good since a small fluctuation in slope can cause a large change in the intercept (Appendix 2).

Several interesting observations can be made employing the data in Table 22. For example, erythro-1,2-diphenyl-1-propylanilino(methyl)-magnesium has a lower E_a than the corresponding threo isomer. This observation reflects the greater steric hindrance involved in eclipsing two phenyl groups in the transition state leading to cis-1,2-diphenylpropene from the threo isomer compared to the steric hindrance involved in eclipsing a methyl and a phenyl group in the transition state leading to trans-1,2-diphenylpropene from the erythro isomer. A comparison of phenylmagnesium isopropoxide and benzylmagnesium isopropoxide indicates that the phenyl compound has a lower E_a. However, the opposite trend is observed when the diisopropylaminomagnesium amides are considered. The order of increasing E_a is $PhCH_2 < Ph < CH_3$. This apparent conflict

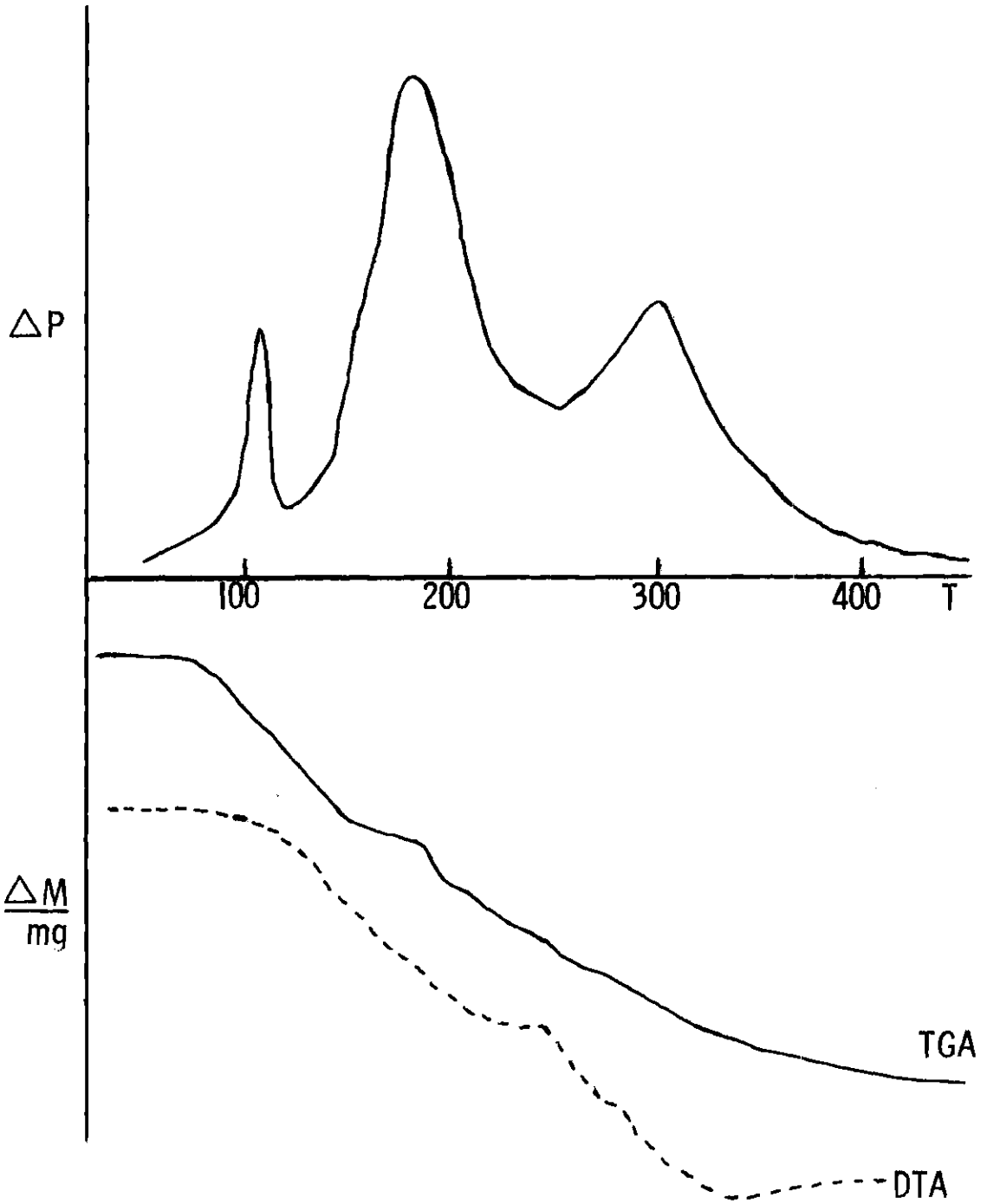

Figure 13. Vacuum DTA-TGA of $PhMgNPr^i_2 \cdot 0.89\ Et_2O$

Table 22. Activation Parameters for Alkoxides and Amides

Compound	E_a (Kcal/mole) at Constant T	E_a (Kcal/mole) at Variable T	A (sec^{-1}) at Constant T	A (sec^{-1}) at Variable T
threo $PhCH_3CHCHPhOMgCH_3 \cdot 0.50\ Et_2O$	19.4	26.7	1.15×10^4	9.52×10^6
erythro $PhCH_3CHCHPhOMgCH_3 \cdot 0.50\ Et_2O$	15.5	9.2	1.26×10^3	8.8
CH_3MgO-⬡	14.6	13.7	1.29×10^2	5.95×10^{-4}
$PhMgOPr^i \cdot 0.16\ Et_2O$	11.8	12.7	3.3	52
$PhCH_2MgOPr^i \cdot 0.56\ Et_2O$	24.7	28.6	2.83×10^6	2.91×10^8
CH_3MgN-⬡$_2$	18.1	8.3	2.55×10^4	9.9×10^{-1}
$PhMgN$-⬡$_2 \cdot 0.94\ PhH$	4.1	9.2	2.96×10^{-3}	1.1
$CH_3MgNPr^i_2$	39.4	23.2	8.35×10^{19}	2.10×10^{10}
$PhMgNPr^i_2 \cdot 0.89\ Et_2O$	14.7	9.3	86	3.3
$PhCH_2MgNPr^i_2 \cdot 1.17\ Et_2O$	11.7	9.2	3.10×10^2	60
CH_3MgSBu^n	13.2	18.7	4.5×10^1	1.11×10^5

in trends can be explained in terms of a variable Ei mechanism as proposed previously.[1] In the case of the alkoxides the transition state exhibits some carbanion character at C_β and magnesium-aryl cleavage is advanced. Therefore, phenylmagnesium isopropoxide has a lower E_a than the benzyl compound since phenyl carbanion is more reactive than benzyl carbanion. On the other hand, the magnesium-amides decompose via a more synchronous transition state. The observed order of increasing E_a's ($PhCH_2 < Ph < CH_3$) indicates that the most stable incipient carbanion is responsible for the lowest E_a. The decomposition reaction was also applied to a representative mercaptan. The E_a calculated for n-butylthio(methyl)magnesium is the same as that for the alkoxides and amides. The rather small values for the Arrhenius factors (A) results in large negative entropies of activation ($\Delta S^{\neq}$) for the alkoxides and amides of magnesium. These entropies of activation fall in the range -32 to -73 e.u. at 200°C. The only exception is diisopropylamino(methyl)magnesium which gave a positive $\Delta S^{\neq}$ (+30 e.u.).

CHAPTER IV

DISCUSSION

The Alkoxides

The thermal decomposition of metal alkoxides of magnesium, aluminum, and zinc proceeds via a unimolecular, cyclic, six-center transition state involving the abstraction of a β-hydrogen from the alkoxide portion by an incipient carbanion to yield a hydrocarbon, an olefin, and a metal oxide. Several studies support this conclusion. The first-order rate constants observed in the decomposition reaction and the fact that no intermediate is observed indicates that the reaction is unimolecular. The syn nature of the elimination reaction is suggested by the decomposition of methylmagnesium erythro and threo 1,2-diphenyl-1-propoxide to give only trans and cis-1,2-diphenylpropene, respectively. The transition state for the threo compound appears more hindered than that of the erythro compound since the threo compound decomposes at a higher temperature and has a higher E_a. The large negative entropies of activation (-32 to -59 e.u.) show that several degrees of freedom are restricted in the transition state and that the transition state is probably cyclic in nature. All these observations are consistent with a cyclic, six-center transition state.

It is interesting that the kinetic isotope effect study shows that the rate-determining step of the decomposition reaction is not abstraction of the β-hydrogen. Instead, the observed inverse isotope

effects imply a more complicated mechansim than suggested in Figure 4. We postulate a spectrum of Ei transition states as described in Figure 14 in analogy to the E_1 - E_2 - E_{1cb} continuum[38] to explain the results of the isotope study. This theory visualizes an Ei mechanism

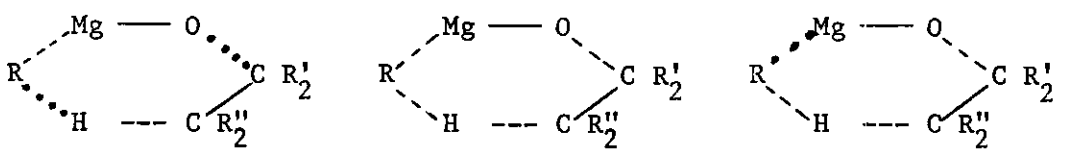

Paenecarbonium extreme | Central | Paenecarbanion extreme

(The strength of the bond increases in the order: ... --- ___).

Figure 14. Variable Ei Transition States

that varies from the extreme of mostly C_α - O rupture and very little C_β - H breaking (paenecarbonium - almost carbonium like) to a central position that is essentially a synchronous breaking of C_α - O and C_β - H bonds to the extreme of mostly C_β - H rupture and very little C_α - O breaking (paenecarbanion - almost carbanion like). The variable Ei transition state as described in Figure 14 postulates that, for an Ei reaction, the lowest energy path from reactants to products is achieved by an optimum adjustment between the degrees of C_α - O and

C_β - H bond rupture at the transition state. The optimum adjustment involves considerable breaking of the bond more easily broken and little breaking of the bond requiring more energy to sever. However, both bonds must be broken before the single reaction step is complete.

The variable Ei transition state theory predicts the maximum kinetic isotope effect for the central transition state in Figure 14. A value for kH/kD > 1 would be expected for the essentially synchronous breaking of C_α - O and C_β - H bonds. The Chugaev reaction (kH/kD = 2.0)[31] and the Acetate Pyrolysis reaction (kH/kD ≃ 2)[31] appear to have a transition state more closely related to this central one.

The kinetic isotope effect for the paenecarbanion transition state would be smaller than that for the central transition state and, in fact, would lead to an inverse isotope effect (kH/kD < 1) in the extreme case.[39] An explanation for the observed inverse isotope effects is based on the following model. In the paenecarbanion transition state considerable C-H bond breaking has occurred due to the abstraction of a proton(or deuterium) from the β-carbon by the incipient carbanion on the metal. This leaves a carbanion at the β-carbon with two remaining C-H (D) bonds. One of these remaining C-H (D) bonds is taken as a hypothetical reactant molecule. It has only a single vibrational frequency (V) which can be calculated for each isotopic species from the expression for a simple harmonic oscillator, namely $V = \frac{1}{2\pi}\sqrt{f/m}$, where f is the force constant, a measure of the stiffness of the bond, and m is the reduced mass. The one vibrational mode becomes the motion along the reaction coordinate in the transition state. Since carbon makes a small contribution to the reduced mass compared to hydrogen or

deuterium, the isotopic ratio of frequencies becomes $\frac{VD}{VH} = \frac{1}{\sqrt{2}}$. The assumption is made that the force constants for a C-H and C-D bond both in the ground state and in the transition state are essentially the same. Of course, there is a change in force constants in going to the transition state since the comparison is between an aliphatic and a vinylic C-H (C-D) bond due to rehybridization at the carbanionic carbon. Therefore, the difference in zero-point vibrational energy between the transition state and the ground state for the deuterated compound is lower than the corresponding energy difference for the hydrogen compound, giving rise to a larger rate constant for the deuterated compound and thus an inverse isotope effect.

Of course, this model represents a considerable simplification. Bonding at six sites is actually changing. However, the major changes are occurring at the carbanion R^- site due to cleavage of the Mg-R bond and at the β-carbon due to C-H bond cleavage. The variable basicity of the carbanion R^- also has an effect. In the paenecarbanion transition state the order of basicity of the carbanion R^- must be greater for hydrogen than for magnesium.

The paenecarbonium transition state resembles an E_1-type mechanism and would have a similar isotope effect. This is, the isotope effect would be less than that for the central transition state, but greater than unity (kH/kD for E_1 = 1 to 3).[40] No example of this extreme Ei transition state is known as yet.

One kinetic isotope effect was found to be greater than unity. The benzylmagnesium isopropoxide compounds gave kH/kD = 1.30. Evidently, in this case the transition state lies closer to the synchronous

transition state.

The variable Ei mechanism explains the apparent conflict in trends in decomposition temperatures. The series of 1,1-diphenylzinc and magnesium compounds shows that the decomposition temperature is independent of the nature of the incipient carbanion base. Apparently, there is considerable carbanion character in these cases, and the decomposition rate is determined by the rate of rehybridization of the carbanion to give the olefin product. The isoproxy magnesium and cyclohexyloxy zinc compounds show a lower decomposition temperature when the incipient carbanion is methyl. In this case the transition state must lie more toward the central one in that the breakage of the C_β - H bond becomes more important. The stronger base (methyl carbanion) can remove the proton from the β-carbon more easily. The nature of the transition state also depends on the type of metal since the cyclohexyloxy magnesium compounds decompose at the same temperature (compared to the cyclohexyloxy zinc compounds). The phenyl magnesium alkoxides give the lowest decomposition temperatures for formation of the most stable carbanion at the β-carbon while the methylmagnesium alkoxides show the reverse order. The explanation here is that for the phenyl magnesium alkoxides there is more carbanion character in the transition state due to a greater portion of C_β - H bond breaking, whereas for the methyl magnesium alkoxides there is less C_β - H bond rupture and less carbanion character. The reversal in decomposition order can then be explained in terms of steric hindrance in the transition state. It is more difficult for bulky alkoxy groups to achieve the correct geometry in the transition state. Therefore, the simplest olefins are

formed at the lowest decomposition temperatures.

Eclipsing effects were studied for the case of the methylmagnesium erythro and threo-1,2-diphenyl-1-propoxides. In the transition state describing the formation of the cis-olefin from erythro substrate, the phenyl groups in C_α and C_β are brought into a partially eclipsed arrangement. The extent of eclipsing depends on the degree of C=C character. Because phenyl groups are large, steric strain is introduced into the transition state when they eclipse. Obviously, the adverse energy effect is greater the flatter the transition state. On the other hand, the eclipsing of a methyl group and a phenyl group in the formation of trans olefin from erythro substrate has a smaller adverse effect since a methyl group is smaller than a phenyl group. Therefore, the erythro/threo rate ratio is a measure of the C=C character in the transition state.[41] The calculation at 200°C gives an erythro/threo rate ratio equal to 7.19. The magnitude of the result shows some C=C character in the transition state. Hence, the paenecarbanion transition state appears to apply here since a purely central transition state would require a considerably larger erythro/threo rate ratio (perhaps 15 to 50).

Comparisons can be made between the Chugaev and Acetate Pyrolysis reactions and the thermal decomposition of alkoxides. The advantages of the newer method include (1) higher yields and equally good stereochemistry and (2) a simpler method in that the alkoxide is easily prepared and does not have to be isolated or purified. The major disadvantage is the limited number of functional groups compatible with an organometallic compound. However, this disadvantage can be

overcome to some extent. The alkoxide can be formed by reaction of the alcohol with a base e.g., diisopropylaminomagnesium bromide as shown in equations 23 and 24. The resultant alkoxide is the same as that prepared from the reaction of methylmagnesium bromide with the alcohol except that the problem of an active organometallic compound

$$CH_3MgBr + HNPr^i_2 \longrightarrow CH_4 + Pr^i_2NMgBr \qquad (23)$$

$$Pr^i_2NMgBr + R'OH \longrightarrow HNPr^i_2 + R'OMgBr \qquad (24)$$

has been avoided. In some cases the problem can be employed to advantage as in the preparation of the alkoxide methylmagnesium 1,1-diphenylethoxide directly by the reaction of dimethylmagnesium with benzophenone.

The Amides

The thermal decomposition of amides proceeds via a unimolecular, cyclic, six-center transition state involving the abstraction of a β-hydrogen by an incipient carbanion to yield a hydrocarbon, an olefin and a residue with empirical formula $(MNR')_x$. The first-order rate constants and the fact that no intermediate is observed indicate that the reaction is unimolecular. The syn nature of the elimination reaction is suggested by the decomposition of threo-1,2-diphenyl-1-propyl-1-anilino(methyl)magnesium to give only cis-1,2-diphenylpropene.

The kinetic isotope effect study shows that the rate-determining step involves the abstraction of the β-hydrogen. In the previous study on the thermal decomposition of the alkoxides of magnesium, zinc, and aluminum an inverse isotope effect (kH/kD < 1) was found and a variable Ei mechanism was proposed to explain the result. For the amides, the transition state is close to a central, synchronous Ei transition state since the kH/kD ratio is about three.

Comparisons can be made between the Hoffman elimination and Cope elimination reactions and the thermal decomposition of amides. The advantages of the newer method include (1) higher yields of olefin and equally good stereochemistry, (2) a simpler method in that the amide is easily prepared and does not have to be isolated or purified, and (3) the method is selective for secondary amines. The major disadvantage is the limited number of functional groups compatible with an organometallic compound.

The Magnazines

Molecular association data on the compound $(MgNPr^i)_x$ in tetrahydrofuran indicates that it exists as a trimeric species at all concentrations. This fact suggests a cyclic structure for $(MgNPr^i)_3$ as shown below (Figure 15 where R = Pr^i). There is the possibility

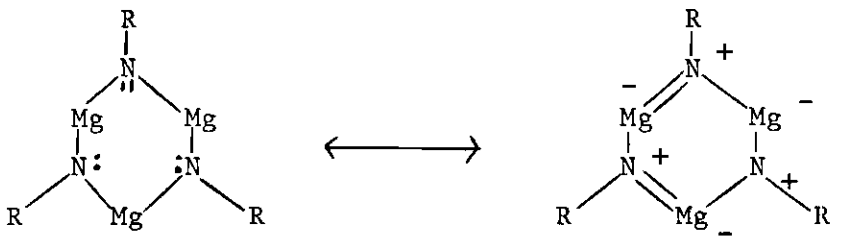

Figure 15. Resonance Structures of N-Substituted Magnazine

that this compound has pseudo-aromatic character analogous to N-substituted borazines by virtue of donation of the lone pair on nitrogen (a Lewis base) onto the magnesium (a Lewis acid). We have assigned the name magnazine to the general class of compounds illustrated in Figure 15 in order to emphasize the presence of magnesium and to be compatible with borazine terminology;[42] hence the name N,N',N'' triisopropylmagnazine.

Other data support the cyclic pseudo-aromatic structure of N,N',N''-triisopropylmagnazine. The infrared bonds at 1855 and 1690 cm^{-1} are indications of Mg = N double bond character. These infrared bands are not found in the starting material, diisopropylamino(methyl)-magnesium ($CH_3MgNPr^i_2$), and are characteristic of the yellow residue only. Any reaction, as with acetic acid or methanol, causes these bands to disappear. These bands are similar when the spectra are obtained in THF or nujol mulls. Additional evidence of a cyclic pseudo-aromatic compound lies in the fact that simple amines, as well as the starting amide, give only end absorption in the uv spectrum due to the $n \rightarrow \sigma^*$ transition at about λ_{max} = 200 nm. The N,N',N''-triisopropylmagnazine, however, gives a band at λ_{max} = 303 nm with a shoulder at λ_{max} = 365 nm in addition to end absorption. These bands illustrate π character since the bands must be due to $\pi \rightarrow \pi^*$ type transitions.

If these new compounds are indeed planar compounds as proposed (Figure 15), then only one type of isopropyl group should be observed in the nmr spectrum and herein lies the problem in absolute identification. Also, if the compound has aromatic character, a ring current effect should be noted in the nmr spectrum in that the methine proton of the

isopropyl group should shift downfield relative to the corresponding proton in such compounds as isopropylamine or bisdiisopropylaminomagnesium ($Mg(NPr^i_2)_2$). However, the nmr spectrum in d_8-THF of N,N',N''-triisopropylmagnazine shows two types of isopropyl groups (two sets of doublets representing the CH_3 groups) in one-to-one ratio. On the other hand, only one of the methine protons could be observed; the signal for the other was probably obscured by solvent. Also, the nmr spectrum in d_4-HOAc shows two types of isopropyl groups in one-to-one ratio. Here both methine protons are observed as septets. The methine proton at 4.29 δ displays a ring current effect in that it is shifted downfield relative to an average value of 3.50 to 3.60 δ for the same proton in bisdiisopropylaminomagnesium or isopropylamine in acetic acid. The other methine proton at 3.59 δ falls in the range of a normal isopropyl group. The conclusion is that two species are present - a planar, pseudo-aromatic one and a non-planar, non-aromatic one.

The molecular weight data describing $(MgNBu)_x$ in benzene gave more information concerning the existence of two species (Figure 11). In refluxing THF the n-butyl compound was found to be trimeric at all concentrations as expected. However, in benzene at low temperature the compound was highly associated. Extrapolation to infinite dilution however gave an i-value equal to six. On the other hand, molecular weight data in refluxing benzene gave an associated species and the i-value extrapolated to three at infinite dilution.

The N,N',N''-tri-n-butylmagnazine data suggest that there is an equilibrium between the trimer and a more highly associated species - a hexamer - as illustrated in Figure 16. In strongly coordinating

solvent such as THF the equilibrium lies toward the planar trimer, especially at higher temperature and in dilute solution, since the electron lone pairs of THF would compete favorably with the electron lone pairs on nitrogen for coordination to the magnesium. The hexameric structure would be expected to be cleaved by THF to give trimeric molecules. In benzene there is no competition for coordination sites on magnesium between the solvent and the lone pair on nitrogen, and the material is highly associated. The basic unit, however, is still the cyclic trimer.

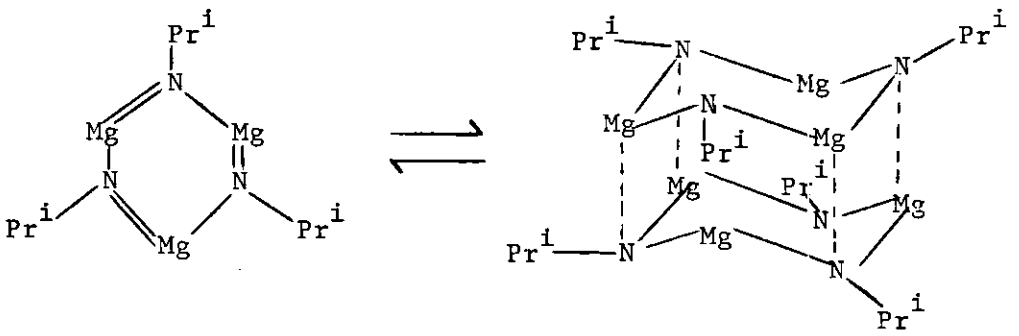

Figure 16. Solution Composition of $(MgNPr^i)_3$

A similar phenomenon occurs in acetic acid. The trimer-hexamer equilibrium exists, but the situation is complicated by the fact that in a short time the material is attacked by the solvent. The acetic acid apparently adds across the Mg = N bond to give $AcOMgNHPr^i$. The infrared spectrum of this product shows the absence of Mg = N character.

An ebullioscopic molecular weight study of N,N',N''-triphenylmagnazine in THF adds additional support for a trimer-hexamer equilibrium

The i-value is 3.4 at all concentrations (Figure 12). In this case there is a trimer-hexamer equilibrium, but the equilibrium does not favor entirely the trimer as it does for N,N',N''-triisopropylmagnazine and N,N',N''-tri-n-butylmagnazine. In fact, the infrared spectrum indicates no Mg = N character, and the uv data shows only absorptions due to the phenyl substituent. Apparently, the N,N',N''-triphenylmagnazine exists as an associated species, not as the trimer. This conclusion is not unreasonable since the electron withdrawing electronic effect of the phenyl substituent would destabilize the trimer relative to the hexamer by electron withdrawal from the ring.

It is interesting to compare the N-substituted magnazines with their boron and aluminum analogs. The borazines have been well characterized and are known to be trimeric, planar aromatic compounds.[43] The poly (N-alkyliminoalanes), on the other hand, have no π character and exist as oligomers of -HAlNR- units with three dimensional structures composed of four to six membered rings. Specifically, a cage structure was found for hexakis (isopropyliminoalane) $(HAlNPr^{i})_6$ by X-ray diffraction on a single crystal.[44] Evidently, the N-substituted magnazines have properties somewhere between these extremes. They possess π character as evidenced by infrared and ultraviolet absorption data in addition to molecular weight data both facts which support the cyclic structure similar to the borazines. However, the nmr data indicate that the degree of planarity and aromatic character is not as advanced as in the borazines but certainly more advanced than in the poly (N-alkyliminoalanes). The trimer-hexamer equilibrium reflects the instability of the aromatic structure relative to the more associated

hexamer in analogy to the poly (N-alkyliminoalanes).

When the trimer-hexamer mixture of $(MgNPr^i)_x$ was treated with methanol so as to exclude all oxygen, the yellow material was converted into a white solid. Analysis of this material as a monoacetic acid salt indicated that it was the dimer $(MgNPr^i)_2 \cdot HOAc$. The original species from methanol unsolvated by acetic acid could be more associated, perhaps as a cubane-like structure; however, the insoluble and nonvolatile nature of the compound would not allow any molecular weight determination.

The N-substituted magnazines have several common features. They are usually yellow and are very air and moisture sensitive requiring that they be handled under an inert atmosphere. Hydrolysis gives the corresponding primary amine in good yield. Elemental analysis data is not reproducible probably due to the formation of magnesium nitride and incomplete combustion. Since the compounds are not volatile, it was not possible to obtain useful mass spectral data. Two characteristic infrared bands occur in the range 2000-1500 cm^{-1}. At least one absorption occurs in the ultraviolet-visible spectrum at about λ_{max} = 300 nm.

Crystallization of all soluble magnazines from solvents such as n-dodecane, THF, and benzene give the same type crystals - very thin flat plates that are unsuitable for single crystal X-ray study. In fact, when the yellow crystals come out of solution, they are very difficult to redissolve indicating that the species is associating as it crystallizes. For example, the magnazine prepared from 1-adamantanamine and dimethylmagnesium (MgN-Ada-1) is soluble in n-dodecane when first prepared. The material can be induced to crystallize from a dodecane/

toluene cosolvent mixture at room temperature as very thin, flat yellow plates which are insoluble in THF. After a few days the compound precipitates completely from n-dodecane solution leaving a colorless supernatant liquid. Isolation of the yellow solid by diethyl ether washing results in a material that is then insoluble in benzene and THF. Obviously, the material has associated to the point that it is no longer soluble. Slow evaporation of the n-dodecane solvent on a high vacuum line at room temperature yielded an amorphous glass as determined by X-ray diffraction data indicating a polymeric material. It was hoped that the sterically bulky adamantyl group would prevent association.

Non-isothermal Kinetics

The activation parameters for the thermal decomposition of the alkoxides and amides of magnesium summarized in Table 22 calculated via isothermal and non-isothermal methods show that the agreement between the energies of activation (E_a) is about $\pm$ 20%.

The advantages of the non-isothermal method are obvious. They include (1) smaller sample size, (2) less time to obtain the data, and (3) better accuracy due to the larger temperature range covered, greater number of data points, and less decomposition in reaching the desired temperature.

The alkoxides and amides of magnesium were found to follow a unimolecular decay law, which in integrated form is $-\ln(1 - \alpha) = kt$, where α is the fraction of material reacted, and k is the Arrhenius rate constant. This decay law indicated that the rate-controlling

process was random nucleation, one nucleus on each particle.[37] That is, reactions of each individual crystal results from the formation of a single nucleus on the surface of that particular particle. Thus, the decomposition rate is controlled by the nucleation process. Since each individual particle in the assemblage may be nucleated with equal probability, the rate of decomposition obeys first-order kinetics.[45]

CHAPTER V

CONCLUSIONS

Alkoxides of magnesium, zinc, and aluminum thermally decompose at 250-350°C to give hydrocarbon, an olefin, and a metal oxide. Kinetic and stereochemical studies indicate that a cyclic, unimolecular six-center transition state is involved. This reaction represents the conversion of an alcohol to an olefin in a syn stereochemical manner and compares favorably as an alternative to the Chugaev and acetate pyrolysis reactions.

Similarly, magnesium, zinc, and aluminum amides thermally decompose at 150-250°C to give hydrocarbon, an olefin, and a residue with empirical formula $(MNR')_x$. Kinetic and stereochemical studies indicate that a cyclic, unimolecular six-center transition state is involved. This reaction represents the conversion of a secondary amine to an olefin in a syn stereochemical manner and compares favorably as an alternative to the Hoffman elimination and Cope elimination reactions.

The compounds $(MgNR')_3$ constitute a new class of pseudo-aromatic compounds analogous to the borazines: N-substituted magnazines. Infrared, ultraviolet-visible, and molecular weight data support this conclusion. However, nmr data indicates that the solution composition is complicated by a trimer-hexamer equilibrium. Hydrolysis of an N-substituted magnazine results in the formation of the

corresponding primary amine in nearly quantitative yield.

The thermal decomposition of the alkoxides and amides of magnesium have been studied by vacuum TGA under both isothermal and non-isothermal conditions. These compounds were found to follow a unimolecular decay law, which in integrated form is $-\ln(1 - \alpha) = kt$, where α is the fraction of material reacted, and k is the Arrhenius rate constant. The rate-controlling process is random nucleation, one nucleus on each particle. Energies of activation calculated by isothermal and non-isothermal methods agree to within $\pm$ 20%.

CHAPTER VI

RECOMMENDATIONS FOR FURTHER RESEARCH

1. Preparation and characterization of the dialkylphosphino derivatives of magnesium, zinc, and aluminum.
2. The thermal decomposition of the dialkylphosphino compounds.
3. Preparation and characterization of compounds with the empirical formula $(MgPR)_x$.

APPENDIX 1

OPERATING INSTRUCTIONS FOR THE METTLER THERMOANALYZER II DTA-TGA

General Considerations

The Mettler Thermoanalyzer II DTA-TGA machine has been adapted to run under a static or dynamic vacuum, or under a static or dynamic argon (or nitrogen) atmosphere. The suggestions listed below for efficient operation are the results of several workers' experience and were obtained at considerable cost.

Care of the Furnace

It is important to handle the quartz furnace with a cotton glove. Oil from the skin can cause the furnace to crack at elevated temperatures. Current price of a new furnace is $850. The furnace can be cleaned with dilute acid and acetone. Care must be exercised to keep acid from the metal portions of the furnace. The furnace is dried with the heat gun before replacing on the balance.

Preconditioning of Aluminum Crucibles

Most DTA-TGA determinations are performed in cylindrical aluminum crucibles with a fritted disk and cap. They are cleaned by brief exposure to dilute acid and final rinsing with acetone. The crucibles are preconditioned by heating in a Muffle furnace at 250°C for several hours prior to use. At that time they are cooled in the glass container provided and weighed.

Preparation of a Reference Crucible

A sample of aluminum oxide (Al_2O_3) is dried in the Muffle furnace at 400°C for several hours. A sample is then loaded into a pretreated, weighed crucible. The reference crucible fits on the right-hand side of the stick (the ceramic rod containing the thermocouple which supports both crucibles). The placement is arbitrary. When the crucible is on the right-hand side of the stick, however, an endothermic process (as shown by Channel 5) is one in which the printer goes to the right on the chart. The current reference crucible contains 75.1 mg Al_2O_3.

Preparation of a Sample Crucible

A pretreated, weighed crucible is taken into the glove box in its glass container. The sample is finely ground in an Agar mortar and then transferred to the crucible using a vibrator to insure uniform particle size. The glass container is capped and removed from the glove box for weighing. If the weight of the sample is not correct, then the crucible is returned to the glove box and the necessary correction made. A typical sample size varies from 20 to 100 mg. An average value of 50 mg is probably best.

Centering of the Stick

The stick that supports the crucibles occasionally needs recentering. The furnace is removed, and a sample crucible and reference crucible are placed on the stick. The viewing tube is placed over the stick, and the balance is released. The stick should center in the target. If it does not, the stick can be correctly positioned by gently moving it with forceps while the balance is clamped.

The stick can be cleaned by gentle wiping with a tissue. It is not removed from the machine for cleaning.

Functions of the Channels

There are six channels on the DTA-TGA printer. Channel 1 is a pressure gauge after the right-hand nitrogen trap, and Channel 2 is a pressure gauge before the liquid nitrogen trap. A peak that appears in the spectrum on Channel 2 that does not appear on Channel 1 indicates a condensable gas. Channels 3 and 4 are weight (TGA) indicators. Channel 4 is ten times more sensitive than Channel 3. Channel 5 is the DTA channel. Movement to the right on the chart indicates an endothermic process. Channel 6 is the temperature channel. The correct temperature is read from Channel 6 using the DTA-TGA ruler.

Operating Instructions for Vacuum DTA-TGA

The following instructions refer to Figure 17. The stopcock numbers in the figure and on the machine are the same.

The first step in running DTA-TGA is to prepare the machine. The condition of the machine should be noted. It should be clean and may be under vacuum or nitrogen atmosphere. If the furnace is clean stopcocks 1, 2, 3, 4, 5, and 7 are closed and the diffusion pump started with liquid nitrogen in only the trap closest to the pump (left one). The furnace should be checked to make sure it has been tightened down. Stopcock 5 is slowly opened. Stopcock 3 is then opened slowly so as to get no bubbles in the mercury of the manometer. If this should happen, close Stopcock 3 again and open the manometer at the O-ring screw clamp to release the pressure and try again. The

next step is crucial. Stopcock 1 should be opened very slowly to the point that only a slight deflection in the manometer is noticed. Another way to watch is to look for the grease at the stopcock to just begin to pull. The stopcock should be left in this position for 10 minutes and then slowly opened further in small increments over the next 20 minutes. This stopcock opens directly into the balance area. A sudden outgassing (or inflow of gas) causes the wire weights on the balance to tangle. If this occurs, the balance has to be removed, and the weights replaced in their proper positions. This operation is tedious, time consuming, and can be expensive since it is often necessary to break the stick (current cost $80) in order to remove the balance. Also, the assistance of the electronics shop is required. The DTA-TGA is evacuated overnight to remove air and moisture. After the preliminary degassing operation has been accomplished, consecutive runs can be made without this requirement of overnight degassing.

When the DTA-TGA has been evacuated overnight or if the furnace is not clean, the next step is to fill the balance with argon. Stopcock 5 is closed. The balance is filled with argon by opening the tank, adjusting the regulator to only 2 psi, turning the needle valve one quarter turn, and opening Stopcock 4 to allow a reading just above 20 on the flowmeter. This flow must be constantly adjusted during the filling. When the balance is full of argon as determined by the manometer, Stopcock 2 (to the mineral oil bubbler) is slowly opened, and the argon is allowed to slowly bubble out for 5 minutes. At this time Stopcocks 2 and 4 are closed, and the needle valve and main argon tank valve are closed. The mineral oil bubbler is removed to

facilitate handling the liquid nitrogen traps.

The above procedure usually takes 20 to 30 minutes. During this period, in order to conserve time, the sample can also be prepared for loading on the balance. The weighed sample crucible in the glass container, a small pair of forceps, and the DTA-TGA wrench are placed on the metal rim of the furnace. The DTA-TGA glove box is positioned over the furnace (without furnace shield), and the glove box is flushed with nitrogen for twenty minutes. If the glove box fits perfectly, its nitrogen bubbler will function. However, this is not required since the nitrogen also escapes at the base of the glove box.

The sample crucible can now be transferred to the balance. While the glove box is still being flushed with nitrogen and with the right hand in the upper right-hand glove and the left hand in the lower left-hand glove, the crucible and forceps are moved inside the glove box to prevent spillage. The wrench is turned three half turns in a counter-clockwise direction to loosen the furnace. The furnace is placed to the right in the glove box. The sample crucible is transferred to the left part of the stick using the forceps and both hands. The furnace is replaced and tightened, and the left hand removed from the glove box. Using the left hand, the recorder is turned on, stopping on Channel 3. To stop on a particular channel the recorder is turned off immediately after the previous channel has printed. The balance is freed, and with the range knob on 100 mg, the course tare knob is adjusted to bring the printer to about 80 on the chart. If the channel will not come on scale, then the balance is clamped, and .1 gram increments are added or subtracted until the channel is on scale.

The balance is tapped, and any deflection in the position of the pointer is noted. If the printer moves, the crucibles are touching the sides of the furnace, and the position of the stick must be changed to correct the problem.

The nitrogen flush is stopped, and the glove box removed along with the wrench and forceps. The furnace shield is placed in position and connected. The coupling will make a click in the proper position. The furnace is now evacuated as described previously.

The evacuation takes about 30 minutes. Liquid nitrogen is also put in the other trap. When Channels 1 and 2 stabilize, the various channels can be set as follows. Channels 1 and 2 are adjusted to about 10 on the chart using the offset knobs. The sensitivity knobs usually are not changed. Channel 3 is positioned at about 80 using the course tare knob. Channel 4 is positioned at about 100 using the fine tare knob. Channel 5 is set with the DTA zero knob (with range set at 50 mv) at 50 in the chart. Channel 6 automatically prints at 0, or slightly below.

The DTA-TGA run is now ready to begin. The heating rate and upper temperature limit are selected. The recirculating system is checked for distilled water and turned on. The appropriate program button is then pushed.

When the DTA-TGA scan is complete, the balance is clamped, the printer is stopped on Channel 1, the furnace control is turned off, and Stopcock 5 is closed. The chart speed is changed to 12 inches per hour (normal speed is 6 inches per hour). Channel 1 is readjusted to be on scale, and the printer is started. Immediately the right-hand

liquid nitrogen trap is dropped. It takes about one hour to print the condensable gas spectrum as followed by Channel 1.

To shut down the DTA-TGA after the condensable gas spectrum has been printed, the printer is stopped on Channel 6, the chart speed returned to 6 inches per hour, and the spectrum is removed from the machine. The recirculating system is turned off as well as the diffusion pump. The balance can be left under vacuum. If the sample is needed, then the procedure of filling the balance with argon is repeated.

Operating Instructions for Argon Atmosphere

The instructions for argon atmosphere DTA-TGA are the same as those for vacuum DTA-TGA. The difference is that when the sample has been loaded on the balance, the balance is not evacuated. Instead, the bubbler is left in place. A dynamic argon atmosphere is maintained by allowing the argon to bubble slowly. A static atmosphere is obtained if the argon source is turned off. No liquid nitrogen is placed in the right-hand trap. Channels 1 and 2 cannot be used under argon and are adjusted to about 100 on the chart. Obviously, there is also no condensable gas spectrum to run later.

Special Operating Instructions

Adjustment of DTA

If the DTA is drifting severely, several factors may have to be corrected. First, centering of the stick should be checked. Then, adjustments to sample weight and reference weight have to be made. By changing the relative ratio the DTA drift can be corrected. This

process is purely trial and error and hence very tedious. It is only done when detailed DTA information is desired.

Interpretation of DTA-TGA Data

Only a few comments are necessary concerning the interpretation of DTA-TGA data. The DTA can be expected to drift. Therefore, sometimes more than one run is needed to distinguish between an endothermic or exothermic process.

Occasionally, a "buoyancy effect" is noticed in the TGA curve. This abnormality causes an apparent increase in weight. It is caused by a large amount of evolved gas pushing down on the balance. The problem can be ignored in terms of calculation of weight loss. A "corrected" TGA curve can be drawn, subtracting out the buoyancy effect.

In the condensable gas spectrum water usually comes at about 70 minutes as a broad peak. Diethyl ether appears at about 30 minutes, and propene comes at about 10 minutes as a sharp peak.

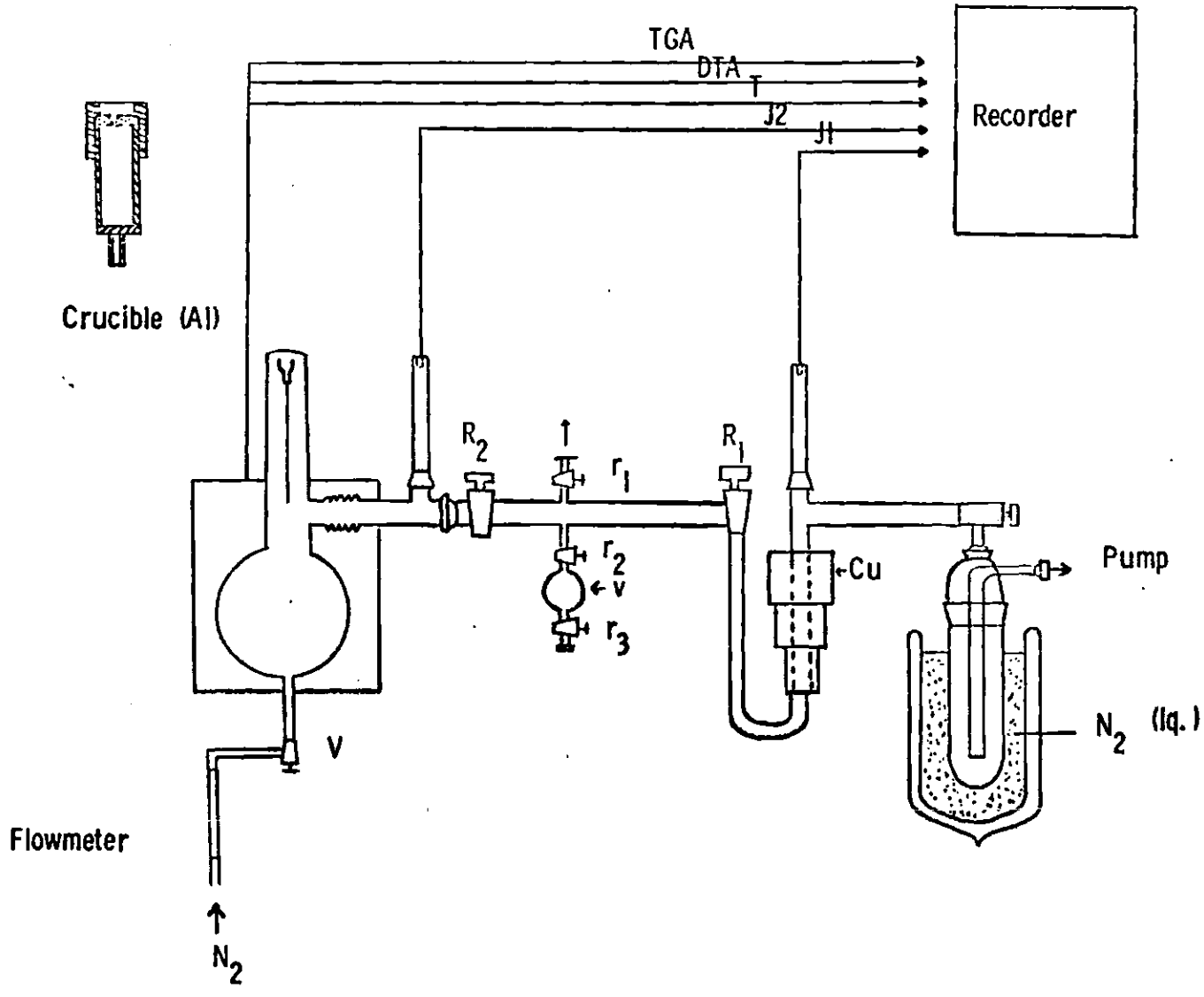

Figure 17. Description of High Vacuum Portion of Mettler Thermoanalyzer II

APPENDIX 2

CALCULATION OF KINETIC PARAMETERS

Kinetic parameters for the alkoxides and amides of magnesium, zinc, and aluminum have been calculated by isothermal and non-isothermal methods via thermogravimetric analysis (TGA). Sample calculations are illustrated for isopropoxy(phenyl)magnesium

$$PhMgOPr^{i} \cdot 0.16\ Et_2O$$

Isothermal Kinetics

The first step in the constant temperature kinetic study was to determine the first-order rate constants at three different temperatures. Data is presented in Table 23 for the rate constant k_1 at 200°C for isopropoxy(phenyl)magnesium. The sample weight was 81.6 mg comprised of 5.6 mg Et_2O and 76.0 mg $PhMgOPr^{i}$. The first stage of decomposition reaction occurs in one step with no apparent intermediate. The observed weight loss is due to the formation of volatile reaction products - benzene and propene in a one-to-one molar ratio. The procedure was to heat the tared sample at 10°C per minute to the desired temperature. When the temperature channel (No. 6) on the DTA-TGA printer was at a constant value, then weight loss data was taken from the TGA curve. The 4.4 mg weight loss at time zero is due to the decomposition that occurs in reaching the desired temperature.

Moles of hydrocarbon lost (benzene) are calculated by solving the simultaneous equations below (shown for time zero data),

$$A = B$$

$$78A + 42B = 4.4 \times 10^{-3}$$

where A equals moles of benzene and B equals moles of propene. The number 4.4×10^{-3} is the weight loss in grams.

The moles of alkoxide remaining are calculated from the following equation (data for time zero substituted):

moles alkoxide remaining = moles alkoxide initially - moles hydrocarbon (benzene)

moles alkoxide remaining = $4.74 \times 10^{-4} - 3.67 \times 10^{-5} = 4.37 \times 10^{-4}$

A linear least squares plot of ln (moles alkoxide) versus time in minutes gives a good straight line as shown by a coefficient of correlation (R) equal to .982. Two other rate constants were calculated in a similar manner and are summarized in Table 24. A plot of ln k versus $^{1}/_{T}$ then allows the energy of activation (E_a) and the Arrhenius preexponential factor (A) to be calculated from the following equations:

$$E_a = -R \times \text{slope}$$

$$E_a = -1.99\ (-5.94 \times 10^3) = 11.8 \times 10^3 \text{ cal/mole}$$

$$E_a = 11.8 \text{ kcal/mole}$$

$$\text{intercept} = \ln A$$

$$5.27 = \ln A$$

$$A = 194 \text{ min}^{-1}$$

$$A = 3.3 \text{ sec}^{-1}$$

The entropy ($\Delta S^{\neq}$) of activation is calculated from the equation

$$S^{\neq} = 2.303\ R \log A - 2.303\ R \log \left(K\ e\ \frac{k'T}{h}\right)$$

where k' is the Boltzman constant, h is Planck's constant, and K is the transmission coefficient which is assumed to be unity. Therefore, the entropy of activation at 200°C for isopropoxy(phenyl)magnesium is -58.8 e.u.

$$S^{\neq} = 2.303(1.99)\log(3.3) - 2.303(1.99)\log \frac{(1)\ (2.303)\ (1.38 \times 10^{-16})(473)}{(6.63 \times 10^{-27})}$$

$$S^{\neq} = 2.4 - 61.2 = -58.8 \text{ e.u.}$$

Non-isothermal Kinetics

Dynamic kinetic data was taken from the TGA curve obtained at a heating rate of 4°C per minute from 25°C to 450°C. The data was applied to the Achar F_1 equation

$$\ln \left(\frac{1}{1 - \alpha} \cdot \frac{d\alpha}{dT}\right) = \ln \left({}^{A}/_{B}\right) - {}^{E_a}/RT,$$

where α is the fraction of sample reacted in time t, R is the gas constant, and B is the heating rate. α is calculated by dividing the weight loss at a given temperature by the total weight loss due to the formation of volatile reaction products - benzene and propene in a one-to-one molar ratio. Weight losses were adjusted for the initial loss of diethyl ether solvent. A sample of isopropoxy(phenyl)-magnesium weighing 58.1 mg was responsible for a total weight loss of 3.9 mg diethyl ether and 38.6 mg benzene and propene. The 11.3 mg weight loss at 280° is due to benzene and propene only. $d\alpha$ at 300° is calculated by subtracting α for 280° from α for 320°. A similar calculation gives dT. The other calculations in Table 25 are self-explanatory.

A linear least squares plot of $\ln \left(\frac{1}{1 - \alpha} \cdot \frac{d\alpha}{dT}\right)$ versus ${}^{1}/_{T}$ gave a straight line (coefficient of correlation (R) equals 0.990) from which the energy of activation (E_a) and Arrhenius preexponential factor (A) can be calculated by the following formulae,

$$E_a = -R \times \text{slope}$$

$$E_a = -1.99\ (-6.39 \times 10^3) = 12.7 \times 10^3 \text{ cal/mole}$$

$$E_a = 12.7 \text{ Kcal/mole}$$

$$\ln\ (^A/_B) = \text{intercept}$$

$$\ln\ (^A/_4) = 6.66$$

$$A = 3.12 \times 10^3 \text{ min}^{-1}$$

$$A = 52 \text{ sec}^{-1}$$

Linear Least Squares Computer Program

Kinetic calculations were conducted on the Georgia Institute of Technology Cyber 74 computer using a simple regression analysis program developed by Dr. A. N. Doherty of St. John's University. The program was designed to describe the primary properties of a least squares linear regression problem. The following instructions constitute a brief introduction to this program.

The program is called from the computer in the following way. The user number and password are obtained in advance from Dr. P. B. Sherry in the Chemistry Department. The return key is used to move to a new line.

The computer will print:	The user types:
User Number:	CMPBSFW
Password:	R864
Recover/System:	BASIC
Old, New, or Lib File:	OLD
File Name:	STATSR/UN=CCLIBKL
READY.	TED, STATSR
Ø ?	69

Data is entered beginning on line 69 in the following format.

line 69	900	Data N
line 70	901	Data X(1), Y(1), X(2), Y(2)...X(N), Y(N)

Since sample data is written into the program, it is necessary to replace this sample data with the new data. For example, in the case of the non-isothermal kinetic data for isopropoxy(phenyl)magnesium, there are four data points. When the number 69 is entered, the following exchange begins.

The computer will print:	The user types:
900 Data 3	
69 ?	R 900 Data 4
69 ?	70
901 Data 1, 3, 3, 5, 3, 6	
70 ?	R 901 Data 1.74, -1.94, 1.69, -1.83, 1.63, -1.65, 1.58, -1.65

```
70?                                    EXIT
Ready.                                 Run
```

When the run is complete, the edit mode can be recalled or the user types in BYE to sign off. The R symbol means replace. If more lines are needed for data, then the symbol I (insert) is used and the line numbering continues as 902 Data, 903 Data, etc. A line is deleted using the symbol D 1, meaning to delete one line.

Table 23. Constant Temperature Kinetic Data (k_1) for $PhMgOPr^i \cdot 0.16\ Et_2O$ at 200°C

Time (min.)	Weight[a] loss (mg)	Hydrocarbon lost (moles)	Alkoxide[b] Remaining (moles)	ln (moles Alkoxide)
0	4.40	3.67×10^{-5}	4.37×10^{-4}	-7.73
30	6.10	5.08×10^{-5}	4.23×10^{-4}	-7.76
60	7.25	6.04×10^{-5}	4.14×10^{-4}	-7.79
90	8.20	6.83×10^{-5}	4.06×10^{-4}	-7.81
120	9.00	7.50×10^{-5}	3.99×10^{-4}	-7.83
150	9.70	8.08×10^{-5}	3.93×10^{-4}	-7.84
180	10.35	8.63×10^{-5}	3.88×10^{-4}	-7.85
210	10.95	9.13×10^{-5}	3.83×10^{-4}	-7.87
240	11.50	9.58×10^{-5}	3.78×10^{-4}	-7.88

[a] The weight loss has been corrected for loss of diethyl ether.

[b] Moles alkoxide initially - moles hydrocarbon lost (benzene) = moles alkoxide remaining.

Table 24. E_a Plot for $PhMgOPr^i \cdot 0.16\ Et_2O$

Temperature	$^1/_T$ ($°K^{-1}$)	k (min^{-1})	R	ln k
200	2.11×10^{-3}	6.00×10^{-4}	0.982	-7.42
235	1.97×10^{-3}	2.10×10^{-3}	0.990	-6.17
285	1.79×10^{-3}	4.21×10^{-3}	0.988	-5.47

Table 25. Achar F_1 Plot for $PhMgOPr^i \cdot 0.16\ Et_2O$

T (°C)	$\frac{1}{T}$ ($°K^{-1}$)	weight[a] loss (mg)	$\alpha = \frac{\text{wt. loss}}{38.6^b}$	$d\alpha$	dT	$\frac{d\alpha}{dT}$	$(1-\alpha)$	$\ln\left(\frac{1}{1-\alpha}\frac{d\alpha}{dT}\right)$
280	1.81×10^{-3}	11.3	0.300	----	--	----	0.700	---
300	1.75×10^{-3}	16.9	0.438	0.260	40	6.50×10^{-3}	0.562	-4.47
320	1.69×10^{-3}	21.6	0.560	0.259	40	6.48×10^{-3}	0.440	-4.21
340	1.63×10^{-3}	26.9	0.697	0.272	40	6.80×10^{-3}	0.303	-3.80
360	1.58×10^{-3}	32.1	0.832	0.225	40	5.63×10^{-3}	0.168	-3.39
380	1.53×10^{-3}	35.6	0.922	----	--	----	0.078	---

[a] The weight loss at T. The weight of diethyl ether has been deducted.

[b] Total weight loss due to benzene and propene but not including the weight loss due to diethyl ether.

APPENDIX 3

CALCULATION OF MOLECULAR WEIGHT DATA

Ebullioscopic Determination of Molecular Association

The molecular associations of the N-substituted magnazines were determined ebullioscopically employing a modified Cottrell boiling point elevation apparatus. Temperature changes were observed using a Beckman differential thermometer, and the pressure was measured using a precision Wallace-Tiernan manometer. Solvent loss was prevented by the recirculation of ice-water through the condenser. Specific details of the procedure have been described.[9]

Calculations of the i-values were made using the following equation:

$$i = \frac{W_2 M_1}{W_1 M_2} \quad \frac{1}{e^{\Delta T_b M_1 / 1000 K_b} - 1} \tag{25}$$

The equation was derived by assuming an ideal but not necessarily dilute solution. The terms include M_1, the formula weight of the solutes; M_2, the molecular weight of the solvent (72.10 g for tetrahydrofuran and 78.11 g for benzene); and K_b, the molal boiling point elevation constant (2.24 for tetrahydrofuran and 2.47 for benzene at 740 mm). The K_b's were determined in advance using benzophenone.

Cryoscopic Determination of Molecular Association

Cryoscopic molecular association studies on the N-substituted magnazines were conducted using an apparatus modified for handling air-sensitive compounds similar to the one described by Salzberg.[10]

The following equation was used for calculations:

$$i = \frac{1000\ K_f W_2}{\Delta T_f\ M_1 W_1} \tag{26}$$

where M_1 is the molecular weight for the empirical formula, W_2 is the weight of dissolved solute, W_1 is the weight of the solvent, and K_f is the molal freezing point-depression constant (3.27 for acetic acid and 5.20 for benzene).

APPENDIX 4

MOLECULAR ASSOCIATION DATA

Isopropylmagnazine in Tetrahydrofuran (Ebullioscopically)

Isopropylmagnazine (gr)	THF (gr)	ΔT_{bp}	Molarity	i-value
0.143	99.449	0.014	0.016	2.8
0.289	103.885	0.027	0.031	2.8
0.433	108.257	0.037	0.044	3.0
0.719	116.940	0.054	0.068	3.1
1.006	125.636	0.072	0.088	3.1

Isopropylmagnazine in Acetic Acid (Cryoscopically)

Isopropylmagnazine (gr)	HOAc (gr)	ΔT_{fp}	Molarity	i-value
0.235	57.035	0.170	0.053	1.01
0.477	62.298	0.312	0.099	0.99
0.953	72.687	0.572	0.169	0.92

n-Butylmagnazine in Tetrahydrofuran (Ebullioscopically)

n-Butylmagnazine (gr)	THF (gr)	ΔT_{bp}	Molarity	i-value
0.254	92.447	0.020	0.025	2.8
0.512	96.767	0.040	0.049	2.7
1.011	105.130	0.065	0.088	3.1
1.483	113.056	0.090	0.120	3.0

n-Butylmagnazine in Benzene (Cryoscopically)

n-Butylmagnazine (gr)	PhH (gr)	ΔT_{fp}	Molarity	i-value
0.257	47.685	0.030	0.050	9.8
0.512	51.889	0.037	0.090	14.5
1.022	60.285	0.050	0.150	18.5
1.516	68.432	0.055	0.200	22.0

n-Butylmagnazine in Benzene (Ebullioscopically)

n-Butylmagnazine (gr)	PhH (gr)	ΔT_{bp}	Molarity	i-value
0.427	91.310	0.020	0.043	6.1
0.931	96.115	0.025	0.088	10.0
1.440	100.978	0.030	0.129	12.3
2.151	107.770	0.030	0.180	17.2

Phenylmagnazine in Tetrahydrofuran (Ebullioscopically)

Phenylmagnazine (gr)	THF (gr)	ΔT_{bp}	Molarity	i-value
0.341	91.772	0.015	0.028	4.1
0.690	95.935	0.035	0.054	3.4
1.103	100.866	0.050	0.082	3.6
1.661	107.509	0.075	0.116	3.4

LITERATURE CITED*

1. J. March, "Advanced Organic Chemistry: Reactions, Mechanisms, and Structure", McGraw-Hill, New York, 1968, p. 753-758.

2. (a) C. H. DePuy and R. W. King, Chem. Rev., 60, 431 (1960).

   (b) W. H. Saunders, Jr., and A. F. Cockerill, "Mechanisms of Elimination Reactions", John Wiley and Sons, New York, 1973.

3. (a) DePuy and King, p. 444.

   (b) H. R. Nace, Org. Reactions, 12, 57 (1962).

   (c) Saunders, Jr., and Cockerill, p. 422.

4. (a) Saunders, Jr. and Cockerill, p. 165.

   (b) A. C. Cope and E. R. Trumbull, Org. Reactions, 11, 317 (1960).

5. (a) Saunders, Jr. and Cockerill, p. 446.

   (b) Cope and Trumbull, p. 361.

   (c) C. H. DePuy and R. W. King, Chem. Rev., 60, 448 (1960).

6. E. C. Ashby and R. Schwartz, J. Chem. Educ., 51, 65 (1974).

7. D. R. Shriver, "The Manipulation of Air Sensitive Compounds", McGraw-Hill, New York, 1969.

8. E. C. Ashby, P. Claudy, and Bousquet, J. Chem. Educ., (in press).

9. F. Walker and E. C. Ashby, J. Chem. Educ., 45, 654 (1968).

10. H. W. Salzberg, J. I. Morrow, S. R. Cohen, and M. E. Green, "A Modern Laboratory Course in Physical Chemistry", Academic Press, New York, 1969, p. 107.

11. C. N. Reilly, R. W. Schmid, and F. S. Sadek, J. Chem. Educ., 36, 619 (1959).

*Journal title abbreviations used are listed in "List of Periodicals," Chemical Abstracts, (1961).

12. (a) W. Schlenk, Chem. Ber., 64, 734 (1931).

(b) Y. Pocker and J. H. Exner, J. Am. Chem. Soc., 90, 6764 (1968).

13. C. R. Noller, Org. Syn., 12, 86 (1932).

14. K. A. Kozeschkow, A. N. Nesmejanou, and W. Z. Petrosaw, Chem. Ber., 67, 1138 (1934).

15. A. W. Lanbengayer, K. Wade, and G. Jengnick, Inorg. Chem., 1, 632 (1962).

16. G. D. Barbaras, C. Dillard, A. E. Finholt, J. Wartik, K. E. Wilzbach and H. D. Schlesinger, J. Am. Chem. Soc., 73, 4858 (1951).

17. H. C. Brown and H. M. Yoon, J. Am. Chem. Soc., 88, 1464 (1966).

18. D. J. Cram and F. A. A. Elhafez, J. Am. Chem. Soc., 74, 5828 (1952).

19. (a) A. McKenzie and H. Wren, J. Chem. Soc., 97, 473 (1910).

(b) A. McKenzie and R. Roger, J. Chem. Soc., 125, 844 (1924).

(c) Reference 21.

(d) D. J. Cram and F. A. A. Elhafez, J. Am. Chem. Soc., 74, 5851 (1952).

20. (a) B. V. Shetty, J. Org. Chem., 26, 3002 (1961).

(b) H. Christol, A. Laurent, and G. Solladie, Bull. Soc. Chim. France, 877 (1963).

21. W. J. Hickinbottom, "Reactions of Organic Compounds", Longmans, Green, and Company, New York, 1936, p. 303.

22. K. A. Schellenberg, J. Org. Chem., 28, 3259 (1963).

23. W. S. Emerson and G. A. Uraneck, J. Am. Chem. Soc., 63, 749 (1941).

24. (a) C. Ainsworth, J. Am. Chem. Soc., 78, 1675 (1956).

(b) E. R. Biehl, S. M. Smith, and P. C. Reeves, J. Org. Chem., 36, 1841 (1971).

25. (a) G. E. Coates, M. L. H. Green, and K. Wade, "Organometallic Compounds", Vol. 1, Meuthuen and Co., London, 1967.

(b) E. C. Ashby, J. Nackashi, and G. E. Parris, J. Am. Chem. Soc., 97, 3162 (1975).

(c) G. E. Coates and D. Ridley, J. Chem. Soc., A, 56 (1967).

26. W. W. Wendlandt, "Thermal Methods of Analysis", John Wiley and Sons, New York, 1974.

27. J. M. Harris and C. C. Wamser, "Fundamentals of Organic Reaction Mechanisms", John Wiley and Sons, New York, 1976, p. 220.

28. G. L. O'Connor and H. R. Nace, J. Am. Chem. Soc., 74, 5454 (1952).

29. R. A. Benkeser and J. J. Hazdra, J. Am. Chem. Soc., 81, 228 (1959).

30. W. J. Bailey and W. F. Hale, J. Am. Chem. Soc., 81, 647 (1959).

31. R. T. Arnold, G. G. Smith, and R. M. Dodson, J. Org. Chem., 15, 1256 (1950).

32. E. R. Alexander and A. Mudrak, J. Am. Chem. Soc., 72, 1810 (1950).

33. (a) G. E. Coates and D. Ridley, J. Chem. Soc., A, 56 (1967).

(b) J. Nackashi, Ph.D. Thesis, Georgia Institute of Technology, 1974.

(c) G. E. Coates and K. Wade, "Organometallic Compounds, The Main Group Elements", Methuen and Company, London, 1967, pp. 101, 137, and 307.

34. E. S. Freeman and B. Carroll, J. Phys. Chem., 62, 394 (1958).

35. A. W. Coats and J. P. Redfern, Nature, 201, 68 (1964).

36. B. N. N. Achar, G. W. Brindley, and J. H. Sharp, Proc. Int. Clay Conf., Jerusalen, 1, 67 (1966).

37. V. Satava, Thermochim. Acta, 2, 423 (1971).

38. J. F. Bunnett, Surv. Progr. Chem., 5, 53 (1969).

39. Saunders, Jr., and Cockerill, p. 17.

40. M. S. Silver, J. Am. Chem. Soc., 83, 3487 (1961).

41. D. J. Cram, F. D. Greene and C. H. DePuy, J. Am. Chem. Soc., 78, 790 (1956).

42. E. K. Mellon, Jr., and J. J. Kagowski, Adv. Inorg. Chem. and Radiochem., 5, 259 (1963).

43. K. Miedenzu and J. W. Dawson, "Boron-Nitrogen Compounds", Academic Press, Inc., New York (1965).

44. S. Cucinella, T. Salvatori, C. Bustelo, G. Perego, and A. Mazzei, J. Organometal. Chem., 78, 185 (1974).

45. A. K. Galwey, "Chemistry of Solids", Chapman and Hall Ltd., London, 1967, p. 166.

VITA

George Fredrick Willard, Jr. was born on May 28, 1950 in Charleston, West Virginia. He attended public school there and later went to Marshall University in Huntington, West Virginia. There he received a B.S. in Chemistry degree with a minor in physics in June 1972, and received an award for being the Outstanding Senior Chemistry Student. In July 1972, he began graduate studies at the Georgia Institute of Technology in Atlanta, Georgia under the direction of Dr. E. C. Ashby in the area of organometallic chemistry.

On June 24, 1971, Fred married the former Kathryn Sue Patton of South Charleston, West Virginia.

In July 1974, he coached his wife, Kathy, during the birth of their first child, George Fredrick Willard III and again in August 1975, during the birth of their second child, Melinda Sue Willard.

After completion of his degree at Georgia Tech, Fred will begin as an Advanced Scientist for Owens-Corning Fiberglas Corporation which has a technical center located in Granville, Ohio.

Fred's chief leisure activities include racquetball which he began in 1973 and woodcarving which he began in 1974. He participated in the 1975 Dahlonega Gold Rush Days and has sold some hand-carved molds for the fabrication of polyurethane wall hangings to an Atlanta contractor.